Spring 2010

Population pharmacokinetics of pyronaridine in the treatment of malaria

Thitima Wattanavijitkul
University of Iowa

POPULATION PHARMACOKINETICS OF PYRONARIDINE IN THE TREATMENT OF MALARIA

by

Thitima Wattanavijitkul

An Abstract

Of a thesis submitted in partial fulfillment
of the requirements for the Doctor of
Philosophy degree in Pharmacy
in the Graduate College of
The University of Iowa

May 2010

Thesis Supervisor: Professor Lawrence L. Fleckenstein

ABSTRACT

A novel pyronaridine-artesunate (PA) combination is being developed as a 3:1 fixed ratio oral combination against *P. falciparum* and *P. vivax* malaria. Pyronaridine (PYR) has been used on a limited basis as monotherapy to treat malaria in some provinces in China since 1970, and there are minimal published data on pharmacokinetics of PYR in humans.

In this thesis, the population pharmacokinetics (PPKs) of PYR is studied in different populations. In Chapter II, we develop a PPKs model in 91 healthy subjects participating in a Phase I study of PA. In addition, data from two Phase II and four Phase III studies of PA are pooled, and PPKs of PYR in 321 adult and 319 pediatric patients are investigated separately in Chapter III and IV, respectively. Chapter V provides comparisons of the results from each population.

PYR pharmacokinetics in each population is best described by a two-compartment model with first order absorption and elimination from the central compartment. Although the same structural model is used, pharmacokinetics of PYR differs among the three populations. PYR is absorbed faster and more variably in patients. The weight-normalized total apparent volumes of distribution (V/F) in adult and pediatric patients are approximately 5 and 3 times larger than in healthy subjects. Adult and pediatric patients have a mean weight-normalized oral clearance (CL/F) approximately 2 times higher than healthy subjects but the drug is eliminated more slowly in patient populations due to a much larger V/F. The average elimination half-lives are 8, 11 and 18 days in healthy, pediatric and adult patient populations, respectively. Pharmacokinetic modeling suggests that lean body weight is an important predictor of apparent central volume (V2/F) in adult patients while actual body weight is a significant covariate of V2/F and CL/F in children.

The parameters obtained from PPK modeling are plausible and estimated with acceptable precision. The final models are evaluated using a nonparametric bootstrap technique and visual predictive check. The final models are robust and adequately capture the overall pyronaridine pharmacokinetics. Further study in a broader patient population will be necessary to examine other covariates that influence pyronaridine pharmacokinetics.

Abstract Approved: _____
Thesis Supervisor

_____
Title and Department

_____
Date

POPULATION PHARMACOKINETICS OF PYRONARIDINE IN THE TREATMENT OF MALARIA

by

Thitima Wattanavijitkul

A thesis submitted in partial fulfillment
of the requirements for the Doctor of
Philosophy degree in Pharmacy
in the Graduate College of
The University of Iowa

May 2010

Thesis Supervisor: Professor Lawrence L. Fleckenstein

Graduate College
The University of Iowa
Iowa City, Iowa

CERTIFICATE OF APPROVAL

_____

PH.D. THESIS

_____

This is to certify that the Ph.D. thesis of

Thitima Wattanavijitkul

has been approved by the Examining Committee
for the thesis requirement for the Doctor of Philosophy
degree in Pharmacy at the May 2010 graduation.

Thesis Committee: _____
Lawrence L. Fleckenstein, Thesis Supervisor

_____
Erika J. Ernst

_____
Lee E. Kirsch

_____
Dawei Liu

_____
Daryl J. Murry

To my dad, Raungrith Kungsamrith, the one who most inspired me for doctoral study.
To my mom and my husband, who have always been the source of my inspiration and encouragement.

All models are wrong, some are useful.
George E. P. Box
Professor of Statistics

ACKNOWLEDGMENTS

I would like to extend my greatest gratitude to Dr. Larry Fleckenstein, who has continuously supported me and given me many comments and suggestions. You have been an inspiration and role model for me.

I would also like to thank my committee members: Dr. Erica Ernst, Dr. Lee Kirsch, Dr. Dawei Liu, and Dr. DJ Murry for all insightful comments and constructive discussion during my defense. Thank you for sharing your valuable ideas and time.

Special thanks to thank Dr. Sarapee Hirankarn for sharing indispensable experiences and Dr. Patrick Dolan for so skillfully helping me edit and improve my work.

My friends and colleagues at the University of Iowa that I am deeply thankful for: Dr. Bee San Tan for being great friend and giving moral support, Denise Morris for being there whenever I needed, Dr. Amal Al Omari, Dr. Jesse Hollanbaugh, Dr. Craig Herman, Janthima Methaneethorn and Carrie Morris for sharing their perspectives on life and study, Paul Imming and Mark Schmidt for spending days and nights analyzing the samples, Grace Kim for double checking data, Dr. Himanshu Naik, Dr. George Lien, and Dr. Sherry Wei for the assistance. It was a pleasure working with you!

To the Thai community of Iowa City. I cannot list every name, but they include: Oitip, Marisa, Jib, Ore, Ake, Todd, Bow, Bird, Ron, Fon, Ow, Jun, Aueng, Putt, Kobkul, Jing, Tar, Toom, Bob, Robert, Brenda, Mem and everyone at Thai Student Association. Thank you for being with me on good days and bad days.

Many thanks to my friends in Thailand for your warm shoulders and encouragement: Siriluck Vatanathum, Dr. Alisara Sangviroon, Dr. Boontarika Chanvorachote, Dr. Aroonwan Lam-ubol, and Dr. Samitada Sungkapo. I would never have come this far without your support.

Last but not least, special thanks to my adorable children, Ohm and Amy who have made my 5 year journey colorful. To the best mom in the world, Vilasluk

Kungsamrith for help raising my children and giving me inspiration. To my late father, Raungrith Kungsamrith who is always on my mind. I did it, dad. Lastly, to my wonderful and patient husband, Songkiat (Art), thanks for your constant support and for allowing me to complete this part of my life.

This thesis and my doctorate would not have been possible without your support. I am glad that each and every one of you is part of my life. Thank you.

ABSTRACT

A novel pyronaridine-artesunate (PA) combination is being developed as a 3:1 fixed ratio oral combination against *P. falciparum* and *P. vivax* malaria. Pyronaridine (PYR) has been used on a limited basis as monotherapy to treat malaria in some provinces in China since 1970, and there are minimal published data on pharmacokinetics of PYR in humans.

In this thesis, the population pharmacokinetics (PPKs) of PYR is studied in different populations. In Chapter II, we develop a PPKs model in 91 healthy subjects participating in a Phase I study of PA. In addition, data from two Phase II and four Phase III studies of PA are pooled, and PPKs of PYR in 321 adult and 319 pediatric patients are investigated separately in Chapter III and IV, respectively. Chapter V provides comparisons of the results from each population.

PYR pharmacokinetics in each population is best described by a two-compartment model with first order absorption and elimination from the central compartment. Although the same structural model is used, pharmacokinetics of PYR differs among the three populations. PYR is absorbed faster and more variably in patients. The weight-normalized total apparent volumes of distribution (V/F) in adult and pediatric patients are approximately 5 and 3 times larger than in healthy subjects. Adult and pediatric patients have a mean weight-normalized oral clearance (CL/F) approximately 2 times higher than healthy subjects but the drug is eliminated more slowly in patient populations due to a much larger V/F. The average elimination half-lives are 8, 11 and 18 days in healthy, pediatric and adult patient populations, respectively. Pharmacokinetic modeling suggests that lean body weight is an important predictor of apparent central volume (V2/F) in adult patients while actual body weight is a significant covariate of V2/F and CL/F in children.

The parameters obtained from PPK modeling are plausible and estimated with acceptable precision. The final models are evaluated using a nonparametric bootstrap technique and visual predictive check. The final models are robust and adequately capture the overall pyronaridine pharmacokinetics. Further study in a broader patient population will be necessary to examine other covariates that influence pyronaridine pharmacokinetics.

TABLE OF CONTENTS

LIST OF TABLES

LIST OF FIGURES

CHAPTER I

INTRODUCTION

Malaria

Malaria, a parasitic infectious disease, is a global health challenge. According to the World Health Organization, half the world's population is at risk of malaria[1]. Although malaria infection is preventable and curable, it can be fatal if not treated promptly. In 2008, there were an estimated 243 million cases and almost a million deaths from the disease[2], making malaria one of the world's leading killers. With the increase in international travel, malaria is becoming a growing health problem in non-endemic industrialized countries[3]. In the United States, approximately 1,500 cases of malaria are reported annually[4, 5]. The majority of reported malaria cases diagnosed each year in the United States is imported from regions where malaria transmission is known to occur.

Malaria is caused by single-celled protozoan parasites of the genus *Plasmodium*. The five species that cause malaria in humans are: *P. falciparum, P. vivax, P. ovale, P. malariae* and a recently confirmed species, *P. knowlesi*[6, 7]. Of these *P. falciparum* is responsible for over 90% of cases and nearly all of the malaria deaths worldwide[1]. *P. vivax* is also common. Vivax malaria is rarely fatal, but *P. vivax* can become dormant in the liver causing relapses that occur months to years after treatment[8]. While malaria parasites can be transmitted by sharing contaminated needles and blood transfusions, almost all malaria is transmitted from one person to another by the bite of a female Anopheles mosquito.

All Plasmodium species have a similar life cycle which involves two hosts: humans and the Anopheles mosquito (figure 1.1). In humans, Plasmodium reproduces asexually by cell division in liver cells and then in red blood cells. In the mosquitoes, the parasite reproduces sexually.

Human malaria infection begins when an infected female Anopheles mosquito bites a human to obtain a blood meal. The mosquito releases saliva containing the parasites in the form of asexual cells (called sporozoites) which rapidly enter the liver cells to reproduce asexually. Each sporozoite develops into schizont, a structure filled with merozoites (another stage of the parasite). This incubation stage is asymptomatic and it lasts a week or more, depending on the Plasmodium species[9]. When the schizont matures, it breaks and releases a massive number of merozoites from the infected hepatocytes. The released merozoites invade other hepatocytes and enter the bloodstream to invade the red blood cells. Some *P. vivax* and *P. ovale* sporozoites can develop a form that remains dormant in the liver for months or years and then later can cause a relapse.

In the blood, the parasites consume hemoglobin and multiply asexually repeatedly inside the erythrocytes. Again, merozoites form schizonts filled with more merozoites. When the schizont matures, it ruptures and releases more merozoites infecting more red blood cells. The majority of symptoms are usually caused by large amounts of free hemoglobin and toxins released into the circulatory system. Early symptoms are non-specific including flu-like illness with cycles of fever and shivering, headache, abdominal discomfort and muscle pain. This is the typical picture of uncomplicated malaria, the mild form of the disease. At this stage, the case-fatality rate is low with prompt and effective treatment. Rapid deterioration is uncommon except with *P.falciparum*. If ineffective drugs are given or treatment is delayed, uncomplicated falciparum malaria can rapidly develop into severe malaria. The rapid destruction of the red blood cells can cause severe anemia and obstruction in the blood vessels to the brain (cerebral malaria) or other vital organs, causing metabolic acidosis, hypoglycemia, acute renal failure, acute pulmonary edema, convulsions, coma and eventually death[10, 11].

Plasmodium completes its life cycle in the mosquito. First, some merozoites develop into male and female sexual forms circulated in human bloodstream. Then the mosquito sucks up these infected erythrocytes filled with gametocytes along with the

blood meal. Once the gametocytes are in the mosquito's gut, they develop into male and female gametes and then mate to produce an oocyst filled with sporozoites. When the oocyst matures, it ruptures and the sporozoites migrate to the mosquito's salivary glands. The life cycle of the parasite starts again when the mosquito bites its next victim.

Despite more than five decades of global efforts bringing the disease under control, malaria still remains a constant threat to public health due to a number of factors: the disease's resistance to traditional treatments, the mosquitoes' resistance to the main insecticides, HIV/AIDS, health and economic problems in endemic areas and population migration into areas where the disease is spread more easily. Although malaria control efforts have been boosted during the past few years with increased international funding and political commitment, eliminating malaria still depends on research and development for more effective tools than currently available medicines and insecticides[7, 12].

Malaria Control

Malaria control relies on the integration of prevention and treatment. The approach to malaria prevention varies by settings[9]. Prevention in endemic areas includes preventive treatment of vulnerable groups, such as pregnant women, and vector control, such as using the insecticide-treated bed nets and indoor insecticide residual spraying. Prevention in travelers from non-endemic countries visiting a malaria risk area involves personal protection to avoid mosquito bites and use of chemoprophylaxis. Malaria vaccine development and testing are ongoing[13].

The primary objective of treating uncomplicated malaria is to cure the infection and prevent progression to severe disease, while the primary objective of antimalarial treatment in severe malaria is to prevent death[14]. The choice of antimalarial drugs usually depends on the species of the parasite and the geographical location, which imply the likely sensitivity of the infecting parasites. Although mono-therapies, such as chloroquine, sulfadoxine-pyrimethamine, amodiaquine, and mefloquine, were highly

effective in the 1960s, those drugs have lost their efficacy due to drug resistance, particularly in *P. falciparum*. To counter the threat of resistance and to improve treatment outcome, the World Health Organization now recommends that confirmed cases of uncomplicated *Plasmodium falciparum* malaria should be treated with an artemisinin-based combination therapy (ACT)[2, 11, 15].

Artemisinin and its derivatives (artesunate, artemether, artemotil, dihydroartemisinin) are highly effective with an excellent safety profile[16]. The drugs produce rapid clearance of parasitemia and rapid resolution of symptoms but they are eliminated rapidly. When used as monotherapy, a 7-day course of treatment is required, but when given in combination with a slowly eliminated partner drug, shorter courses of treatment (3 days) are effective and will enhance patient compliance[14-16]. The choice of the partner drug depends on resistance patterns, efficacy, cost, and tolerability.

Pyronaridine

Pyronaridine is a Mannich derivative originally synthesized at the Institute of Parasitic Diseases, Chinese Academy of Preventive Medicine, China in 1970[17, 18]. It obtained marketing authorization in China in 1980 for the treatment of malaria[18]. Although the drug has proven to be safe and efficacious[19-29], pyronaridine has only been used experimentally outside China because of the failure to meet international regulatory standards[30, 31].

The chemical name of pyronaridine is 2-methoxy-7-chloro-10-[3', 5'-bis (pyrrolidino-methyl)-4'-hydroxyanilino] benzo-(b)-1, 5-naphthyridine[20] (figure 1.2). It is available as the free base and the salt form, pyronaridine tetraphosphate, containing 57% base. Solubility of pyronaridine and pyronaridine tetraphosphate was determined in several solvents including methanol, distilled water, n-octanol, ethanol and chloroform[32]. Pyronaridine base is sparingly soluble in chloroform (1.34%w/v) while it is slightly soluble in methanol (0.29%) and ethanol (0.42%) and very slightly soluble in octanol

(0.09%) and distilled water (0.02%). Pyronaridine tetraphosphate, the form which has been used in clinical treatment of malaria, occurs as an odorless hydroscopic yellow powder. It is sparingly soluble in water (1.46%) while only very slightly soluble in other solvents[18, 32]. Four pKa values were obtained for the tetraphosphate titrated which when extrapolated to the base (7.08 ± 0.05, 7.39 ± 0.07, 9.88 ± 0.05 and 10.30 ± 0.10). These findings suggest that at physiological pH, the drug gets ionized to some extent. However, log P value determination implied that the base (log P of 0.26 ± 0.02) has affinity for lipid membranes.

Pyronaridine is a blood schizontocide (acts on intraerythrocytic forms). The mechanism of action of pyronaridine is similar to chloroquine in that they both interfere with the digestive system of the parasites[33, 34]. Pyronaridine inhibits hemozoin production thereby interfering in heme detoxification and consequently poisoning the parasite. Malaria parasites digest host's hemoglobin, the major source of amino acids of parasites, in the parasite acidic food vacuole. Heme, the by-product of this parasitic digestion, is very toxic to the parasites. Thus, the parasites release hematin in large amounts in its digestive food vacuole to detoxify free heme by converting heme to harmless hemozoin (a red malaria pigment). It has been reported that Pyronaridine inhibits *in vitro* β-hematin formation, a process that closely parallels hemozoin synthesis with the same IC_{50} as chloroquine[35]. In addition, pyronaridine can enhance heme-induced lysis of human red blood cells but at about 1/100 of the concentration seen with chloquine[35].

The antimalarial activity of pyronaridine has been clearly demonstrated in both preclinical and clinical studies. Unfortunately, most of the data, especially before 1990, are either not available or published only in Chinese. A series of *in vitro* and *in vivo* studies showed that pyronaridine acted as a highly effective blood schizontocide against chloroquine-sensitive and resistant parasites, exhibited low toxicity[18-26, 29]. The drug does not appear to show cross-resistance with chloroquine[18, 23, 26, 36], although a correlation between chloroquine and pyronaridine responses was found[37-39]. In the 1970s, clinical

trials on the treatment of symptomatic malaria against both *P. falciparum* and *P. vivax* in more than 1,000 cases in China had revealed that the efficacy of pyronaridine was comparable to that of chloroquine[22, 24]. Several falciparum malaria patients who had been refractory to chloroquine treatment or had multi-drug resistance were also effectively cured[22]. All patients tolerated the therapeutic dosages of pyronaridine well. Following oral administration, the main side effects included nausea, diarrhea, slight abdominal pains, vomiting, palpitations, headache, and skin rash. Although there was local irritation with the intramuscular injection, no other adverse effects were observed when the drug was given by either intramuscular or intravenous route[23, 24]. In 1980, pyronaridine was formally released as a new antimalarial drug for use in China. The total oral dosage was 1.2 g divided into 3 or 4 doses. Two doses were given on the 1st day and the rest were given once daily on the following one or 2 days. The total dosage by intramuscular injection or intravenous drip was 0.3 g divided into 2 doses with an 8-hour interval[18].

Only a few clinical studies have been published in the international English literature. Two clinical trials in adults with uncomplicated falciparum malaria in Thailand[27] and Cameroon[28] showed that oral pyronaridine was well-tolerated and effective. In Thailand, two pyronaridine regimens, a mean total dose of 25.6 mg/kg over 3 days and 36.7 mg/kg over 5 days[27, 40], were evaluated in 101 patients. Cure rates, defined as no recrudescence during a 28-day follow-up period, for the two groups were 63% and 88% respectively. The drug was well-tolerated in both groups. In a clinical study performed in Cameroon, pyronaridine was also well-tolerated and showed 100% efficacy during a 14-day follow-up period in 40 adult patients treated with pyronaridine 32 mg/kg divided over 3 days[28]. The safety and efficacy of pyronaridine at the same dose was later confirmed in 41 Cameroonian children (5-15 years old) with acute uncomplicated falciparum malaria[41] and 22 Cameroonian patients (6-55 years old) with *P. ovale*- and *P. malariae*-infection[42].

Due to the known benefits of artemisinin-based combination therapy (ACT), currently a fixed-dose combination of pyronaridine and artesunate as a once-daily oral treatment for uncomplicated *P. falciparum* and *P. vivax* malaria is being developed. To date, over 2,900 healthy subjects and malaria patients have been exposed to this product and it has showed favorable efficacy and safety profile. A multi-objective Phase I study was completed in 2005 and two Phase II studies to assess the tolerability, safety and pharmacokinetics in adults and children[43] were completed in 2007. Four pivotal Phase III trials involving a total of 3,533 patients in 18 countries were completed in 2008. In all cases, the Phase III trials achieved their primary endpoints of non-inferiority compared with current standard of care at 28 days[44].

Up to now, there is very limited published data on pharmacokinetics of pyronaridine in humans. Pyronaridine pharmacokinetics after single I.M. and oral dosing has been studied in ten malaria Chinese patients in 1987[45]. A spectrofluorometric method was used for quantification of pyronaridine drug levels. A linear 2-compartment model was adequately fitted to the concentration-time course. It exhibited a long elimination half-life and large apparent volume of distribution indicating an extensive tissue distribution.

There was evidence that pyronaridine is not evenly distributed in rabbit blood. Blood pyronaridine concentrations are substantially higher than plasma concentrations after intramuscular injection[46, 47]. The partitioning of pyronaridine between blood cells and plasma was studied in human, dog, rat, and rabbit whole blood at the Clinical Pharmacokinetics Laboratory at College of Pharmacy, the University of Iowa (unpublished data). The partitioning ratio, defined as the concentration in blood cells divided by the concentration in plasma, varied among the species studied and different occasions studied. Humans had the average partitioning ratio in the range of 1.6 to 2.9. Since there is an uptake of the drug by blood cells and blood is the target organ, we believe blood is the preferred biological matrix for pharmacokinetic studies.

Pyronaridine is eliminated mainly by metabolism. Data from Phase I study demonstrated that the fraction eliminated unchanged in urine was about 1%. *In vitro* incubation of pyronaridine with human liver microsomes resulted in the formation of 9 metabolites[48]. None of the metabolites are known to be pharmacologically active and no clear major metabolic pathway was identified.

Pharmacometrics

Pharmacometrics can be defined as the science of developing and applying mathematical and statistical models to understand and predict a drug's pharmacokinetics and pharmacodynamics (drug models) and biomarker-outcomes behavior (disease models). In addition, these models can be linked and applied to support innovative study designs (trial models) [49-52]. A broader definition emphasizing its multidisciplinary nature has been proposed[53].

Pharmacometrics is playing a major role in drug development and therapeutics. This term first appeared in the literature in the 1980s when it tended to focus on the application of population methods, particularly population pharmacokinetics[49]. Later this discipline has been applied to different area of drug development and therapeutics as it provides critical information to support drug development and regulatory decisions[50]. The role of pharmacometrics at the US Food and Drug Administration (FDA) in making drug approval and labeling decisions from 2000 to 2006 was evaluated in two surveys[54, 55]. The results showed that the impact of pharmacometric reviews was viewed as either pivotal or supportive for at least 85% of New Drug Applications (NDAs). These surveys indicated pharmacometric reviews contribute to key regulatory decisions even though they are not pre-specified[55].

Of all different aspects of pharmacometrics, typical focus of this field has been on drug models[51]. Roles of population pharmacokinetics on drug development and regulatory decisions has been recognized by regulatory agencies as emphasized in

guidelines on population pharmacokinetics published by both US FDA[56] and European Medicines Agency (EMEA)[57].

Population Pharmacokinetics

Pharmacokinetic studies involve examining the time course of drugs or substances in the body in attempt to explain biologic processes with mathematical expressions. Traditionally, pharmacokinetic properties of a drug were derived from data collected from intensive experimentation in healthy volunteers or highly selected patients or so-called rich data-studies. However, it is not always feasible to obtain such data (extensive sampling) in relevant patient populations. Consequently, data analysis techniques that are capable of utilizing sparse data to obtain the central tendency of the pharmacokinetic information of target population are of great interest. This type of analysis or the population approach has been applied to pharmacokinetic and pharmacodynamic data analysis since the 1970s[58].

Population pharmacokinetics (PPK) can be defined as the study of the sources and correlates of variability in drug concentrations among individuals who are the target patient population receiving clinically relevant doses of a drug of interest[56, 59]. It seeks not only to understand the mean population response but it also recognizes variability as an important characteristic that should be identified and measured. Then it seeks to explain the variability by identifying patient factors, such age, weight, or disease state, to derive information about an individual which may not be obtained from each individual directly.

There are two common methods for obtaining estimates of the mean and the variability: the traditional two-stage approach and the nonlinear mixed-effects modeling approach[56]. The latter is more widely used and usually referred to as the population approach[56, 57].

The standard two-stage approach involves estimating pharmacokinetic parameters for each subject through nonlinear regression using an individual's dense concentration-

time data in the first stage. Then in the second stage, the individual parameters are then pooled to provide measures of central tendency and variability using descriptive statistics. Analysis of dependencies between parameters and covariates can also be included using classical statistical approach in this second stage. This method provides an adequate mean estimate of population characteristics, but the variance and covariance are likely to be upwardly biased[60-62].

The nonlinear mixed-effects modeling approach is a more sophisticated method and can be used to analyze data as a single-stage approach. Instead of modeling data from each individual separately, data from all individuals are modeled simultaneously. Means and different levels of variability are simultaneously obtained for all individuals. This method allows for the use of sparse data. It has become widely accepted to the extent that the term population pharmacokinetics is commonly used synonymously with nonlinear mixed effects models[56, 63]. The term mixed refers to both fixed and random effects which characterize the population mean values and their variability, respectively. Among the software programs available for the analysis of population pharmacokinetic data, NONMEM® (ICON Development Solutions, Ellicott City, MD) is perhaps the most widely used package[57, 59]. In this thesis, NONMEM was used and, therefore, the nomenclature used is relevant to NONMEM.

Population Pharmacokinetic Model Development

A brief description of the PPK model development is given below, while the details can be found elsewhere[63-65]. The PPK models are developed in three main steps: structural model development, covariate model development and model evaluation.

The structural model usually means the model that best describes the data in the absence of covariates[63]. The observed concentration-time data are described in NONMEM in terms of fixed effect parameters and random effect parameters[66]. Fixed effect parameters, referred to as θs, may include the mean values of the relevant structural

pharmacokinetic model parameters or parameters relating the structural model parameters to demographic and pathophysiological variables. Random effect parameters often include the inter-subject variability, ω^2, and the residual intrasubject variability, σ^2. To represent the underlying pharmacokinetics of a drug, selection of the compartmental (ADVAN1 to ADVAN12) model for NONMEM analysis is normally based on preliminary analysis of individual profile with extensive sampling and visual inspection of the concentration-time profiles. Model selection decisions are usually based on a number of different criteria, such as the minimum objective function value (MOFV), Aikake Information Criterion (AIC), goodness-of-fit plots, and the precision of parameter estimates.

Once the structural model is identified, covariate models are then developed. A covariate is any variable that is specific to an individual, such as demographic and pathophysiological variables[63]. How the covariate is incorporated into the structural model is dependent on the type of variable the covariate is, e.g. continuous or categorical variables, and the relationship between the covariate and the structural model parameter. Initially, significant covariates can be identified by graphic analysis, and generalized additive model (GAM) analysis[67]. Potential covariates can be further examined using a stepwise procedure in NONMEM.

After a reasonable model is developed, the performance of the model should be examined. There are various methods available to evaluate a model[56, 57, 68, 69], for example, boostrap analysis and Visual Predictive Check (VPC). Bootstrap analysis is a resampling technique that resample the observed data with replacement repeatedly to create random samples, or bootstrap data sets, and compute the sampling distribution. The bootstrap parameter estimates obtained from the final model can be used as a guide to the distribution of an underlying population. VPC plot is a plot of the 90% confidence intervals of simulated concentrations and it is plotted together with observed

concentrations. If a majority of the observed values judged by visual inspection, lies within the intervals, the final model is said to be predictive.

Thesis Overview and Research Objectives

Pyronaridine, a highly active antimalarial agent, has been used on a limited basis as a monotherapy in treating malaria in China since the 1980s. To date, there is very limited published data on the pharmacokinetics of pyronaridine in humans. The present studies provide a basic description of the pharmacokinetics of pyronaridine, and is the first PPK analysis of pyronaridine in the literature.

The overall objectives of this thesis are to investigate the pharmacokinetic properties of pyronaridine in healthy subjects as well as malaria patients using a nonlinear mixed-effect modeling approach and to evaluate the effect of clinical covariates and other related factors on the pharmacokinetics of pyronaridine. The data were obtained from 7 clinical trials of an oral product containing pyronaridine/artesunate in a fixed combination in the ratio of 3:1 (Pyramax®). The thesis is organized in six chapters and each chapter stands on its own. Chapter II presents the PPK analysis of pyronaridine in healthy subjects participating in a multi-objective Phase I study in Korea (SP-C-001-03). Chapter III and IV focus on the PPKs of pyronaridine in adult and pediatric malaria patients, respectively, participating in two Phase II(SP-C-002-05[43], SP-C-003-05) and four Phase III (SP-C-004-06, SP-C-005-06[70], SP-C-006-06 and SP-C-007-07) clinical studies in Asia and Africa. Chapter V provides comparisons of PPKs of pyronaridine in each population and the last chapter provides a brief summary of the findings. NONMEM control files and output summary are included in the appendices.

Figure 1.1 The Life Cycle of Malaria[71, 72]

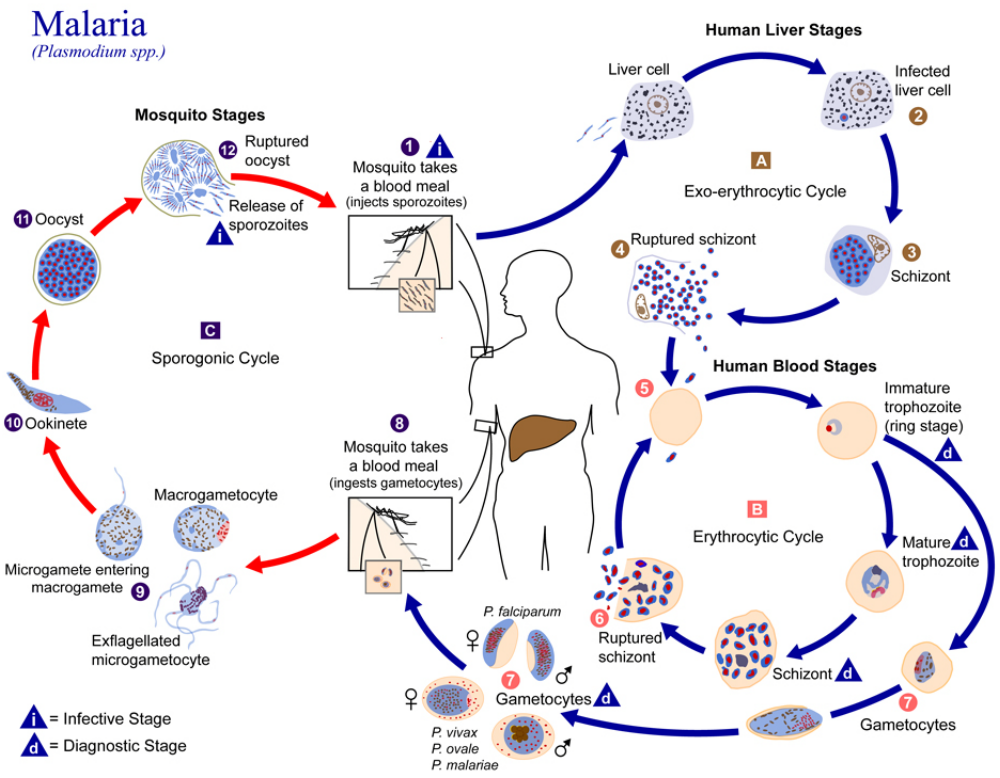

Note: The malaria parasite life cycle involves two hosts. During a blood meal, a malaria-infected female Anopheles mosquito inoculates sporozoites into the human host ❶. Sporozoites infect liver cells ❷and mature into schizonts ❸, which rupture and release merozoites ❹. (Of note, in P. vivax and P. ovale a dormant stage [hypnozoites] can persist in the liver and cause relapses by invading the bloodstream weeks, or even years later.) After this initial replication in the liver (exo-erythrocytic schizogony A), the parasites undergo asexual multiplication in the erythrocytes (erythrocytic schizogony B). Merozoites infect red blood cells ❺. The ring stage trophozoites mature into schizonts, which rupture releasing merozoites ❻. Some parasites differentiate into sexual erythrocytic stages (gametocytes) ❼. Blood stage parasites are responsible for the clinical manifestations of the disease. The gametocytes, male (microgametocytes) and female (macrogametocytes), are ingested by an Anopheles mosquito during a blood meal ❽. The parasites' multiplication in the mosquito is known as the sporogonic cycle C. While in the mosquito's stomach, the microgametes penetrate the macrogametes generating zygotes ❾. The zygotes in turn become motile and elongated (ookinetes) ❿ which invade the midgut wall of the mosquito where they develop into oocysts ⓫. The oocysts grow, rupture, and release sporozoites ⓬, which make their way to the mosquito's salivary glands. Inoculation of the sporozoites ❶into a new human host perpetuates the malaria life cycle.

Figure 1.2 Chemical structure of pyronaridine tetraphosphate (2-methoxy-7-chloro-10-[3',5'-bis-(pyrolidinyl-1-methyl) -4'-hydroxyanilinol]benzo[b] - 1,5-naphthyridines)

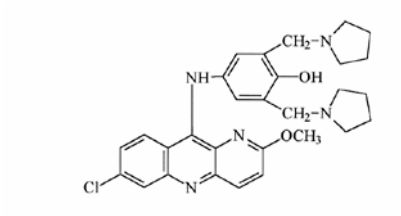

$4H_3PO_4$

$C_{29}H_{32}N_5O_2Cl \cdot 4H_3PO_4$ MW 910.04

CHAPTER II

POPULATION PHARMACOKINETICS OF PYRONARIDINE IN HEALTHY SUBJECTS

Introduction

Artemisinin-based combination therapy (ACT) is recommended by the World Health Organization to minimize the emergence and spread of antimalarial resistance[2]. Combining an artemisinin drug with a long half-life partner drug improves the efficacy, allows for short treatment courses and also reduces the likelihood of the resistance. Pyronaridine is a promising partner drug in artemisin-base combination therapies[43, 73]. Currently an oral fixed-dose combination product containing Pyronaridine tetraphosphate and Artesunate (PA) is being developed, as a 3-day treatment for uncomplicated *P. falciparum* and *P. vivax* malaria. To date, over 2,900 healthy subjects and patients with malaria have been exposed to PA combination and it has showed a favorable efficacy profile with only minor or moderate adverse events reported[43, 74].

Pyronaridine is a Mannich base anti-malarial drug synthesized in China in 1970[17, 18]. Pyronaridine monotherapy has been shown to be well tolerated and effective against both *Plasmodium falciparum* and *Plasmodium vivax* in adult and pediatric patients in chloroquine resistant areas[22, 23, 27, 28, 41]. It is effective against the erythrocytic stage of several species of malaria parasites[25, 29, 75]. The mechanism of action is similar to chloroquine, as it inhibits β-hematin formation, disrupting hematin detoxification in malaria parasites[35]. Although it has been used in eastern Asia for many years, to date there is very limited published data on pharmacokinetics of pyronaridine in humans. Pyronaridine pharmacokinetics after single IM and oral dosing has been studied in ten Chinese patients in 1987[45]. The concentration-time course was adequately fitted to a linear 2-compartment model. It exhibited a long elimination half-life and large apparent volume distribution indicating an extensive tissue distribution. Pyronaridine is

concentrated in red blood cells[46, 47]. The partitioning of pyronaridine between blood cells and plasma was studied in different species at the Clinical Pharmacokinetics Laboratory at College of Pharmacy, the University of Iowa (unpublished data). The partition ratio varied among the species and occasions. In humans, the concentration of pyronaridine in blood cells is approximately 1.6 to 2.9 times higher than in plasma. Pyronaridine is eliminated primarily by metabolism. The fraction eliminated unchanged in urine was about 1% (unpublished data). *In vitro* incubation of pyronaridine with human liver microsomes resulted in the formation of 9 inactive metabolites[48]. However, no clear major metabolic pathway was identified.

Recently an oral fixed-dose PA combination product has completed Phase III trials. In order to analyze sparse data from Phase III clinical trials, it is useful to have preliminary knowledge of the pharmacokinetic behavior of pyronaridine. Given the extensive concentration-time profiles over a wide dose range available from a four-part Phase I study, it is of interest to develop a population pharmacokinetic (PPK) model to characterize pyronaridine pharmacokinetics and its variability. Therefore, in this study, we present for the first time the PPKs of pyronaridine on full-profile sampling data from fasting healthy Korean subjects who participated in a four-part Phase I study conducted in series to assess the safety, tolerability and pharmacokinetics of orally administered PA. The effects of available clinical covariates on pharmacokinetic variability are also investigated.

Materials and Methods

Data from a four-part Phase I clinical study to assess the safety, tolerability and pharmacokinetics of the combination of orally administered PA in healthy Korean subjects were pooled for this population pharmacokinetic analysis. The study was conducted at the Clinical Trial Centre of Seoul National University, Seoul, Korea in accordance with the Guidelines of Good Clinical Practice and the Declaration of

Helsinki. The protocol was reviewed and approved by the Institutional Review Board of Seoul National University. Written informed consent was obtained from all subjects prior to their participation.

Subjects

Subjects were healthy adult Korean men and women who met the following criteria: age, 19 to 40 years, weight, 50 to 70 kg with a body mass index of 18-28 kg/m^2, no abnormalities on the basis of a physical examination, electrocardiogram (ECG) and thorough review of medical history and clinical laboratory results (complete blood count, routine kidney and liver function tests), abstinence from caffeine, grapefruit and alcohol-containing products from 72 hours before dosing through the duration of study. Volunteers were excluded if they were smokers (>10 cigarettes per day), had positive results on screening for alcohol abuse, had taken certain over-the-counter medications or herbal medicines within 2 weeks before study, had used any of the known inhibitors (e.g., ketoconazole) or inducers (e.g., rifampicin) of drug metabolism within one month before the study start, had undergone gastric surgery, or any surgical procedure that might interfere with gastrointestinal absorption. Pregnant and breastfeeding women were excluded from the study.

Study Design

Part 1 was a double blind, randomized, parallel, placebo-controlled, single ascending dose study to evaluate safety, tolerability and pharmacokinetics of PA after single dose administration at following doses: PA 6+2 mg/kg (pyronaridine tetraphosphate 6 mg/kg + artesunate 2 mg/kg), PA 9+3 mg/kg, PA 12+4 mg/kg or PA 15+5 mg/kg. At each dose level, nine subjects were enrolled with seven receiving the study drug and two receiving placebo.

Part II was a 2-cohort, parallel, 2-period, randomized crossover study of a single oral dose of PA vs. each of the individual drugs at the same dose to investigate the

potential drug interaction between pyronaridine and artesunate. Twenty participants were randomly assigned into two cohorts to compare PA with pyronaridine (cohort 1), or PA with artesunate (cohort 2). The two study periods were separated by a 21-day washout interval.

Part III was conducted to explore the effect of food on the pharmacokinetics of PA. The study design was a 2-period, randomized, single oral dose fasted vs. fed crossover study. Of the 20 subjects enrolled into the study, 10 were randomly assigned to each of the fasted or the fed arms of the study. The test meal was a standard high-fat and high calorie breakfast. There was a washout period of 21 days between the two periods.

Part IV aimed to evaluate safety, tolerability and pharmacokinetics of PA after multiple dose administration. The study design was the same as Part I except that subjects received PA once daily for three consecutive days and at each dose level, eight subjects were enrolled with six receiving the study drug and two receiving placebo.

Table 2.1 summarizes the study designs and sampling times for the four-part Phase I study. All study drugs and placebos were provided by Shin Poong Pharmaceuticals (Seoul, Korea). Study drug was given with approximately 240 mL of water to each subject, under supervision, after an overnight fast. No food intake was allowed up to 4 hours post-dose except fed arm of the food interaction study (Part 3). It is worth mentioning that results from non-compartmental analysis showed that mean pyronaridine $AUC_{0-\infty}$ values were 20% greater when given with high fat food as compared to fasting. To obtain more reliable and precise parameter estimates, only pharmacokinetic data after the study drug was given at fasting condition were included in this analysis.

Determination of Blood Pyronaridine Concentrations

Whole blood samples were collected at intervals for pyronaridine bioanalysis (Table 2.1) and were stored frozen at -80°C until analyzed. Pyronaridine concentrations

in blood were determined using validated high performance liquid chromatography, as previously described[47]. Briefly, blood sample of 0.5 mL was spiked with 200 ng of amodiaquine, an internal standard. A 1.25 mL of 500 mM Sodium Phosphate Tribasic dodecahydrate buffer (pH = 10.3) was added to the blood and mixed briefly on a vortex mixer, and followed by the addition 8 mL of diethyl ether. The mixture was homogenized on rugged rotor mixer for 15 minutes, and then centrifuged for 10 min (2500 rpm). The organic layer was transferred to a new glass test tube and then dried in an evaporator (N-Vap Berlin, MA, USA) under a flow of nitrogen at room temperature. The dried sample was then dissolved in 100 µL of solution containing acetonitrile–0.02 M KH_2PO_4 (27:73, v/v). A 50-µl aliquot was injected onto the chromatographic system.

The calibration curves were linear over concentrations ranging from 5.7 (the lower limit of quantitation) to 855 ng/mL. Samples with a concentration higher than 855 ng/mL were diluted so that the concentration fell within the range of the calibration curve. The coefficient of variation for intra-day and inter-day precision ranged from 3.0 to 5.9% and 5.0 to 10.0%, respectively.

Population Pharmacokinetic Analysis

Structural Model

The population pharmacokinetic analyses were performed using NONMEM® version VI level 2.0 (Icon development solutions, Ellicott city, MD)[76]. The compiler was Intel Fortran Complier v10.2 (Intel Corporation, Santa Clara, CA) with 2.82 GHz Intel Pentium III Xeon running Microsoft Windows XP Professional x64 Edition (Microsoft Corporation, Seattle, WA). NONMEM output was processed using PDx-Pop 3.10 (ICON Development Solutions, Ellicott City, MD) and Xpose version 4.0 (Uppsala University, Uppsala, Sweden)[77]. Graphical plots were produced using S-PLUS version 8.0 (Insightful Inc, Seattle, WA) and R 2.8.1 (Free Software Foundation, Boston, MA).

Both untransformed and log-transformed blood pyronaridine concentrations were analyzed and compared. Concentration measurements below the lower limit of quantitation were treated as missing and were excluded from the dataset. Based on the exploratory data analysis, two- and three- compartment models with different absorption models were fitted to pyronaridine data of all subjects to determine the best structural model. The first-order conditional estimation (FOCE) methods with and without interaction were tested for parameter estimation. The models were parameterised in terms of clearances and distribution volumes using the PREDPP subroutine supplied in NONMEM. Inter-subject variability (ISV) of the pharmacokinetic parameters was modeled assuming a log-normal distribution, as follow:

$$\theta_i = \theta_{TV} \bullet \exp(\eta_i)$$

where θ_i is the estimated parameter value for individual i, θ_{TV} represents the population's typical value for the corresponding parameter and η_i is the deviation of θ_i from θ_{TV}. The η random effects were assumed to be independent and symmetrically distributed with zero mean and variance ω^2, which represents the ISV of the parameter. The magnitude of ISV was expressed as coefficient of variation (%CV). An additive error model, a proportional error model and a combined proportional-additive error model were tested to explain the residual variability (RV) of untransformed data. For the log-transformed predictions, RV was described with an additive error model as follows:

$$\ln C_{ij} = \ln C_{pred,ij} + \varepsilon_{ij}$$

where C_{ij} and $C_{pred,ij}$ represent the jth observed and model predicted concentrations, respectively, for individual i and ε_{ij} denotes the additive residual random error for individual i and observation j. The ε random effects were assumed to be independent and symmetrically distributed with mean of zero and variance σ^2.

Model selection decisions were based on a number of different criteria, including minimum objective function value (MOFV) generated by NONMEM, Akaike's

Information criterion (AIC), condition number, visual examination of index plots, the precision of the parameter estimates (%RSE) and the reductions in both ISV and RV.

Covariate model

Once the base model was identified, the possible influence of the subject-specific covariates on the estimated pharmacokinetic parameters was assessed. Correlations between tested covariates were examined by graphical analysis. Categorical covariates included in the analysis were sex (female or male) and co-administration of artesunate (PA combination or pyronaridine monotherapy). The available continuous covariates were age, body weight (WT), height (HT), lean body weight (LBW), and body mass index (BMI). LBW and BMI were calculated as follows.

$$Females: \quad LBW\ (kg) = 1.07\ \cdot WT(kg) - \frac{148 \cdot WT^2(kg^2)}{HT^2(cm^2)}$$

$$Males: \quad LBW\ (kg) = 1.10\ \cdot WT(kg) - \frac{128 \cdot WT^2(kg^2)}{HT^2(cm^2)}$$

$$BMI\ (kg/m^2) = \frac{WT(kg)}{HT^2(m^2)}$$

Model building process was guided by physiologic plausibility, the generalized additive model (GAM) as implemented in Xpose[67] and graphic explorations. Plots of the individual empirical Bayes estimates of the parameters versus covariates were generated to visualize potential relationships. Covariate selection was performed by a stepwise forward addition and backward deletion procedure using NONMEM. All continuous covariates were scaled or centered with the median values so that the population estimates represent those of an average patient and were tested using linear, power, and exponential functions as illustrated in the following equations.

$\theta_i = \theta_{TV} + \theta_F \bullet (COV - COVmedian)$, for linear function;

$\theta_i = \theta_{TV} \bullet (COV/COVmedian)^{\theta_F}$, for power function;

$\theta_i = \theta_{TV} \bullet EXP(\theta_F \bullet (COV - COVmedian))$, for exponential function;

where θ_i is the estimated parameter value for individual i, θ_{TV} represents the typical value for the parameter of an individual with median value of the covariate (COV=COV_{median}), and θ_F is a factor describing the influence of the covariate (COV) expressed as deviation per unit of the covariate from the median value (COV_{median}) of the study population. The influences of binary covariates on the parameter were modeled using an additive relationship, as follows:

$$\theta_i = \theta_{TV} + \theta_F \bullet COV ;$$

where θ_{TV} represents the parameter value for subjects with the categorical covariate coded as 0, and θ_F is the additional change in the parameter in subjects with the categorical covariate coded as 1.

Model discrimination was based on the improvement of the minimum objective function values (MOFVs), a statistic that is proportional to minus twice the log likelihood of the data. In the case of hierarchical models, the change in the MOFV produced by the inclusion of a parameter is asymptotically distributed as chi-square, with the number of degrees of freedom equal to one or the number of parameter added to the model. In forward addition step, a decrease in the MOFV of 3.84 was considered statistically significant (p-value < 0.05) for addition of one parameter to a candidate model. The stepwise addition of covariates into the model continued until all significant covariates were incorporated in the model. In backward elimination step, each covariate in the fully parameterized model was removed, one at a time. The covariate remained in the final model if its removal resulted in an increase in MOFV of at least 10.83, corresponding to a p-value of 0.001. A more stringent criterion is used in this step to avoid any possible false-positives. The process was repeated until all remaining covariates in the model are significant.

Once the final model was identified, one hundred concentration-time profiles were then simulated for each dose level of pyronaridine to visualize the profiles in a 70-kg subject.

Model evaluation

One thousand bootstrap datasets was generated by repeated random sampling with replacement from the NONMEM input data file, and the final NONMEM model was fitted to the bootstrap datasets. The mean and 95% confidence intervals for the PPK parameters was derived, and compared with the estimates from the original dataset to evaluate the stability of the model. The bootstrap 95% confidence interval was calculated based on the percentile of the empirical distribution of the estimated parameters from the bootstrap runs.

The predictive performance of the final model was assessed by a visual predictive check. One thousand observations at each sampling point were simulated from the final model. The median and the 5^{th} and 95^{th} quintiles were calculated from all simulated concentrations. All measured pyronaridine concentrations were then compared with the corresponding 90% prediction intervals.

Additionally, the condition number was also used to ascertain stability of parameter estimates. The condition number is calculated as the ratio of the highest Eigen value to the lowest Eigen value from the covariance matrix. A condition number of greater than 1000 is evidence of ill-conditioning.

Non-compartmental analysis

The pharmacokinetic parameters estimated from population modeling were compared with those calculated from a non-compartmental analysis (NCA) using WinNonlin Professional Version 5.0 (Pharsight Corporation, Mountain View, CA, USA). The following pharmacokinetic parameters of pyronaridine from 76 single-dose concentration-time profiles at fasted condition were estimated by NCA: elimination half-

life ($T_{1/2\,\beta}$); area under the curve ($AUC_{0-\infty}$); apparent total volume of distribution (V/F); oral clearance (CL/F), where F is a bioavailability.

In order to compare the results from the final PPK model with NCA, $T_{1/2\,\beta}$, $AUC_{0-\infty}$ and V/F were derived from the final parameter estimates by the following equations:

$$T_{1/2\,\beta} = \frac{Ln(2)}{\beta}\,;\ \beta = \frac{1}{2}\left[k_{12} + k_{21} + k_{10} - \sqrt{(k_{12} + k_{21} + k_{10})^2 - 4k_{21} \cdot k_{10}}\right]$$

$$AUC_{0-\infty} = F \bullet Dose/CL$$

$$V/F = V2/F + V3/F$$

Results

Data of 91 participating subjects (54 males) with a median age of 23 years and a median weight of 61.5 kg receiving PA under fasting conditions were pooled for the analysis. Demographic and pertinent clinical data of subjects were shown in Table 2.2. Of a total of 1,967 pyronaridine concentration measurements, 33 measurements (1.7% of total samples) were below lower limit of quantitation and were not included in the analysis. Seventy-three percent of the available data (1,406-of-1,934 observation records) were from single dose studies (Part I to III). The pyronaridine blood concentration versus time for each dose level in Part I study is shown in Figure 2.1. Based on graphical inspection of the concentration-time profile showing multiphasic disposition, 2- and 3-compartment pharmacokinetic models were evaluated. There was clear evidence that modeling the log-transformed data was better than untransformed data by visual inspection of diagnostic plots. Therefore, all blood pyronaridine concentrations were transformed into their natural logarithms before the analysis.

The data was best described by the 2-compartment model with first-order absorption and elimination from central compartment as implemented in NONMEM using its ADVAN4 TRAN4 subroutine. The analysis was performed using the first-order

conditional estimation with interaction (FOCEi) method for parameter estimation. The estimated structural model parameters included absorption rate constant (Ka), apparent central volume of distribution (V2/F), apparent peripheral volume of distribution (V3/F), oral clearance (CL/F) and inter-compartmental clearance (Q/F) where F is oral bioavailability. The data did not support ISV on V3/F as shown by poor precision of the parameter estimates and removing this term did not significantly increase either the MOFV or AIC (5.00, 3.01 respectively). The 3-compartment models were not supported by the data as evidenced by either inability to converge successfully or model instability (condition number > 1,000).

During graphic inspection, we found that females were significantly smaller than males. Since many physiologic parameters, such as blood flow or organ size, are dependent of WT, sex was not considered further during the development of the covariate model. The GAM analysis indicated that none of the tested covariates had significant effect on Ka. All candidate covariates were selected by a stepwise procedure using NONMEM. After the stepwise forward addition, two covariates retained in the fully parameterized model included LBW on V2/F and AGE on CL/F. Following the stepwise forward addition, the stepwise backward deletion was done to refine the model. Through this process, none of the two covariates was significant enough to remain in the final model. Co-administration of artesunate did not show significant effect on any of pharmacokinetics of pyronaridine.

The population pharmacokinetic parameters were estimated with a high degree of precision as listed in Table 2.3. The relative standard errors (% RSEs) of estimation for the pharmacokinetic parameters were with a range from 4.3% to 10.1%. The estimates for ISV were associated with a higher degree of uncertainty (20.2% to 41.5%). The ISV for Ka, V2/F, CL/F and Q were 53.9%, 24.3, 45.1% and 30.9%, respectively. Table 2.4 summarizes the pharmacokinetic parameters of 76 single-dose concentration-time profiles at fasted condition determined by noncompartmental analysis. Mean parameter

estimated or derived from PPK model (CL/F, V/F, $T_{½\beta}$ and AUC) were comparable with those calculated by non-compartmental analysis as presented in Table 2.5.

The diagnostic plots of the model are also shown in Figure 2.2. In general, the plots showed an acceptable fit of the model to the observed data. The upper left and right panels show the plots between the population-predicted (PRED) and individual-predicted concentrations (IPRED) versus observed pyronaridine concentrations, respectively. A good correlation in the plots was evidenced, suggesting that the resulting model fits the observed data well. The lower panels are the conditional weighted residual (CWRES) plots. The distribution of CWRES values for model-predicted concentrations was around zero and relatively symmetric across the range of both the predicted concentrations and time after administration, although peak concentrations in relatively few individuals were overestimated. Figure 2.3 illustrates the good fit for the final model to data from six randomly selected individual subjects representative of the population for each part of the study. The final parameter estimates and their variance were used to simulate pyronaridine concentrations after once-daily administration for three days. Figure 2.4 shows the median values of 100 simulated profiles corresponded to the oral doses of pyronaridine tetraphosphate of 6, 9, 12, and 15 mg/kg in 70-kg subjects. The median concentrations at day 21 for each dose were 10.1, 15.2, 20.2 and 25.3 ng/mL, respectively.

The results of the bootstrap analysis are listed in Table 2.3. The mean parameter estimates resulting from the bootstrap analysis were very similar to the population estimates of the final model. The final population estimates were within the 95% confidence intervals obtained by 1,000 bootstrap runs. These results indicate that the model was stable and robust. Figure 2.5 shows the results of the visual predictive check for each part of the study. The final model adequately described the observed concentrations. Overall, 11.88% of the pyronaridine observations were not contained within the 90% prediction interval.

Discussion

Based on the noncompartmental analysis of each part of the study, there was a linear and dose-proportional relationship between Cmax and $AUC_{0-\infty}$ of pyronaridine with increasing pyronaridine tetraphosphate dose over the 6 – 15 mg/kg dose range. There were no significant differences in the pharmacokinetics of pyronaridine when it was administered alone or in combination with artesunate. The mean pyronaridine Cmax and $AUC_{0-\infty}$ values were higher when administered with high fat breakfasts (17.7% and 20.4%, respectively), compared to fasting. Initially we attempted to analyze all available data but excluding the pharmacokinetic profiles of pyronaridine under fed conditions resulted in less complex models providing more reliable and precise parameter estimates. Since a majority of the data was from fasting subjects and it is not very common for malaria patients to have high-fat meals, we decided to exclude the profiles under fed conditions.

In the current PPK analyses, a total of 1,934 observations from 100 concentration-time profiles were included. After oral administration under fasting conditions, pyronaridine was absorbed with an average absorption half-life of one hour with moderately high degree of variability (ISV of 54%). This study confirms that pyronaridine exhibits a large total apparent volume of distribution (V/F = 85 L/kg), which is similar to that reported by Feng et al[45]. In their study, mean apparent volume of distribution of pyronaridine after 4 Chinese patients were given a single dose (204 mg) I.M. was 71.5 L/kg. This large apparent volume of distribution indicates that pyronaridine is extensively distributed to peripheral tissues. The mean pyronaridine elimination half-life derived from the final PPK model was 8.4 days, which is much longer reported previously by Feng et al[45] (2.6 days). However, in their study, pyronaridine levels were measured only up to 3 days after dosing using a spectrofluorometric method, so the shorter elimination half-life is not unexpected. The half-life of 8.4 days might still be underestimated since no samples were collected beyond 10 days after dosing.

Covariates including age, sex, WT, HT, LBW, BMI and co-administration with artesunate were assessed in this analysis. Although the full model indicated that subjects with higher LBW tended to have a greater V2/F and older subjects tended to have higher CL/F, none of the tested covariates were significant enough to remain in the model. However, these results must be interpreted in a context of relatively narrow range of characteristics of the healthy subjects examined in the Phase I studies.

Kurth et al[29] assessed the *in vitro* activity of pyronaridine against clinical isolates of *P. falciparum* from Gabon. A geometric mean cut-off concentration of 9.3 nM (or 4.8 ng/mL) and fifty percent effective concentration (EC_{50}) of 1.9 nM (or 1.0 ng/mL) were reported. This EC_{50} is similar to results from previous studies with laboratory strains and field isolates obtained by a different drug sensitivity assay (values between 2.2 and 3.8nM)[73, 78, 79]. Our simulation showed that pyronaridine concentrations from the studied doses would remain above the EC_{50} for at least 21 days after first dose administation. The long duration at which concentrations remain above EC_{50} suggests prolonged activity after dosing.

The final model was internally evaluated by nonparametric bootstrapping and showed good robustness. The results from randomly selected combinations of data were very similar to those estimated with the original data set. In addition, the predictive check indicated that the model was appropriate by the symmetrical distribution of the raw data around the median. An overall of 11.88% of the observations were outside the 90% prediction interval. Although there was a tendency of slight under-estimation observed in peak concentration range, the pharmacokinetic parameters of pyronaridine were estimated with high degree of precision and consistent with noncompartmental analysis.

In conclusion, this study is the first population pharmacokinetics analysis of pyronaridine, the promising antimalarial agent. The pharmacokinetics of pyronaridine in healthy adult Korean subjects was best characterized with a two-compartment model with first-order absorption and elimination. None of the tested covariates were identified as

important covariates for the drug's pharmacokinetics, most likely because the population was relatively homogenous. The pharmacokinetic parameters of pyronaridine were estimated with high degree of precision and consistent with noncompartmental analysis. The final model was found to be stable and robust with acceptable predictive power. This analysis will serve as a comparison to future works in malaria patients.

Table 2.1 Study design and data characteristics

	Part 1 Single ascending dose	Part 2 Drug Interaction	Part 3 Food Interaction	Part 4 Multiple ascending dose
Study Design	A single ascending dose, randomized, double-blind placebo-controlled study	A randomized, blinded, crossover study of a single dose of PA vs. each of the individual drugs	A 2-period, randomized, single oral dose of PA fasted vs. fed crossover study	A multiple ascending dose, randomized, double-blind placebo-controlled study
Study Drug*	PA 6+2, PA 9+3, PA 12+4, or PA 15+5	Cohort 1 PA 12+4 vs. PP 12 Cohort 2 PA 12+4 vs. AS 4	PA 12+4	PA 6+2, PA 9+3, PA 12+4, or PA 15+5
PP* dose	6, 9, 12, or 15 mg/kg Single dose	12 mg/kg Single dose	12 mg/kg Single dose	6, 9, 12,or 15 mg/kg Multiple dose (once daily for 3 days)
Sampling Times	Predose, 20, 40, 60, 80, 100 minutes, 2, 2.5, 3, 4, 5, 8, 12, 24, 48, 72, 120, 168 and 240 hours after dosing.	Same as part 1.	Same as part 1.	Immediately before each dose, and, 20, 40, 60, 80, 100 minutes, 2, 2.5, 3, 4, 5, 8, 12, 24, 48, 72, 120, 168 and 240 hours after the third dose.
Number of Subjects	28	20	19[¥]	24
Number of concentration-time profiles	28	29	19	24
Number of observations	512	541	353	528

* PA 6+2 = Pyronaridine tetraphosphate (PP) 6 mg/kg + Artesunate (AS) 2 mg/kg; PA 9+3 = PP 9 mg/kg + AS 3 mg/kg; PA 12+4 = PP 12 mg/kg + AS 4 mg/kg; PA 15+5 = PP 15 mg/kg + AS 5 mg/kg.

[¥] One subject has only fed profile and, therefore, was not included in the analysis.

Table 2.2 Demographic and clinical data of participating subjects

Characteristics	Mean (SD)	Median (Range)
Age (years)	23.3 (3.2)	23.0 (19-40)
Weight (kg)	60.8 (6.3)	61.5 (50.1-70.0)
Lean Body Weight (kg)	48.7 (6.3)	50.2 (37.9-57.4)
Height (cm)	169.4 (7.5)	171.0 (154.0-183.0)
Body Mass Index (kg/m^2)	21.1 (1.4)	21.1 (18.1-23.8)
Sex	Count	Percent
Male	54	59.4
Female	37	40.6

Table 2.3 Pharmacokinetics of pyronaridine estimated by the final population model and results of bootstrap analysis

Parameter	Estimate (%RSE)		Bootstrap estimate (95% CI)
Ka (d^{-1})	15.4 (10.1)		15.3 (12.3 – 18.1)
V2/F (L)	738 (5.9)		723 (639 – 796)
V3/F (L)	4390 (8.0)		4366 (3840 – 5170)
CL/F (L/d)	614 (4.3)		615 (558 – 670)
Q/F (L/d)	1270 (5.2)		1276 (1140 – 1440)
ISV		ISV (%CV)	
ISV -Ka	0.291 (20.2)	53.9	0.277 (0.173 – 0.393)
ISV –V2/F	0.059 (41.5)	24.3	0.048 (0.019 – 0.084)
ISV -CL/F	0.203 (22.4)	45.1	0.174 (0.099 – 0.259)
ISV -Q/F	0.096 (37.2)	30.9	0.111 (0.034 – 0.253)
RV (additive error)	0.150 (10.7)		0.147 (0.117 – 0.180)
Derived parameters (mean $\pm$ SD)			
$T_{½\alpha}$ (d)	0.25 $\pm$ 0.04		
$T_{½\beta}$ (d)	8.40 $\pm$ 2.63		

Note: Ka first-order absorption rate constant, V2 central volume of distribution, V3 peripheral volume of distribution, CL clearance, Q intercompartmental clearance, F oral bioavailability, ISV inter-subject variability, RV residual variability, $T_{½\alpha}$ distribution half-life, $T_{½\beta}$ elimination half-life, %RSE relative standard error [(SE/mean)x100%], %CV coefficient of variation [(SD/ESTIMATE)x100%].

Table 2.4 Pharmacokinetics of pyronaridine from single-dose profiles at fasting condition as determined by noncompartmental analysis (mean ± SD).

Study Drug	n	Half-life (hr)	Cmax (ng/mL)	Tmax (hr)	CL/F (L/hr/kg)	V/F (L/kg)	$AUC_{0-\infty}$ (ng-hr/mL)
Part 1Single dose study							
- PA 6+2	7	393 ± 252¥	186 ± 85	2.2 ± 1.6	0.50 ± 0.22¥	227 ± 68¥	8713 ± 5920¥
- PA 9+3	7	188 ± 109	262 ± 85	2.1 ± 1.3	0.77 ± 0.41	177 ± 57	7667 ± 2482
- PA 12+4	7	150 ± 36	467 ± 217	1.6 ± 0.3	0.60 ± 0.20	130 ± 56	12430 ± 4087
- PA 15+5	7	168 ± 48	792 ± 321	4.8 ± 4.5	0.43 ± 0.12	103 ± 57	20841 ± 4839
Part 2 Drug Interaction							
- PA 12+4	19	185 ± 70	616 ± 178	3.0 ± 2.7	0.36 ± 0.13	87 ± 22	22127 ± 11410
- PP 12	10	196 ± 142	662 ± 130	3.5 ± 3.2	0.30 ± 0.12	133 ± 55	25204 ± 8346
Part 3 Food Interaction							
- PA 12+4 Fasting	19	205 ± 122§	483 ± 134	4.4 ± 3.1	0.40 ± 0.17§	106 ± 40§	19947 ± 7444§

* PA 6+2 = Pyronaridine tetraphosphate (PP) 6 mg/kg + Artesunate (AS) 2 mg/kg; PA 9+3 = PP 9 mg/kg + AS 3 mg/kg; PA 12+4 = PP 12 mg/kg + AS 4 mg/kg; PA 15+5 = PP 15 mg/kg + AS 5 mg/kg.

¥ n=4 because three subjects had measureable concentrations up to only 3 days.

§ n=18 because one subjects had measureable concentrations up to only 3 days.

Table 2.5 Pharmacokinetics of pyronaridine derived from the final model parameter estimates compared with those calculated from non-compartmental analysis (mean ± SD)

	Population Analysis	Non-compartmental Analysis
CL/F (L/hr/kg)	0.47 ± 0.24	0.46 ± 0.27
V/F (L/kg)	85 ± 9	112 ± 55
$T_{½\beta}$ (d)	8.4 ± 2.6	8.3 ± 4.9
$AUC_{0-\infty}$ (ng-hr/mL)	16086 ± 7520	18937 ± 9574

Figure 2.1 Observed pyronaridine (PYR) concentration-time profiles after single ascending oral doses of pyronaridine tetraphosphate (PP) and artesunate combination.

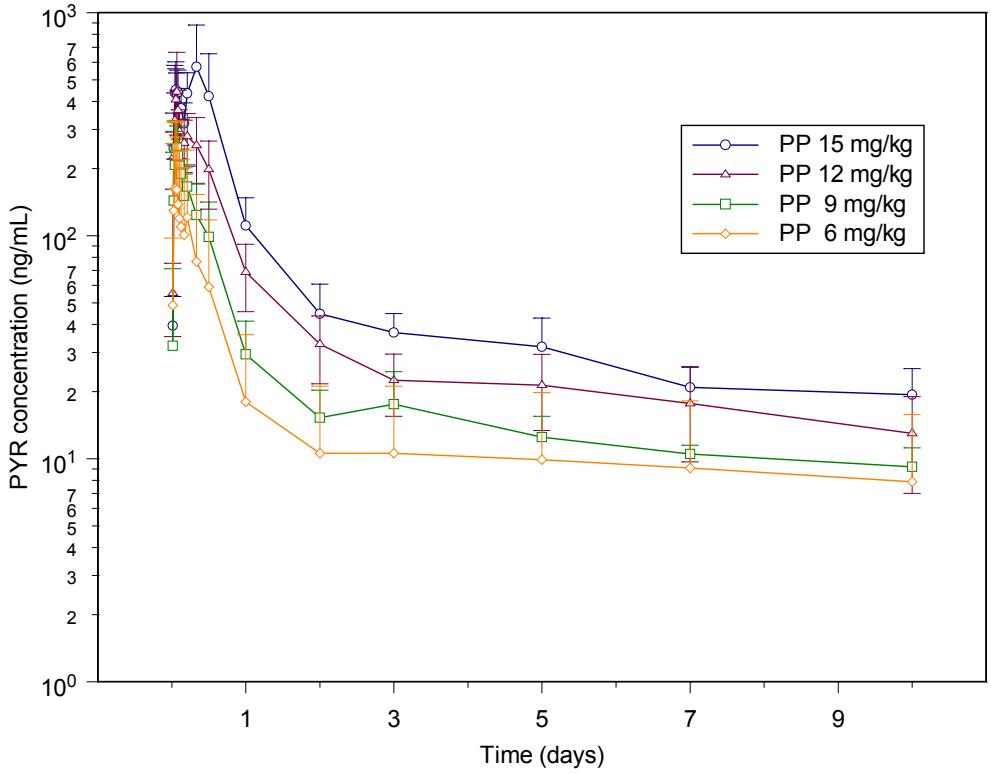

Figure 2.2 Goodness of fit plots of pyronaridine for the final model.
The upper left and right panels show population and individual predicted concentration versus observed concentration. The solid lines are lines of identity. The lower panels are the conditional weighted residual plots for the final model.

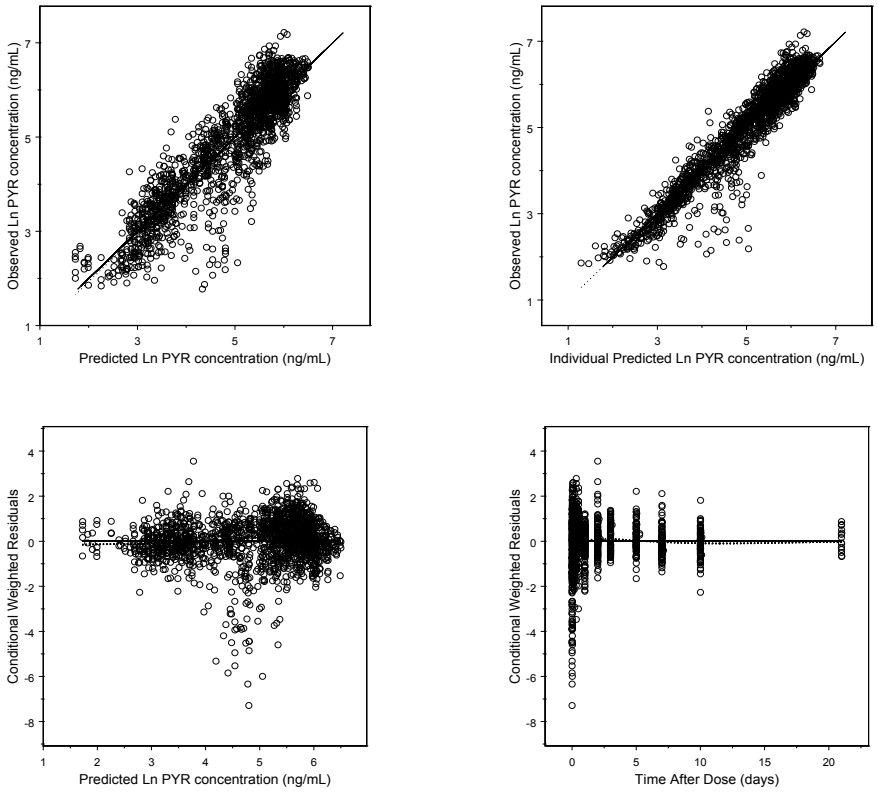

Figure 2.3 Observed and predicted blood pyronaridine concentration-time profiles for 6 randomly selected subjects

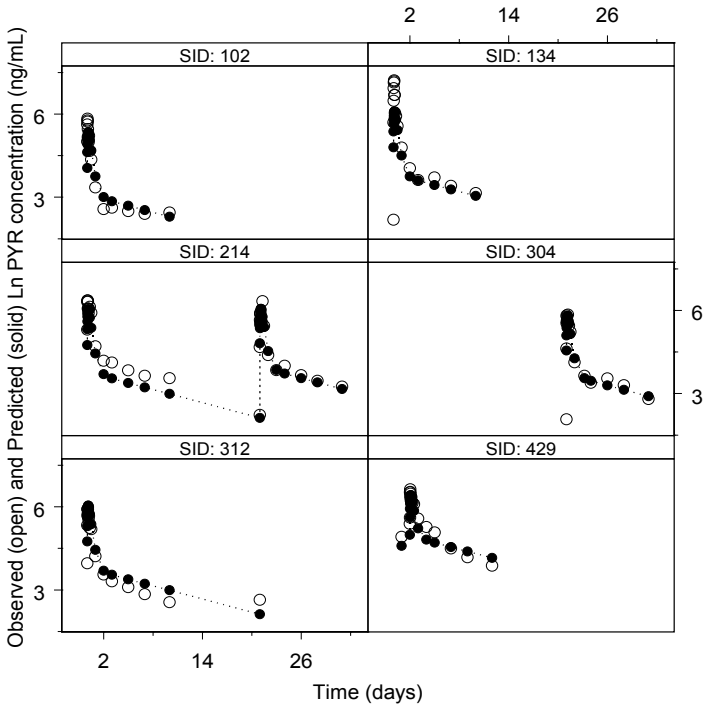

Figure 2.4 Simulated concentration-time profiles for a 3-dose regimen from the final model. The lines represent the median values of 100 simulated profiles of 70-kg subjects at each dose level.

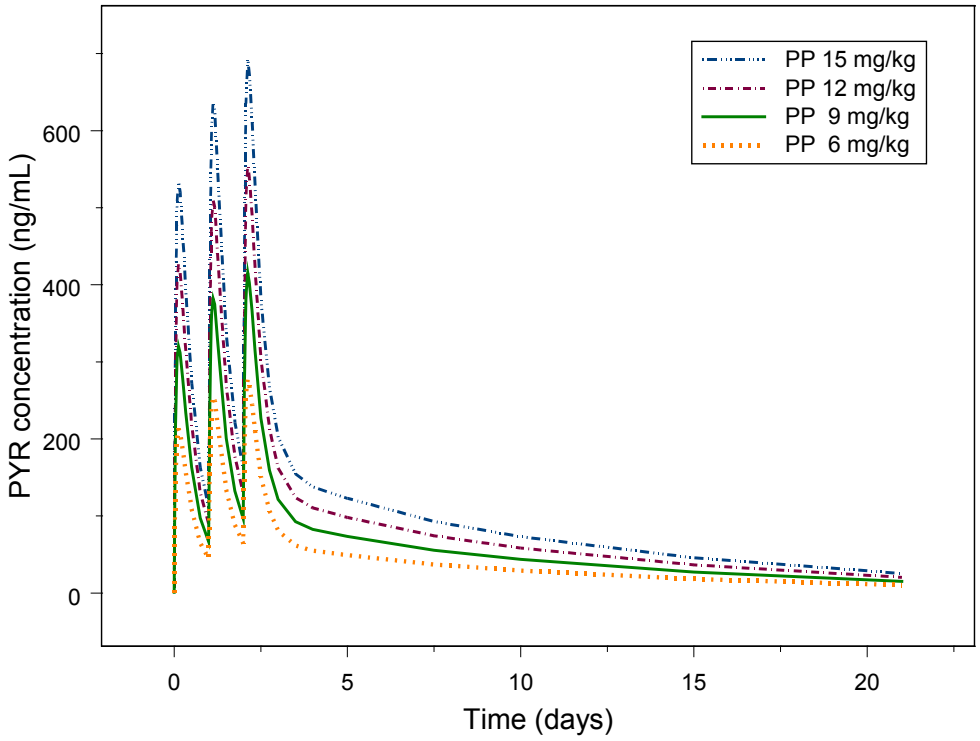

Figure 2.5 Visual Predictive Check of the final model for each part of the study. The open circles represent the observed concentrations, solid lines represent the 5th and 95th quantiles, the dashed line represents the 10th and 90th quantiles, and the dotted line represents the 50th percentile obtained from the simulations.

Part 1 Single ascending dose study

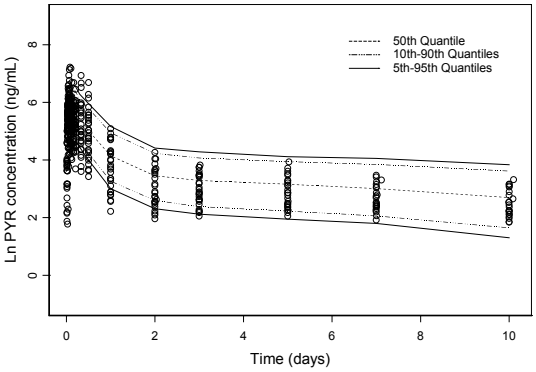

Part 2 Drug interaction study

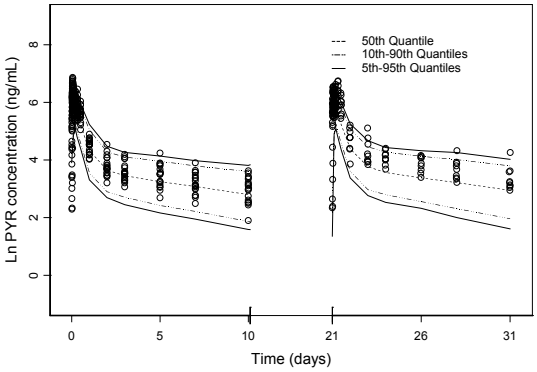

Part 3 Food interaction study

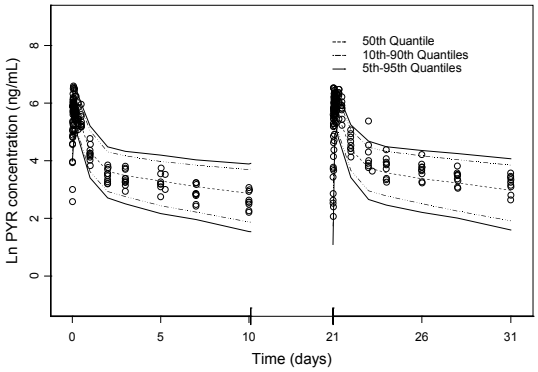

Part 4 Multiple ascending dose study

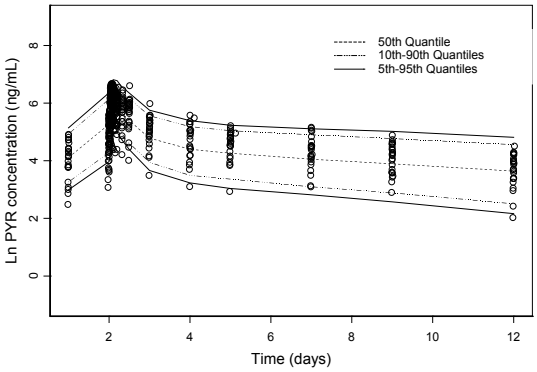

CHAPTER III

POPULATION PHARMACOKINETICS OF PYRONARIDINE FOLLOWING ORAL PYRONARIDINE/ARTESUNATE TREATMENT IN ADULT MALARIA PATIENTS

Introduction

Half of the world's population is at risk of malaria, and an estimated 243 million cases led to estimated 863,000 deaths in 2008[2]. Malaria is curable and preventable, but it can be fatal if not treated promptly. Currently artemisinin-based combination therapies (ACTs) are considered by World Health Organization to be the best antimalarials in terms of efficacy and a lower propensity to resistance[2, 15]. Artemisinin and its derivatives produce rapid clearance of parasitemia and fast resolution of symptoms but they are eliminated rapidly. In order to prevent the occurrence of drug resistance to artemisinins and to address the issue of their relatively short half-lives, combining an artemisinin drug with a long half-life partner drug is recommended.

Pyronaridine, a Mannich base anti-malarial drug synthesized in China in 1970s[25], is a promising partner drug in artemisinin-base combination therapies. It is effective against erythrocytic stage of several species of malaria parasites[28, 80]. The mechanism of action is similar to chloroquine, as it inhibits β-hematin formation, disrupting hematin detoxification in malaria parasites[35]. Clinical studies have showed that pyronaridine is safe and efficacious against *P. falciparum* even in the area with chloroquine-resistant strains[28, 40, 41]. The combination of pyronaridine and artesunate exhibited an enhanced effect over monotherapy *in vitro* and *in vivo* studies[73]. Currently an oral combination product containing pyronaridine tetraphosphate and artesunate (PA) in fixed combination in the ratio of 3:1 has completed Phase III clinical trials in Asia and Africa as a 3-day oral therapy for use in children and adults to treat acute, uncomplicated falciparum and blood

stage vivax malaria. To date, this combination has showed a favorable efficacy and safety profile[43].

The population pharmacokinetics of pyronaridine has been investigated in 91 healthy subjects in Phase I studies reported in the previous chapter. A two-compartment model with first-order absorption and elimination best described the disposition of pyronaridine. Pyronaridine exhibits a large total apparent volume of distribution (85 L/kg) with mean elimination half-life of 8.4 days. Pyronaridine is known to be concentrated in red blood cells[46, 47]. The partitioning study of pyronaridine (Schmidt et. al, unpublished data) revealed that the concentration of pyronaridine in blood cells is approximately 1.6 to 2.9 times higher than in plasma. Pyronaridine is eliminated mainly by metabolism. However no active metabolite was identified.

In this study, we examine the population pharmacokinetics of pyronaridine using a nonlinear mixed-effect modeling approach in adult malaria patients (15 - 60 years) participating in Phase II and Phase III clinical studies. We also investigate the influence of several clinical covariates on the pharmacokinetics of pyronaridine in this heterogeneous patient population.

Materials and Methods

Blood concentrations of pyronaridine in adults participating in a Phase II study (SP-C-002-05) and three Phase III studies (SP-C-004-06, SP-C-005-06 and SP-C-006-06) were included in the pharmacokinetic analysis. The PA combination was given orally once a day for 3 consecutive days.

Subjects and Study designs

SP-C-002-05 was a double-blind, randomized, multicenter, Phase II study to determine the clinical effective dose of orally administered PA (3:1) in adult patients (15-60 years, 35-75 kg), with acute uncomplicated *Plasmodium falciparum* malaria. Patients were randomized to receive PA6+2 mg/kg (pyronaridine tetraphosphate 6 mg/kg +

artesunate 2 mg/kg), PA9+3 mg/kg, or PA12+4 mg/kg. Pharmacokinetics of pyronaridine was investigated in 14 subjects with extensive blood sampling at one study site.

All Phase III studies were conducted as multicenter, randomized, controlled, blinded designs to confirm the efficacy and safety of the fixed combination of PA (180:60 mg tablet) with GMP gold standard comparators. **SP-C-004-06** and **SP-C-005-06**[70] were conducted to compare the efficacy and safety of PA with that of mefloquine plus artesunate and with that of the combination of artemether/lumefantrine (Coartem®), respectively, in children and adult patients (3-60 years) with uncomplicated *Plasmodium falciparum* malaria. The aim of **SP-C-006-06** was to compare the safety and efficacy of PA with that of chloroquine in children and adult patients with acute *P. vivax* malaria. To be part of the Phase III studies, a patient needed to fulfill the following criteria: age, 3 - 60 years, weight, 20 to 90kg, acute uncomplicated malaria and no significant concomitant disease or clinical laboratory abnormalities. The efficacy endpoints and schedule of assessments selected generally followed the current WHO guidelines for monitoring drug efficacy[81]. PA (180:60) tablets were supplied by Shin Poong Pharm Co. Ltd. The dosing regimen depended on body weight. Subjects weighing 20-25 kg, were given one tablet; subjects weighing 26-44 kg, two tablets; 45-64 kg, three tablets and 65-90 kg, four tablets.

The trials were conducted in accordance with the Guidelines of Good Clinical Practice and the Declaration of Helsinki. Written informed consent, in accordance with local practice, was obtained from each subject. Approval for the study was granted by the local Ethics Committee.

Malaria is more common and more severe in children. Although a small number of patients were reported as treatment failures, there were a larger number of treatment failures in the pediatric population. To gain more insight in adult and pediatric populations, we decided to perform the population pharmacokinetic analysis separately

for each group. A cut-off of 14 years of age was used according to the inclusion criteria for clinical protocols in pediatric studies included in this analysis.

Sample Collection and Storage

For the Phase II study (SP-C-002-05), blood samples were collected for pharmacokinetic analysis of pyronaridine at the following time points: Predose and 0.5, 1, 1.5, 2, 2.5, 4, 8, 16, 24 hours and 3, 5, 12, 19, 26 days after the third dose. For all Phase III studies at all participating clinical study sites, unless determined otherwise by the sponsor, the investigator was required to collect one or two blood samples from each patient at two different time points. One sample was drawn between Day 0 (post dose) and Day 3, and a second between Day 4 and Day 42. The actual times were recorded. Blood samples (2 mL) were drawn into heparinized tubes (Vacutainer tubes). Two approximately equal volume aliquots of the blood were transferred to screw cap cryovials (Nalgene No.: 50000012) and frozen at or below -80°C in a laboratory freezer. They were later shipped separately via air express frozen on dry ice to the Clinical Pharmacokinetics Laboratory at College of Pharmacy, the University of Iowa. All samples were stored at -80°C until drug analysis was performed.

Determination of blood pyronaridine concentrations

Pyronaridine concentration in blood were quantified by a validated liquid chromatography-mass spectrometric method (LC/MS) as described elsewhere[82]. Briefly, blood sample of 0.3 mL was spiked with 100 ng of amodiaquine, an internal standard. A 0.75 mL of 500 mM Sodium Phosphate Tribasic dodecahydrate buffer (pH = 10.3) was added to the blood and mixed briefly on a vortex mixer, and followed by the addition 4.5 mL of ether. The mixture was vortexed for 15 minutes, and then centrifuged for 10 min (2500 rpm). The organic layer was transferred to a new glass tube and then dried in an evaporator (N-Vap Berlin, MA, USA) under a flow of nitrogen at room temperature. The residue was then reconstituted with 200 µL of solution containing acetonitrile and 0.02 M

KH_2PO_4 (13:87, v/v). Test tubes were shaken for 1 min, sonicated for 10 min at 35 ◦C and again vortexed for 1 min before transferring the liquid layer to an autoinjector vial. A 15 µL aliquot of this solution was injected onto the chromatographic system. For lower QC (11.4 ng/mL) and calibration point (5.7 ng/mL) 75 µL of the solution was injected onto the column.

Chromatographic analysis was carried out on a Shimadzu Model 2010A liquid chromatograph and mass spectrometer (Shimadzu, Columbia, MD, USA) using a LC-10AD VP Solvent Delivery system (Pump: A, B). The injection was made with a Shimadzu SIL-10AD VP automatic injector and analysis used Shimadzu model 2010A data analysis software Lab Solutions Version 3.30. The column was stored in a CTO-10AS VP column oven (Shimadzu, Columbia, MD, USA). The limit of detection is in the range of 5.7–855 ng/mL. The intra-day coefficients of variation for pyronaridine samples (11.4, 285, 760 ng/mL) were 11.1, 4.8 and 2.2%, respectively. Coefficients of variation of inter-day analysis of pyronaridine samples (11.4, 285, 760 ng/mL) were 15.9, 9.7 and 7.8%, respectively.

Population Pharmacokinetic Analysis

Structural Model

The population pharmacokinetic analyses were performed using NONMEM® version VI level 2.0 (Icon development solutions, Ellicott city, MD)[76]. The compiler was Intel Fortran Complier v10.2 (Intel Corporation, Santa Clara, CA) with 2.82 GHz Intel Pentium III Xeon running Microsoft Windows XP Professional x64 Edition (Microsoft Corporation, Seattle, WA). NONMEM output was processed using PDx-Pop 3.10 (ICON Development Solutions, Ellicott City, MD) and Xpose version 4.0 (Uppsala University, Uppsala, Sweden)[77]. Graphical plots were produced using S-PLUS version 8.0 (Insightful Inc, Seattle, WA) and R 2.8.1 (Free Software Foundation, Boston, MA).

Blood pyronaridine concentrations were natural log-transformed before the analysis. All models were fitted using the first-order conditional estimation method with interaction (FOCEI). Concentration measurements below the lower limit of quantitation were treated as missing and were excluded from the dataset. Based on the exploratory data analysis, two- and three- compartment models with different absorption models were fitted to pyronaridine data to determine the best structural model. The models were parameterised in terms of clearances and distribution volumes using the PREDPP subroutine supplied in NONMEM. Inter-subject variability (ISV) of the pharmacokinetic parameters was modeled assuming a log-normal distribution, as follow:

$$\theta_i = \theta_{TV} \bullet \exp(\eta_i)$$

where θ_i is the estimated parameter value for individual i, θ_{TV} represents the population's typical value for the corresponding parameter and η_i is the deviation of θ_i from θ_{TV}. The η random effects were assumed to be independent and symmetrically distributed with zero mean and variance ω^2, which represents the ISV of the parameter. The magnitude of ISV was expressed as coefficient of variation (%CV).

The residual variability (RV) was described with an additive error model as follows:

$$\ln C_{ij} = \ln C_{pred,ij} + \varepsilon_{ij}$$

where C_{ij} and $C_{pred,ij}$ represent the jth observed and model predicted concentrations, respectively, for individual i and ε_{ij} denotes the additive residual random error for individual i and observation j. The ε random effects were assumed to be independent and symmetrically distributed with mean of zero and variance σ^2.

Model selection was guided by the plausibility of the estimates, minimum objective function value (MOFV), equal to minus twice the log-likelihood function, Akaike Information Criterion (AIC), equal to MOFV plus two times the number of parameters, condition number, defined as the ratio of the largest Eigen value to the

smallest Eigen value, visual inspection of diagnostic plots and the precision of parameter estimates.

Covariate model

Once the base model was identified, the possible influence of the subject-specific covariates on the estimated pharmacokinetic parameters was assessed. Correlations between tested covariates were examined by graphical analysis. Continuous covariates examined include age, total body weight (WT), height (HT), baseline hematocrit (HCT), baseline hemoglobin (HGB), baseline erythrocyte count (RBC), lean body weight (LBW), and body mass index (BMI). LBW and BMI were calculated as follows.

$$Females: \quad LBW\ (kg) = 1.07\ \cdot WT(kg) - \frac{148 \cdot WT^2(kg^2)}{HT^2(cm^2)}$$

$$Males: \quad LBW\ (kg) = 1.10\ \cdot WT(kg) - \frac{128 \cdot WT^2(kg^2)}{HT^2(cm^2)}$$

$$BMI\ (kg/m^2) = \frac{WT(kg)}{HT^2(m^2)}$$

Categorical covariates included in the analysis were sex (female or male), geographic region (Asia or Africa), baseline parasite count (using a cut off of 50,000 /μL), baseline aspartate aminotransferases (AST) and baseline alanine aminotransferases (ALT) (using a cut off of 1.5 x upper limit of normal range at each study).

Model building process was guided by physiologic plausibility, the generalized additive model (GAM) as implemented in Xpose[67] and graphic explorations. Plots of the individual empirical Bayes estimates of the parameters versus covariates were generated to visualize potential relationships. The potential covariates were tested for statistical significance using a stepwise forward addition and backward deletion procedure. All continuous covariates were scaled or centered with the median values so that the population estimates represent those of an average patient and were tested using linear, power, and exponential functions as illustrated in the following equations.

$\theta_i = \theta_{TV} + \theta_F \bullet (COV - COVmedian)$, for linear function;

$\theta_i = \theta_{TV} \bullet (COV/COVmedian)^{\theta_F}$, for power function;

$\theta_i = \theta_{TV} \bullet EXP(\theta_F \bullet (COV - COVmedian))$, for exponential function;

where θ_i is the estimated parameter value for individual i, θ_{TV} represents the typical value for the parameter of an individual with median value of the covariate (COV=COV_{median}), and θ_F is a factor describing the influence of the covariate (COV) expressed as deviation per unit of the covariate from the median value (COV_{median}) of the study population. The influences of binary covariates on the parameter were modeled using an additive relationship, as follows:

$$\theta_i = \theta_{TV} + \theta_F \bullet COV ;$$

where θ_{TV} represents the parameter value for subjects with the categorical covariate coded as 0, and θ_F is the additional change in the parameter in subjects with the categorical covariate coded as 1.

Discrimination between two nested models was based on the improvement of the MOFV which is equal to twice the negative log likelihood of the data. A decrease in the MOFV (which approximately follows the χ^2 distribution, where the degrees of freedom is the difference in the number of estimated parameters) of 3.84 units was considered statistically significant ($P<0.05$) for addition of one parameter to a candidate model. The stepwise addition of covariates into the model would continue until a decrease of 3.84 cannot be reached any longer. This would be the fully parameterised population pharmacokinetic model. To determine if all the covariates included in the fully parameterised population pharmacokinetic model continued to provide significant influence on the population model, the covariates included in the full model would be stepwise sequentially removed and the resulting reduced model evaluated to determine if there was significant model degradation. The significance of the covariate was tested using the nested model criteria at a more stringent p-value of 0.001, resulting in a change

in OFV of 10.83, to avoid false-positives. The process was repeated until all remaining covariates in the model were significant. In addition to using the stated statistical criteria, clinical consideration were also taken into account. For categorical variables, at least a 20% change in the affected parameter is needed for the covariate to be considered clinically meaningful.

Model evaluation

The robustness of the final model was evaluated using the nonparametric bootstrap approach. A 1,000 bootstrap datasets were generated by repeated random sampling with replacement from the NONMEM input data file, and the final NONMEM model was fitted to the bootstrap datasets. The mean and 95% confidence intervals for the population pharmacokinetic parameters were calculated, and compared with the estimates from the original dataset. The bootstrap 95% confidence interval was calculated based on the percentile of the empirical distribution of the estimated parameters from the bootstrap runs.

Visual predictive check was performed to evaluate the predictive ability of the final model. A thousand virtual observations at each sampling time point were simulated using the final model and its parameter estimates. The observed data were then plotted with the 5th, 50th and 95th percentiles of the simulated data. The percent of observations outside the 90% prediction interval was also calculated.

The condition number is calculated as the ratio of the largest Eigen value to the smallest Eigen value, was also used to ascertain stability of parameter estimates.

Results

Data from a Phase II and three Phase III studies in adult patients were pooled for the analysis. Among 878 blood samples collected to determine pyronaridine level, the concentrations of pyronaridine in 206 (23.5%) samples were below the limit of quantitation (BLQ values) and three observations (0.3%) were identified as possible

outliers as the data points were far from bulk of the data. A total of 699 blood pyronaridine concentration data collected from 321 adult patients with uncomplicated falciparum and vivax malaria were available for the analysis. The plots of natural log-transformed blood pyronaridine concentrations versus time and time after dose are shown in Figure 3.1 and 3.2, respectively. The numbers of observations, demographic and clinical characteristics of subjects in each clinical study are listed in Tables 3.1 and 3.2. The patient population was predominantly male (71%) with a mean age (± SD) of 28.4 (± 10.3) years and mean weight (± SD) of 52.5 (± 8.1) kg. The average PP dose received was 10.0 ± 1.1 mg/kg. There was a greater proportion of Asian patients than African patients (74% and 26% respectively).

Based on graphical inspection of the concentration-time plots showing multiphasic disposition, two- and three-compartment pharmacokinetic models were evaluated. The data was best described by the 2-compartment model with first-order absorption and elimination from central compartment was implemented in NONMEM using its ADVAN4 TRAN4 subroutine. The estimated structural model parameters included absorption rate constant (Ka), apparent central volume of distribution (V2/F), apparent peripheral volume of distribution (V3/F), oral clearance (CL/F) and inter-compartmental clearance (Q/F) where F is oral bioavailability. Intersubject variability (ISV) on all parameters was initially included into the model; however, the data supported only ISV on Ka, V2/F and CL/F. Including ISV terms on Q/F and V3/F resulted in the model instability and unreasonable parameter estimates. There was no significant correlation between model parameters. The 3-compartment model was not supported by the data as evidenced by inability to converge the models successfully and unreasonable parameter estimates.

A summary of the clinical covariates evaluated is shown in Table 3.2. Correlations between continuous covariates were examined. Significant correlations among weight based covariates, such as between WT and LBW, and among RBC indices,

such as HGB and HCT, were found. A total of 13 covariates were initially screened by GAM analysis, graphical exploration and physiologic plausibility. None of the tested covariates was identified as potential covariates on Ka. HT was not found to be a potential covariate on any pharmacokinetic parameters and, therefore, was not included in subsequent evaluation. There was a substantially smaller proportion of females in the Asian studies compared to the African studies (19% and 59% respectively). Consequently only sex, not geographic region, was brought forward to further model development.

The remaining covariates were further evaluated for statistical significance in NONMEM using a stepwise procedure. NONMEM screening showed that both LBW and WT might be important predictors of CL/F and V2/F but LBW appeared to be more important covariates as evidenced by more significant improvements in the MOFV (a decrease of 17.43 versus 8.68, respectively). In forward addition step 1 and 2, LBW was included into the model as a predictor of V2/F and CL/F, respectively. The effect of Age on V2/F was included step 3. No more significant improvements were obtained in round 4. During backward elimination, the effect of AGE on V2/F and LBW on CL/F were not significant enough to remain in the model using the criteria stated in method section. As a result, LBW as a predictor of V2/F was the only covariate incorporated in the model.

The final population pharmacokinetic model for pyronaridine is a two-compartment model with first-order absorption and elimination from the central compartment. Apparent central volume was parameterized as a power function of LBW centered at its median value. The model is described by the following equations.

$$\text{TVKA } (d^{-1}) = \theta_1 * \exp(\eta_1)$$

$$\text{TVCL/F (L/d)} = \theta_2 * \exp(\eta_2)$$

$$\text{TVV2/F (L)} = [\theta_3 * \exp((\text{LBW}-42.9)* \theta_6] * \exp(\eta_3)$$

$$\text{TVV3/F (L)} = \theta_4$$

$$\text{TVQ/F (L/d)} = \theta_5$$

The final parameter estimates given by this model are summarized in Table 3.3. All parameters were estimated with acceptable precision. Pyronaridine was rapidly absorbed with a typical value of Ka of 1.22 hr^{-1} with high ISV (109%). The population estimates of CL/F and V2/F were 1,180 L/d with 50.2% ISV and 8,540 L with 82.4% ISV, respectively. The population estimates of V3/F and Q/F were 13,200 L and 1,720 L/d, respectively. The mean distribution and elimination half-lives of pyronaridine were estimated to be 1.7 and 18.1 days. The goodness-of-fit plots are shown in Figure 3.3 and 3.4. The observed concentrations versus population and individual predicted concentrations plots illustrated no significant deviations from the line of identity, suggested reasonable fit. The conditional weighted residual (CWRES) values were generally distributed around zero and relatively symmetric with the exception of a slight under-prediction at low concentrations or at 42 days after first dose. However, there was no observation outside the acceptable limits of $\pm$5. Figure 3.5 shows the individual fit for subjects with intensive sampling.

The final model was fitted repeatedly to 1,000 bootstrap samples. The mean parameter estimates obtained from the bootstrap replicates are summarized in Table 3.3. The final model provided estimates within the 95% confidence intervals obtained by 1,000 bootstrap runs. Results of the visual predictive check are presented in Figure 3.6. Overall, the final model adequately described the observed concentrations. About 11.23% of the pyronaridine observations respectively were not contained within the 90% prediction interval. The condition number of the final model was 30.8 indicating that the model was stable.

Discussion

This study reports for the first time the population pharmacokinetic study of pyronaridine in malaria patients. A total of 699 blood PYR concentration data collected from 321 adult patients participating one Phase II and three Phase III clinical studies were

included in the analysis. Extensive blood sampling scheme was used in the Phase II study while a sparse number of samples per subject at different time points collected during clinical visits in Phase III studies. Pyronaridine concentrations were measured for 28 days in the Phase II study, 42 days in Phase III studies. Thus, Phase III studies yielded many more BLQ samples.

Our analysis revealed that the pharmacokinetics of pyronaridine in adult patients was best described using a two-compartment model with first-order absorption and elimination, the same structural model describing the pharmacokinetics of the drug in healthy subjects. Goodness-of-fit plots from the final model suggested a reasonable fit of the model to the data (Figure 3.3 and 3.4). The final model provided all parameter estimates with acceptable precision. The final estimates lie within the 95% confidence intervals obtained by bootstrap runs. The visual predictive check showed that the final population model adequately captured the majority of the data. Limitation of the model appeared to be mainly during the first three days but this finding is not unexpected given the typical variability observed during oral drug absorption.

In our study, the main physiological variables showed significant influence on pyronaridine disposition was LBW, the strongest predictor of central apparent of distribution (V2/F). Pyronaridine has a large volume of distribution. We expected that WT should be a significant covariate of volume of distribution, particularly the apparent peripheral volume (V3/F) but we could not investigate that because ISV term on V3/F was not included in the model. Although it was evident that pyronaridine is concentrated in blood cells[46, 47], RBC indices at baseline did not appear to be a significant covariate on V2/F. It would be interesting to investigate the effect of RBC indices as time-varying covariates in future studies.

In the previous chapter, a 2-compartment model was fitted to pyronaridine blood concentrations in healthy volunteers receiving different doses of pyronaridine tetraphosphate (PP 6 - 15 mg/kg, median dose of 12 mg/kg). The same structural model

also best described the present data from patients and we found that the pharmacokinetics of pyronaridine in patients is different from healthy subjects. Following the oral administration of 9 mg/kg of PP, pyronaridine absorption was faster and more variable in patients than in healthy subjects (Ka = 29.2 d^{-1} with ISV of 109% vs. 15.4 d^{-1} with ISV of 54%, in patients and healthy subject, respectively). The typical value of oral clearance in patients was 1.0 L/hr/kg (ISV 50%) which was double of that in healthy volunteers (0.5 L/hr/kg, ISV 45%). Total apparent volume of distribution (V/F) were much higher and more variable (V/F = 466 vs. 85 L/kg, ISV 82% vs. 42%, in patients and healthy subject, respectively). The differences in oral clearance and apparent volume of distribution could also be due to the fact that the bioavailability of the drug in patients is lower than in healthy subjects.

The higher variability in patient studies is not unexpected. Although the bioanalysis of pyronaridine was carried out in the same lab, the studies in patients were done in a wider range in subject characteristics and for a longer duration of the study. It should be noted that the bioanalysis methods used in the healthy population[47] and the patient population study[82] were different, but the extraction procedures and the sensitivity of the two methods were the same. The typical weight of malaria patients is usually less than the average of normal population. In this present study, the median actual body weight of patients was 52 kg with median LBW of 43 kg. Given the fact that patients are usually small and lean, the apparent peripheral compartment volume of pyronaridine (V3/F) may not be much different among patients. This could be a reason that the model could not estimate the ISV of V3/F. Anemia is one of the symptoms frequently observed in malaria. Since pyronaridine is known to be concentrated in RBCs, the destruction of RBCs, the increased splenic clearance of RBCs and the decreased production of erythrocytes in the bone marrow could explain the large and variable central compartment volume of pyronaridine in patients (212 L/kg). Although oral clearance of pyronaridine in patients was higher, the average elimination half-life in patients was

longer than in healthy subjects (18 vs. 8 days) due to a much larger volume of distribution,. However, the sampling times in the Phase III studies were considerably longer than in the Phase I studies (42 and 10 days after the first dose, respectively). The elimination half-lives in healthy subjects could be underestimated due to too short sampling times.

In conclusion, a two-compartment model with first-order absorption and elimination best described the pharmacokinetics of pyronaridine in malaria patients. LBW was identified as a significant predictor of V2/F. The final model was stable and showed good robustness. The pharmacokinetic parameters of pyronaridine were plausible and estimated with acceptable precision.

Table 3.1 A summary of data characteristics.

Characteristics	Phase II SP-C-002-05	Phase III SP-C-004-06	Phase III SP-C-005-06	Phase III SP-C-006-06	Total
Total number of observations	217	439	129	93	878
- Number of observations excluded as BLQ (%)	2 (0.9%)	110 (25.1%)	39 (30.2%)	55 (59.1%)	206 (23.5%)
- Number of observations excluded as outliers	0	0	2	1	3
- Number of observations included in the analysis	215	329	88	37	669

Table 3.2 A summary of demographic and clinical characteristics of subjects.

Characteristics	Phase II SP-C-002-05	Phase III SP-C-004-06	Phase III SP-C-005-06	Phase III SP-C-006-06	Total
Number of subjects included in the analysis	14	219	61	27	321
Mean PP dose received ± S.D. (mg/kg)	9.4 ± 2.3	10.0 ± 1.1	10.0 ± 0.9	10.2 ± 1.0	10.0 ± 1.1
Median age (range) (years)	32.5 (18-60)	26 (15-58)	21 (15-55)	24 (15-53)	26 (15-60)
Median weight (range) (kg)	53.8 (45.0-74.5)	51.8 (24.8-72.3)	54.0 (33.0-80.0)	51.0 (35.0-67.0)	52.0 (24.8-80.0)
Median height (range) (cm)	161 (150-178)	162 (127-175)	156 (131-174)	162 (142-173)	161 (127-178)
Median BMI (range) (kg/m^2)	20.3 (17.0-32.0)	19.9 (14.0-26.9)	21.9 (15.4-35.6)	18.9 (16.3-27.1)	20.1 (14.0-35.6)
Median LBW (range) (kg)	42.5 (34.8-48.9)	43.1 (22.4-56.5)	42.6 (28.2-57.1)	42.5 (29.5-52.3)	42.9 (22.4-57.1)
Gender [N (%)] Female	11 (79%)	42 (19%)	34 (56%)	6 (22%)	93 (29%)
Male	3 (21%)	177 (81%)	27 (44%)	21 (78%)	228 (71%)
Geographical region [N (%)] Asia	0 (0%)	212 (97%)	0 (0%)	27 (100%)	239 (74%)
Africa	14 (100%)	7 (3%)	61 (100%)	0 (0%)	82 (26%)
Baseline parasite count (range) (per μL)	3,081 (1,457-55,257)	12,490 (1,040-97,500)	8,113 (1,143-39,304)	11,462 (1,822-73,248)	11,490 (1,040-97,500)
Median baseline Alanine Aminotransferase (range) (U/L)	16 (9-167)	22 (6-91)	22 (11-53)	18 (10-122)	22 (6-167)
Median baseline Aspartate Aminotransferase (range) (U/L)	37 (21-236)	30 (5-114)	36 (18-73)	31 (17-138)	32 (5-236)
Median baseline hematocrit (range) (%)	37.3 (30.2-44.0)	36.8 (24.0-50.0)	36.6 (29.3-56.0)	37.4 (28.6-45.5)	37.0 (24.0-56.0)
Median baseline hemoglobin (range) (g/L)	125 (100-148)	124 (80-171)	128 (91-195)	122 (95-163)	125 (80-195)
Median baseline erythrocyte count (range) ($x10^{12}$ /L)	4.4 (3.4-5.2)	4.6 (2.6-6.5)	4.7 (3.6-7.3)	4.7 (3.3-8.6)	4.6 (2.6-8.6)

Table 3.3 Parameter estimates obtained with the final model describing pyronaridine population pharmacokinetics in adult patients.

Parameter	Estimate	%RSE	%CV	Bootstrap estimate (95% CI)
Ka (d^{-1})	29.2	20.0		34.4 (11.0 – 67.2)
CL/F (L/d)	1,180	10.0		1,175 (876 – 1,470)
V2/F (L)	8,540	7.3		7,960 (2,120 – 9,610)
V3/F (L)	13,200	24.2		14,630 (9,240 – 25,200)
Q/F (L/d)	1,720	22.7		2,226 (1,160 – 6,670)
θ_6 LBW on V2/F	0.041	23.7		0.037 (-0.086 – 0.068)
ISV				
ISV-Ka	1.190	41.9	109.0	2.067 (0.083 – 9.780)
ISV-CL/F	0.252	15.9	50.2	0.253 (0.152 – 0.347)
ISV-V2/F	0.679	12.6	82.4	0.722 (0.501 – 1.550)
RV (additive error)				
RV	0.143	15.4		0.151 (0.107 – 0.238)
Weight-normalized parameters (mean $\pm$ SD)				
CL/F (L/d/kg)	24.0 $\pm$ 8.1			
V2/F (L/kg)	212 $\pm$ 171			
V3/F (L/kg)	254*			
Derived parameters (mean $\pm$ SD)				
$T_{½\alpha}$ (d)	1.7 $\pm$ 0.8			
$T_{½\beta}$ (d)	18.1 $\pm$ 5.5			

Note: Ka first-order absorption rate constant, F oral bioavailability, CL clearance, V2 central volume of distribution, V3 peripheral volume of distribution, Q intercompartmental clearance, $T_{½\alpha}$ distribution half-life, $T_{½\beta}$ elimination half-life, %RSE relative standard error [(SE/mean)x100%], %CV coefficient of variation [(SD/ESTIMATE)x100%].

*Represents V3/F value for a subject with median weight as no ISV on this parameter.

Figure 3.1 Natural log-transformed blood pyronaridine concentrations versus time. The solid line is loess smoothing lines.

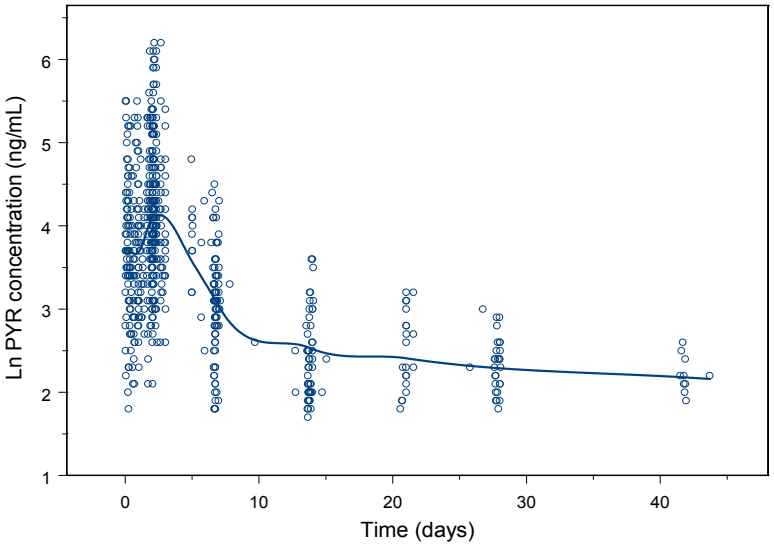

Figure 3.2 Natural log-transformed blood pyronaridine concentrations versus time after dose. The solid line is loess smoothing lines.

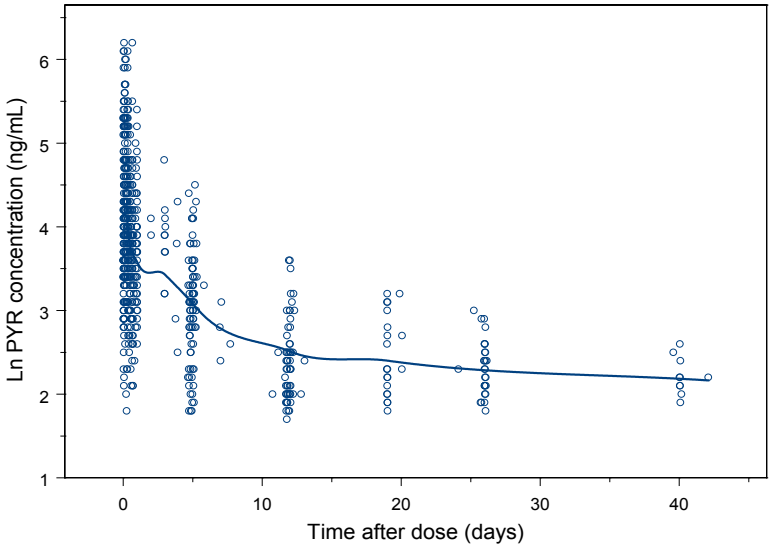

Figure 3.3 Observed concentrations versus Population and individual predicted concentrations plots for the final model. The solid lines are lines of identity.

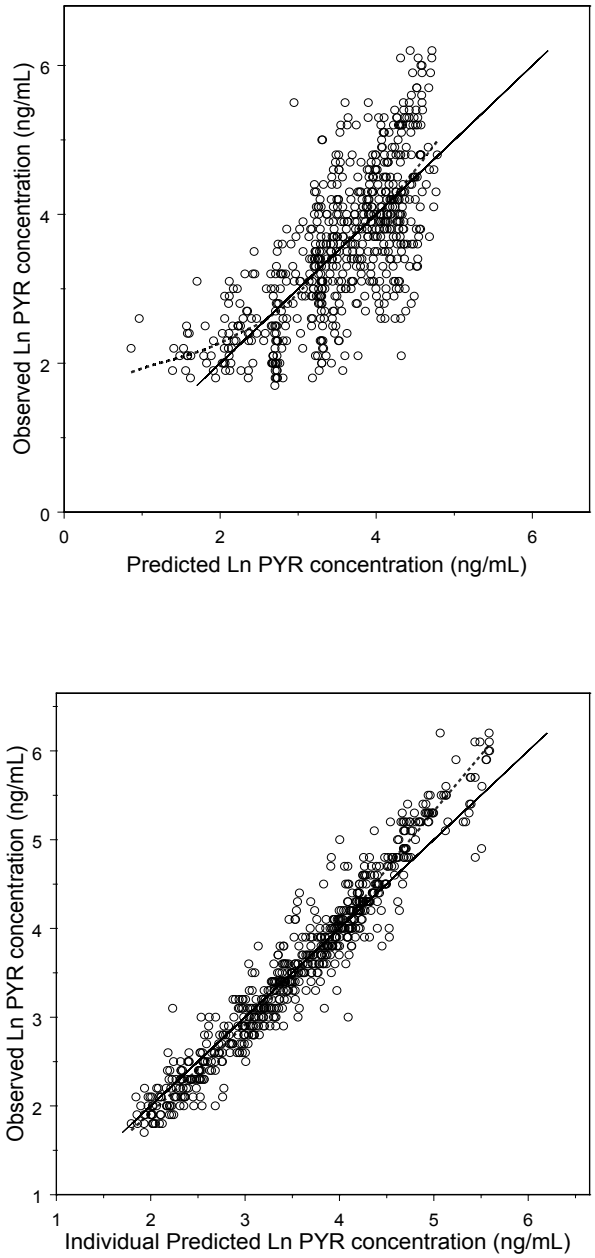

Figure 3.4 Conditional weighted residual plots for the final model. The dotted lines are smoothing lines.

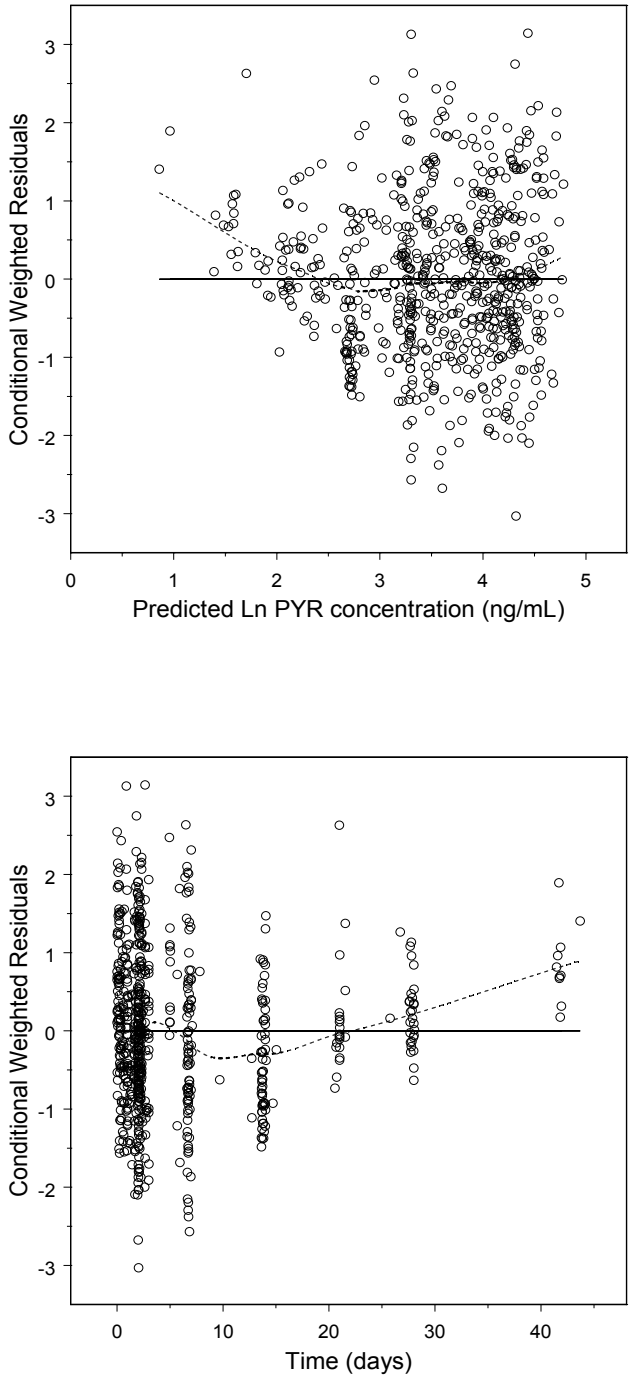

Figure 3.5 Plots of pyronaridine observations (open) and predictions (solid) from the final model for individual subjects with intensive pharmacokinetic sampling.

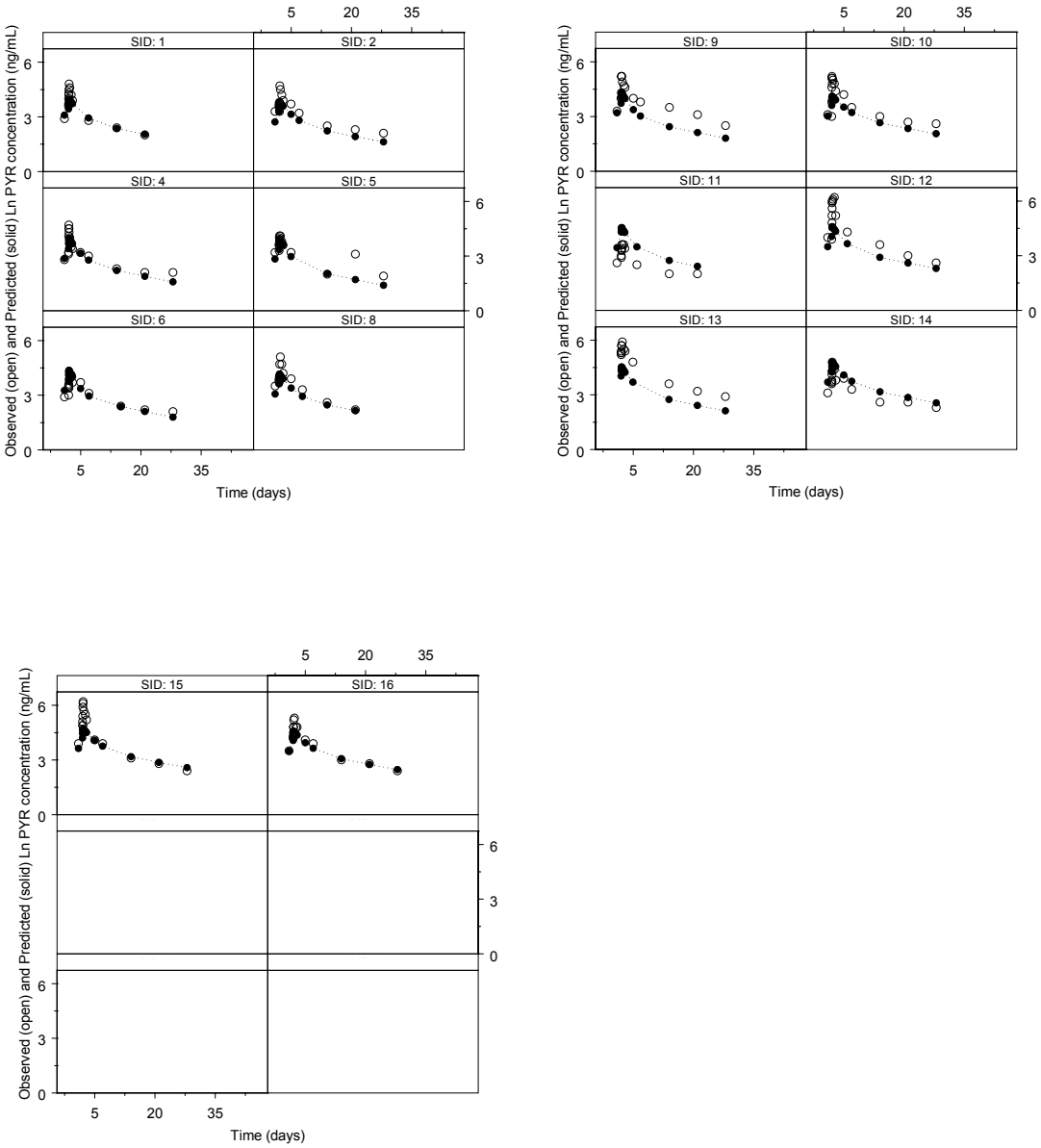

Figure 3.6 Visual Predictive Check of the final model in the adult population. The open circles represent the observed concentrations, solid lines represent the 5th and 95th quantiles, the dashed line represents the 10th and 90th quantiles, and the dotted line represents the 50th percentile obtained from the simulations. The lower graph shows an expanded time scale

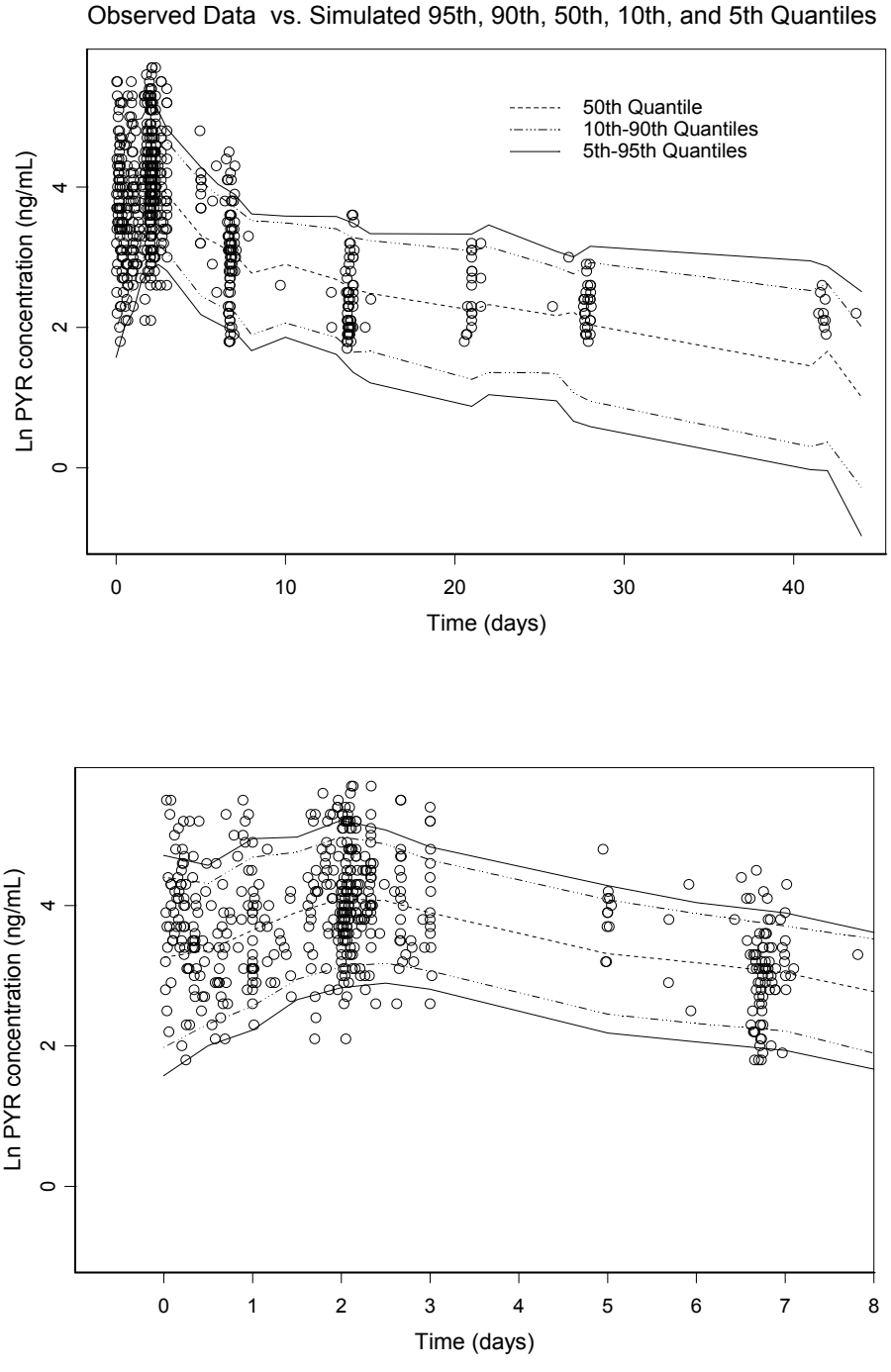

CHAPTER IV
POPULATION PHARMACOKINETICS OF PYRONARIDINE FOLLOWING ORAL PYRONARIDINE/ARTESUNATE TREATMENT IN PEDIATRIC MALARIA PATIENTS

Introduction

Malaria is a major disease affecting infants and young children in regions where it is endemic. There were an estimated 243 million cases, causing 863,000 deaths in 2008[2]. Most of the deaths were of African children under 5 years of age[1]. Not only does malaria result in illness and death, but malaria also hinders children's schooling and social development[83]. One of major obstacles to malaria control is drug resistance in the *plasmodium* parasite. In many parts of the world, the drugs traditionally used to treat uncomplicated malaria have become ineffective due to the development of drug resistance. To counter the threat of resistance, the World Health Organization currently recommends artemisinin-based combination therapies (ACTs) for treating uncomplicated malaria[2, 15]. Artemisinin and its derivatives clear parasitemia rapidly but they are also eliminated rapidly. In order to reduce the risk of further resistance and to address the issue of their relatively short half-lives, combining an artemisinin drug with a long half-life partner drug is recommended.

Pyronaridine, a promising partner drug in ACTs, was synthesized in China in 1970s[25]. It inhibits the formation of β-hematin *in vitro* and enhances hematin-induced lysis of infected erythrocytes[35]. Pyronaridine has been used extensively as a monotherapy to treat malaria in the Hunan and Yunan Provinces, China, where it has been found to be safe and effective in the treatment of uncomplicated malaria[84]. The combination of pyronaridine and artesunate exhibits an enhanced effect over monotherapy *in vitro* and *in vivo* studies[73]. Recently an oral combination product containing pyronaridine tetraphosphate and artesunate (PA) in fixed combination in the ratio of 3:1 has completed

Phase III clinical trials in Asia and Africa as a 3-day oral therapy for use in children and adults to treat acute, uncomplicated falciparum and blood stage vivax malaria. To date, this combination has demonstrated favorable efficacy and safety[43, 85].

In Chapter III, we investigated the population pharmacokinetics (PPKs) of pyronaridine in 321 adult patients participating one Phase II and three Phase III clinical studies. A two-compartment model with first-order absorption and elimination best described the disposition of pyronaridine. Pyronaridine exhibits a large total apparent volume of distribution (466 L/kg) with a mean elimination half-life of 18 days.

Since children are more susceptible to malaria compared to adults, in this study, we characterize the population pharmacokinetics of pyronaridine using a nonlinear mixed-effect modeling approach in pediatric malaria patients participating in Phase II and Phase III clinical studies. The influence of several clinical covariates on the pharmacokinetics of pyronaridine in this heterogeneous patient population was examined. In addition, since there were some treatment-failure patients with pyronaridine measurements, we also investigate pharmacokinetics of pyronaridine in this group to achieve a rational optimization of the treatment.

Materials and Methods

Blood concentrations of pyronaridine in children participating in a Phase II study (SP-C-003-05) and four Phase III studies (SP-C-004-06, SP-C-005-06, SP-C-006-06 and SP-C-007-07) were included in the pharmacokinetic analysis. The PA combination was given orally once a day for 3 consecutive days.

Subjects and Study designs

SP-C-003-05 was an open-label, dose-escalation Phase II study. The aim was to investigate the safety, tolerability and pharmacokinetics of the fixed-dose PA (3:1) combination in tablets and granules formulations for the treatment of uncomplicated falciparum malaria in pediatric patients (2-14 years) in Gabon. PA was administered as

co-formulated tablets at the following dose levels: PA6+2 mg/kg, PA9+3 mg/kg, and PA12+4 mg/kg. A pediatric granule co-formulation was investigated at PA9+3 mg/kg. Extensive blood sampling scheme was used for pharmacokinetic analysis of pyronaridine. The details of this study were described elsewhere[43].

SP-C-004-06, SP-C-005-06 and **SP-C-006-06** were Phase III studies in adult and pediatric patients (3-60 years). The study designs were multicenter, randomized, controlled, blinded designs to confirm the efficacy and safety of the fixed combination of PA (180:60 mg tablet) with GMP gold standard comparators. **SP-C-004-06** and **SP-C-005-06**[70] were conducted to compare the efficacy and safety of PA with that of mefloquine plus artesunate and with that of the combination of artemether/lumefantrine (Coartem®), respectively, in children and adult patients with uncomplicated *Plasmodium falciparum* malaria. The aim of **SP-C-006-06** was to compare the safety and efficacy of PA with that of chloroquine in children and adult patients with acute *P. vivax* malaria. To be part of these three Phase III studies, a patient needed to fulfill the following criteria: age, 3 - 60 years, weight, 20 to 90kg, acute uncomplicated malaria and no significant concomitant disease or clinical laboratory abnormalities. **SP-C-007-07** was a Phase III study in infants and children (between $\geq$ 5 kg and < 25 kg) to assess safety and efficacy of a granule formulation (60:20 mg) (pediatric PYRAMAX®) versus Coartem® crushed tablets with acute uncomplicated *P. falciparum* malaria.

The efficacy endpoints and schedule of assessments selected generally followed the current WHO guidelines for monitoring drug efficacy[81]. PA (180:60) tablets and PA(60:20) granule formulation were supplied by Shin Poong Pharm Co. Ltd. The dosing regimen depended on body weight. In adult and pediatric studies, subjects weighing 20-25 kg, were given one tablet; subjects weighing 26-44 kg, two tablets; 45-64 kg, three tablets and 65-90 kg, four tablets. In SP-C-007-07, subjects weighing 5-<9 kg, were given one sachet; 9-<17, two sachets; 17-<25, three sachets. The trials were conducted in accordance with the Guidelines of Good Clinical Practice and the Declaration of

Helsinki. Written informed consent, in accordance with local practice, was obtained from each subject. Approval for the study was granted by the local Ethics Committee.

Malaria is more common and more severe in children. Although a small number of patients were reported as treatment failures, there were a larger number of treatment failures in the pediatric population. To gain more insight in adult and pediatric populations, we decided to perform the population pharmacokinetic analysis separately for each group. A cut-off of 14 years of age was used according to the inclusion criteria for clinical protocols in pediatric studies (SP-C-003-05 and SP-C-007-07) included in this analysis.

Sample Collection and Storage

For the Phase II pediatric study (SP-C-003-05), blood samples were collected for pharmacokinetic analysis of pyronaridine at the following time points: 0(predose), 0.5, 1, 1.5, 2.5, 4, 8, 12, and 1(predose), 2(predose), 3, 7, 14 and 21 days after first dose administration.

For all Phase III studies at all participating clinical study sites, unless determined otherwise by the sponsor, the investigator was required to collect one or two blood samples from each patient at two different time points. One sample was drawn between Day 0 (post dose) and Day 3, and a second between Day 4 and Day 42. The actual times were recorded. Blood samples (1 mL) were drawn into heparinized tubes (Vacutainer tubes). Two approximately equal volume aliquots of the blood were transferred to screw cap cryovials (Nalgene No.: 50000012) and frozen at or below -80°C in a laboratory freezer. They were later shipped separately via air express frozen on dry ice to the Clinical Pharmacokinetics Laboratory at College of Pharmacy, the University of Iowa. All samples were stored at -80°C until drug analysis was performed.

Determination of blood pyronaridine concentrations

Pyronaridine concentration in blood were quantified by a validated liquid chromatography-mass spectrometric method (LC/MS) as described elsewhere[82]. Briefly, blood sample of 0.3 mL was spiked with 100 ng of amodiaquine, an internal standard. A 0.75 mL of 500 mM Sodium Phosphate Tribasic dodecahydrate buffer (pH = 10.3) was added to the blood and mixed briefly on a vortex mixer, and followed by the addition 4.5 mL of ether. The mixture was vortexed for 15 minutes, and then centrifuged for 10 min (2500 rpm). The organic layer was transferred to a new glass tube and then dried in an evaporator (N-Vap Berlin, MA, USA) under a flow of nitrogen at room temperature. The residue was then reconstituted with 200 µL of solution containing acetonitrile and 0.02 M KH_2PO_4 (13:87, v/v). Test tubes were shaken for 1 min, sonicated for 10 min at 35 ◦C and again vortexed for 1 min before transferring the liquid layer to an autoinjector vial. A 15 µL aliquot of this solution was injected onto the chromatographic system. For lower QC (11.4 ng/mL) and calibration point (5.7 ng/mL) 75 µL of the solution was injected onto the column.

Chromatographic analysis was carried out on a Shimadzu Model 2010A liquid chromatograph and mass spectrometer (Shimadzu, Columbia, MD, USA) using a LC-10AD VP Solvent Delivery system (Pump: A, B). The injection was made with a Shimadzu SIL-10AD VP automatic injector and analysis used Shimadzu model 2010A data analysis software Lab Solutions Version 3.30. The column was stored in a CTO-10AS VP column oven (Shimadzu, Columbia, MD, USA). The limit of detection is in the range of 5.7–855 ng/mL. The intra-day coefficients of variation for pyronaridine samples (11.4, 285, 760 ng/mL) were 11.1, 4.8 and 2.2%, respectively. Coefficients of variation of inter-day analysis of pyronaridine samples (11.4, 285, 760 ng/mL) were 15.9, 9.7 and 7.8%, respectively.

Population Pharmacokinetic Analysis

Structural Model

The population pharmacokinetic analyses were performed using NONMEM® version VI level 2.0 (Icon development solutions, Ellicott city, MD)[76]. The compiler was Intel Fortran Complier v10.2 (Intel Corporation, Santa Clara, CA) with 2.82 GHz Intel Pentium III Xeon running Microsoft Windows XP Professional x64 Edition (Microsoft Corporation, Seattle, WA). NONMEM output was processed using PDx-Pop 3.10 (ICON Development Solutions, Ellicott City, MD) and Xpose version 4.0 (Uppsala University, Uppsala, Sweden)[77]. Graphical plots were produced using S-PLUS version 8.0 (Insightful Inc, Seattle, WA) and R 2.8.1 (Free Software Foundation, Boston, MA).

Blood pyronaridine concentrations were natural log-transformed before the analysis. All models were fitted using the first-order conditional estimation method with interaction (FOCEI). Concentration measurements below the lower limit of quantitation were treated as missing and were excluded from the dataset. Based on the exploratory data analysis, two- and three- compartment models with different absorption models were fitted to pyronaridine data to determine the best structural model. The models were parameterised in terms of clearances and distribution volumes using the PREDPP subroutine supplied in NONMEM. Inter-subject variability (ISV) of the pharmacokinetic parameters was modeled assuming a log-normal distribution, as follow:

$$\theta_i = \theta_{TV} \bullet \exp(\eta_i)$$

where θ_i is the estimated parameter value for individual i, θ_{TV} represents the population's typical value for the corresponding parameter and η_i is the deviation of θ_i from θ_{TV}. The η random effects were assumed to be independent and symmetrically distributed with zero mean and variance ω^2, which represents the ISV of the parameter. The magnitude of ISV was expressed as coefficient of variation (%CV).

The residual variability (RV) was described with an additive error model as follows:

$$\ln C_{ij} = \ln C_{pred,ij} + \varepsilon_{ij}$$

where C_{ij} and $C_{pred,ij}$ represent the jth observed and model predicted concentrations, respectively, for individual i and ε_{ij} denotes the additive residual random error for individual i and observation j. The ε random effects were assumed to be independent and symmetrically distributed with mean of zero and variance σ^2.

Model selection was guided by the plausibility of the estimates, minimum objective function value (MOFV), equal to minus twice the log-likelihood function, Akaike Information Criterion (AIC), equal to MOFV plus two times the number of parameters, condition number, defined as the ratio of the largest Eigen value to the smallest Eigen value, visual inspection of diagnostic plots and the precision of parameter estimates.

Covariate model

Once the base model was identified, the possible influence of the subject-specific covariates on the estimated pharmacokinetic parameters was assessed. Correlations between tested covariates were examined by graphical analysis. Continuous covariates examined include age, total body weight (WT), height (HT), baseline hematocrit (HCT), baseline hemoglobin (HGB), baseline erythrocyte count (RBC), lean body weight (LBW), and body mass index (BMI). LBW and BMI were calculated as follows.

$$Females: \quad LBW\ (kg) = 1.07\ \cdot WT(kg) - \frac{148 \cdot WT^2(kg^2)}{HT^2(cm^2)}$$

$$Males: \quad LBW\ (kg) = 1.10\ \cdot WT(kg) - \frac{128 \cdot WT^2(kg^2)}{HT^2(cm^2)}$$

$$BMI\ (kg/m^2) = \frac{WT(kg)}{HT^2(m^2)}$$

Categorical covariates included in the analysis were sex (female or male), geographic region (Asia or Africa), formulation (tablet or granule), baseline parasite count (using a cut off of 50,000 /μL), baseline aspartate aminotransferases (AST) and baseline alanine aminotransferases (ALT) (using a cut off of 1.5 x upper limit of normal range at each study).

Model building process was guided by physiologic plausibility, the generalized additive model (GAM) as implemented in Xpose[67] and graphic explorations. Plots of the individual empirical Bayes estimates of the parameters versus covariates were generated to visualize potential relationships. The potential covariates were tested for statistical significance using a stepwise forward addition and backward deletion procedure. All continuous covariates were scaled or centered with the median values so that the population estimates represent those of an average patient and were tested using linear, power, and exponential functions as illustrated in the following equations.

$\theta_i = \theta_{TV} + \theta_F \bullet (COV - COVmedian)$, for linear function;

$\theta_i = \theta_{TV} \bullet (COV/COVmedian)^{\theta_F}$, for power function;

$\theta_i = \theta_{TV} \bullet EXP(\theta_F \bullet (COV - COVmedian))$, for exponential function;

where θ_i is the estimated parameter value for individual i, θ_{TV} represents the typical value for the parameter of an individual with median value of the covariate (COV=COV_{median}), and θ_F is a factor describing the influence of the covariate (COV) expressed as deviation per unit of the covariate from the median value (COV_{median}) of the study population. The influences of binary covariates on the parameter were modeled using an additive relationship, as follows:

$$\theta_i = \theta_{TV} + \theta_F \bullet COV ;$$

where θ_{TV} represents the parameter value for subjects with the categorical covariate coded as 0, and θ_F is the additional change in the parameter in subjects with the categorical covariate coded as 1.

Discrimination between two nested models was based on the improvement of the MOFV which is equal to twice the negative log likelihood of the data. A decrease in the MOFV (which approximately follows the χ^2 distribution, where the degrees of freedom is the difference in the number of estimated parameters) of 3.84 units was considered statistically significant ($P<0.05$) for addition of one parameter to a candidate model. The stepwise addition of covariates into the model would continue until a decrease of 3.84 cannot be reached any longer. This would be the fully parameterised population pharmacokinetic model. To determine if all the covariates included in the fully parameterised population pharmacokinetic model continued to provide significant influence on the population model, the covariates included in the full model would be stepwise sequentially removed and the resulting reduced model evaluated to determine if there was significant model degradation. The significance of the covariate was tested using the nested model criteria at a more stringent p-value of 0.001, resulting in a change in OFV of 10.83, to avoid false-positives. The process was repeated until all remaining covariates in the model were significant. In addition to using the stated statistical criteria, clinical consideration were also taken into account. For categorical variables, at least a 20% change in the affected parameter is needed for the covariate to be considered clinically meaningful.

Model evaluation

The robustness of the final model was evaluated using the nonparametric bootstrap approach. A 1,000 bootstrap datasets were generated by repeated random sampling with replacement from the NONMEM input data file, and the final NONMEM model was fitted to the bootstrap datasets. The mean and 95% confidence intervals for the PPK parameters were calculated, and compared with the estimates from the original dataset. The bootstrap 95% confidence interval was calculated based on the percentile of the empirical distribution of the estimated parameters from the bootstrap runs.

Visual predictive check was performed to evaluate the predictive ability of the final model. A thousand virtual observations at each sampling time point were simulated using the final model and its parameter estimates. The observed data were then plotted with the 5th, 50th and 95th percentiles of the simulated data. The percent of observations outside the 90% prediction interval was also calculated.

The condition number is calculated as the ratio of the largest Eigen value to the smallest Eigen value, was also used to ascertain stability of parameter estimates.

Treatment Failure Subpopulation Analysis

As part of clinical Phase III protocols, a blood sample was requested for assay of pyronaridine at the time of treatment failure or parasitemia reappearance. Treatment failure was characterized by either re-infection or recrudescence. The detailed differentiation was described elsewhere[70]. To achieve a rational optimization of the treatment for future studies, an analysis of the subpopulation of treatment failures was also performed by comparing demographic characteristics and population pharmacokinetic parameter estimates of patients in this group with those of the other group. All statistical analyses were conducted using SPSS 17 (SPSS Inc., Chicago, IL). Graphical analysis and Shapiro-Wilk test were first performed to check for normality of the data. The results revealed that not all variables to be tested followed normal distribution. Therefore, two-sided Wilcoxon–Mann–Whitney test was used to compare the two subpopulations. A significance level of 0.05 was used

Results

Data from a Phase II and four Phase III studies in pediatric patients were pooled for the analysis. A total of 1,272 blood samples were collected to determine pyronaridine level. The concentrations of pyronaridine in 239 (18.8%) samples were below the limit of quantitation (BLQ values). There were only 3 observations after day 31 and they were excluded from the analysis as possible outliers. The pharmacokinetic data of pyronaridine

comprised 1,030 blood levels from 319 pediatric patients with uncomplicated falciparum and vivax malaria. The plots of natural log-transformed blood PYR concentration versus time and time after dose of PYR are shown Demographic and clinical characteristics of pediatric subjects are summarized in Figure 4.1 and 4.2, respectively. The numbers of observations, demographic and clinical characteristics of subjects in each clinical study are listed in Tables 4.1 and 4.2. The pediatric patient population equally well represented by males (47%) and females (53%) with a mean age (± SD) of 7.6 (± 3.3) years and mean weight (± SD) of 23.1 (± 7.8) kg. The average PP dose received was 9.9 ± 2.2 mg/kg. The majority of the pediatric population was African patients (92%).

Based on graphical inspection of the concentration-time plots showing multiphasic disposition, two- and three-compartment pharmacokinetic models were evaluated. The data was best described by the 2-compartment model with first-order absorption and elimination from central compartment was implemented in NONMEM using its ADVAN4 TRAN4 subroutine. The estimated structural model parameters included absorption rate constant (Ka), apparent central volume of distribution (V2/F), apparent peripheral volume of distribution (V3/F), oral clearance (CL/F) and inter-compartmental clearance (Q/F) where F is oral bioavailability. Intersubject variability (ISV) on all parameters was initially included into the model; however, the data supported only ISV on Ka, V2/F and CL/F. Including ISV terms on Q/F and V3/F resulted in the model instability and unreasonable parameter estimates. There was no significant correlation between model parameters. The 3-compartment model was not supported by the data as evidenced by inability to converge the models successfully and unreasonable parameter estimates.

A summary of the clinical covariates evaluated is shown in Table 4.2. There was no record of HT of one patient, so HT, BMI and LBW of this subject were not included in the analysis. Correlations between continuous covariates were examined. Significant correlations among weight based covariates, such as between WT and LBW, and among

red blood cell indices such as between HGB and HCT, were found. All covariates were initially screened by GAM analysis, graphical exploration and physiologic plausibility. Graphical analysis revealed that the granule formulation was given to a significantly younger and smaller pediatric population than those received tablets as can be seen in Figure 4.3. The average age (± SD) of patients receiving granule formulation and tablet formulation were 4.8 ± 2.0 and 8.9 ± 3.0 years, respectively. The mean weight (± SD) of patients receiving granule formulation and tablet formulation were 16.6 ± 3.9 and 26.0 ± 7.4 kg, respectively. Hence, the effect of FORM was tested on only Ka. Likewise, relationship between GEO and AGE was found. African children were significantly younger and smaller than Asian children (Figure 4.4). The average age (± SD) of African and Asian children were 7.3 ± 3.2 and 11.5 ± 2.0 years and the mean weight (± SD) were 22.8 ± 7.8 and 27.3 ± 6.4 kg, respectively. Also, since 92% of the pediatric population was African, we decided not to test the effect of GEO in further step. Height was not identified as potential covariates on any pharmacokinetic parameters and, therefore, was not included in subsequent evaluation.

The remaining candidate covariates were evaluated in NONMEM using a stepwise procedure. NONMEM screening showed that WT appeared to be the most importance covariate on CL/F in forward addition step 1. Since LBW and AGE had significant correlation with WT; therefore, to use a consistent marker for body size, LBW and AGE were not brought forward into the next step. WT as a predictor of V2/F showed the best improvement in the model in round 2 of forward addition. The process was repeated until no further improvement. The full model had WT on CL/F, WT on V2/F, FORM on Ka and HGB on CL/F. During backward elimination, the effect of FORM on Ka and HGB on CL/F did not reach the level of significance required to remain in the model; therefore, they were removed from the model.

The final population pharmacokinetic model for PYR is a two-compartment model with first-order absorption and elimination from the central compartment. Two

covariates incorporated into the model are WT on CL/F and WT on V2/F. The model is described by the following equations.

$$\text{TVKA } (d^{-1}) = \theta_1 * \exp(\eta_1)$$

$$\text{TVCL/F (L/d)} = \theta_2 * (WT/22)^{**}\theta_6 * \exp(\eta_2)$$

$$\text{TVV2/F (L)} = \theta_3 * (WT/22)^{**}\theta_7 * \exp(\eta_3)$$

$$\text{TVV3/F (L)} = \theta_4$$

$$\text{TVQ/F (L/d)} = \theta_5$$

The final parameter estimates given by this model are summarized in Table 4.3. All parameters were estimated with acceptable precision. Pyronaridine was rapidly absorbed with a population mean value of Ka of 1.17 hr^{-1} with ISV of 81.9%. The typical values of CL/F and V2/F were 429 L/d with 39.6% ISV and 2,780 L with 92.3% ISV, respectively. The typical values of V3/F and Q/F were 1,980 L and 524 L/d. The population means distribution and elimination half-lives of PYR were estimated to be 1.3 and 11.0 days. The goodness-of-fit plots are shown in Figure 4.5 and 4.6. The observed concentrations versus population and individual predicted concentrations plots illustrated no significant deviations from the line of identity, suggested reasonable fit with the exception of a slight under-prediction at low concentrations. No obvious bias pattern was apparent in the plot of the conditional weighted residual (CWRES) values versus population predicted concentrations and CWRES versus time. The values were generally distributed around zero and relatively symmetric. Figure 4.7 shows the individual fit for subjects with intensive sampling.

The final PPK model was fitted repeatedly to 1,000 bootstrap samples. The mean parameter estimates obtained from the 1,000 bootstrap replicates are summarized in Table 4.3. The final model provided estimates within the 95% confidence intervals obtained by 1,000 bootstrap runs. Figure 4.8 shows the results of the visual predictive check. Overall, the final model adequately described the observed concentrations. About 11.55% of the pyronaridine observations were not contained within the 90% prediction

interval. The condition number of the final model was 17.5 indicating that the model was stable.

Treatment failure subgroup analysis

There were 51 blood samples for pyronaridine analysis that were drawn from pediatric patients at the time of study withdrawal due to parasites reappearance during follow-up. These subjects were classified as treatment failures. Patients' demographic and baseline characteristics in the treatment failure group are summarized in Table 4.4. Patients in the treatment failure had generally comparable characteristics with the population characteristics in Table 4.2. However, the treatment failure group tended to receive a pyronaridine tetraphosphate (PP) dose slightly lower than the average of the pediatric population. Moreover the average age of children in treatment failure group was younger, thus smaller body size, than the others.

These blood samples were drawn during day 20 to 46 after the initiation of the treatment. Only 5 samples (8.9%) were drawn before 27 days after the first dose and only one samples had measurable pyronaridine concentrations. The remaining samples had pyronaridine levels below the limit of quantitation. However, there were a total of 41 observations from 23 children in this treatment failure group collected either before or at the time of withdrawal and these data were included in population pharmacokinetics analysis. The comparison of pharmacokinetic parameter estimates obtained from the final model between treatment failure group and the success group was done as shown in Table 4.5. This comparison shows that the treatment failure group, on the average, had statistically significant longer elimination half-life ($t_{½\beta}$) and higher weight-normalized central compartment volume (V2/F).

Discussion

PA fixed combination in the ratio of 3:1 has been evaluated extensively in clinical Phase II and Phase III studies for use in children and adults to treat acute, uncomplicated

falciparum and blood stage vivax malaria. In this study, we reports for the first time the population pharmacokinetic study of pyronaridine in pediatric malaria patients. A total of 1,030 blood PYR concentration data collected from 319 pediatric patients participating one Phase II and four Phase III clinical studies were included in the analysis. Extensive blood sampling scheme was used in the Phase II study while a sparse number of samples per subject at different time points collected during clinical visits in Phase III studies. The number of BLQ samples was larger in Phase III studies because pyronaridine concentrations were measured for 42 days in Phase III studies and only 21 days in the Phase II study.

Our analysis revealed that the pharmacokinetics of pyronaridine in pediatric patients was best described using a two-compartment model with first-order absorption and elimination, the same structural model describing the pharmacokinetics of the drug in healthy adult subjects and adult patients reported in the previous chapters. Goodness-of-fit plots from the final model suggested a reasonable fit of the model to the data. The final model provided all parameter estimates with acceptable precision. The model is robust as evidence by the bootstrap analysis and the visual predictive check showed that the final population model adequately captured the majority of the data. Similar to results of adult data set, limitation of the model appeared to be mainly during the first three days most likely due to variability observed during oral drug absorption.

We attempted to analyze the combined data of adult and pediatric patients using allometric scaling on body weight. Either a fixed exponent allometric scaling approach, the exponent fixed at 0.75 for all clearance and 1 for the volume of distribution terms, or an unfixed approach were not supported by the data as evidenced by inability to converge the models successfully. This could be due to the fact that pyronaridine pharmacokinetics and its variability in these two populations are different and could not be adequately explained by the body weight.

Other than 13 covariates tested in the adult population in the previous chapter, we also examined the effect of formulation (FORM) in this data set because a granule formulation was given in SP-C-003-05 (n=15) and SP-C-007-07 (n=83). However, the effect of FORM on Ka was not significant enough for it to remain in the model. In this study, the main physiological variables showed significant influence on pyronaridine disposition in children was the actual body weight (WT). Pyronaridine oral clearance (CL/F) and central volume of distribution (V2/F) was significantly related to body weight (WT) as indicated by in considerable decreases in the objective function value as well as the inter-subject variability of the parameters. These findings are anticipated because WT is generally the most important fixed effect parameter in the pediatric population and the drug was administered on a weight basis. Although it was evident that pyronaridine is concentrated in blood cells[46, 47], red blood cell indices at baseline did not appear to be a significant covariate on V2/F. It would be interesting to investigate the effect of red blood cell indices as time-varying covariates in future studies.

Comparing the weight normalized parameters of children with adults in the previous chapter, pediatric patients have lower oral clearance and volume of distribution of pyronaridine. The oral clearance in children was 17% lower than adults (20 vs. 24 L/d/kg). Similarly, the average values for V2/F and V3/F in children were lower than in adults about 18% (174 vs. 212 L/kg) and 65% (90 vs. 254 L/kg), respectively. These reductions were in harmony with the shorter elimination half-lives in the pediatric population, namely 11 vs. 18 days for children and adults, respectively. Differences in oral clearance and apparent volume of distribution could be due to the drug's bioavailability in adults being lower than in children.

Interestingly, despite the fact that the dose protocols were similar across all Phase III studies, the final average PP dose in the treatment failure group was slightly lower than the average of the population. This suggests that these patients also received a lower than average artesunate dose. In addition, the majority of patients in treatment failure

group were young children who may be more vulnerable because they have not built up any immunity to the disease.

Comparison of pharmacokinetic parameter estimates for pediatric patients in treatment failure (n=23) and success (n=296) revealed a statistically significant higher weight-normalized volumes of distribution. This would result in lower blood concentrations of PYR which may have contributed to the clinical failures. These results should be interpreted cautiously, since the parameter estimates were obtained from limited available pyronaridine concentration data (23 pediatric subjects out of a total of 51 pediatric subjects in treatment failure group).

In conclusion, a two-compartment model with first-order absorption and elimination best described the pharmacokinetics of pyronaridine in children with uncomplicated malaria. WT was identified as a significant predictor of CL/F and V2/F. The final model was stable and showed good robustness. The pharmacokinetic parameters of pyronaridine were plausible and estimated with acceptable precision.

Table 4.1 A summary of data characteristics.

Characteristics	Phase II SP-C-003-05	Phase III SP-C-004-06	Phase III SP-C-005-06	Phase III SP-C-006-06	Phase III SP-C-007-07	Total
Total number of observations	702	73	296	13	188	1272
- Number of observations excluded as BLQ (%)	14 (2%)	23 (31.5%)	108 (36.5%)	7 (53.8%)	87 (46.3%)	239 (18.8%)
- Number of observations excluded as outliers	0	1	1	0	1	3
- Number of observations included in the analysis	688	49	187	6	100	1,030

Table 4.2 A summary of demographic and clinical characteristics of subjects.

Characteristics	Phase II SP-C-003-05	Phase III SP-C-004-06	Phase III SP-C-005-06	Phase III SP-C-006-06	Phase III SP-C-007-07	Total
Number of subjects included in the analysis	57	34	139	6	83	319
Mean PP dose received ± S.D. (mg/kg)	10.0 ± 2.8	9.6 ± 2.1	10.2 ± 2.3	10.1 ± 2.7	9.3 ± 1.4	9.9 ± 2.2
Median age (range) (years)	5.0 (2.0-14.0)	10.5 (5-14)	9.0 (5-14)	11.0 (9-14)	5 (0.6-10.0)	7 (0.6-14)
Median weight (range) (kg)	16.2 (10.0-36.4)	24.2 (20.0-45.0)	26.5 (20.0-48.0)	25.8 (20.0-46.7)	17.0 (9.0-24.3)	22.0 (9.0-48.0)
Median height (range) (cm)	107 (85-153)	132.5 (100-155)	128 (101-160)	136 (114-156)	104 (65-134)	120 (65-160)
Median BMI (range) (kg/m^2)	15.0 (12.8-17.6)	14.7 (11.0-20.0)	16.6 (11.5-26.5)	15.5 (13.6-19.2)	15.0 (6.0-23.0)	15.6 (6.0-26.5)
Median LBW (range) (kg)	14.4 (8.7-31.7)	22.0 (15.5-34.8)	22.8 (15.6-40.7)	22.8 (18.1-39.9)	14.7 (7.3-22.0)	19.5 (7.3-40.7)
Gender [N (%)] Female	28 (49%)	17 (50%)	76 (55%)	2 (33%)	45 (54%)	168 (53%)
Male	29 (51%)	17 (50%)	63 (45%)	4 (67%)	38 (46%)	151 (47%)
Geographical region [N (%)] Asia	0 (0%)	18 (53%)	0 (0%)	6 (100%)	0 (0%)	24 (8%)
Africa	57 (100%)	16 (47%)	139 (100%)	0 (0%)	83 (100%)	295 (92%)
Baseline parasite count (range) (per μL)	6,304 (1,072-174,241)	12,809 (1,201-92,500)	14,033 (1,000-93,923)	9,559 (1,193-51,947)	14,400 (153-188,488)	11,560 (153-188,488)
Median baseline Alanine Aminotransferase (range) (U/L)	18 (5-70)	19 (11-95)	22 (11-87)	16 (10-27)	22 (6-61)	21 (5-95)
Median baseline Aspartate Aminotransferase (range) (U/L)	32 (18-71)	37 (15-104)	40 (22-91)	35 (28-40)	38 (13-150)	38 (13-150)
Median baseline hematocrit (range) (%)	29.6 (24.3-38.2)	33.0 (23.9-40.0)	33.7 (24.1-57.2)	32.1 (29.1-40.6)	30.0 (22.5-36.9)	32.2 (22.5-57.2)
Median baseline hemoglobin (range) (g/L)	102 (74-129)	110 (82-130)	115 (84-208)	103 (93-135)	100 (80-123)	107 (74-208)
Median baseline erythrocyte count (range) ($x10^{12}$ /L)	4.1 (3.3-6.0)	4.4 (3.3-5.5)	4.5 (3.1-7.1)	4.3 (3.6-5.4)	4.2 (2.9-5.7)	4.3 (2.9-7.1)

Table 4.3 Parameter estimates obtained with the final model describing pyronaridine population pharmacokinetics in pediatric patients.

Parameter	Estimate	%RSE	%CV	Bootstrap estimate (95% CI)
Ka (d^{-1})	28.0	14.8		28.8 (21.4 – 38.4)
CL/F (L/d)	429	6.5		429 (376 – 511)
V2/F (L)	2,780	6.2		2,791 (2,410 – 3,210)
V3/F (L)	1,980	11.2		1,982 (1,560 – 2,470)
Q/F (L/d)	524	10.0		536 (432 – 672)
θ_6 WT on CL/F	1.17	11.6		1.19 (0.87 – 1.50)
θ_7 WT on V2/F	0.83	20.7		0.80 (0.40 – 1.19)
ISV				
ISV-Ka	0.671	26.7	81.9	0.689 (0.346 – 1.080)
ISV-CL/F	0.157	40.6	39.6	0.158 (0.064 – 0.337)
ISV-V2/F	0.852	9.0	92.3	0.849 (0.690 – 1.030)
RV (additive error)				
RV	0.226	13.1		0.227 (0.175 – 0.283)
Weight-normalized parameters (mean $\pm$ SD)				
CL/F (L/d/kg)	20.0 $\pm$ 4.5			
V2/F (L/kg)	174 $\pm$ 156			
V3/F (L/kg)	90*			
Derived parameters (mean $\pm$ SD)				
$T_{½\alpha}$ (d)	1.3 $\pm$ 0.5			
$T_{½\beta}$ (d)	11.0 $\pm$ 5.6			

Note: Ka firsrt-order absorption rate constant, F oral bioavailability, CL clearance, V2 central volume of distribution, V3 peripheral volume of distribution, Q intercompartmental clearance, $T_{½\alpha}$ distribution half-life, $T_{½\beta}$ elimination half-life, %RSE relative standard error [(SE/mean)x100%], %CV coefficient of variation [(SD/ESTIMATE)x100%].

*Represents V3/F value for a subject with median weight as no ISV on this parameter.

Table 4.4 Demographic and baseline characteristics for pediatric patients in treatment failure group.

	Pediatric Patients (n=51)
Number of treatment failures in each clinical study	
- SP-C-003-05	1
- SP-C-004-05	1
- SP-C-005-06	12
- SP-C-006-06	-
- SP-C-007-07	37
Gender (F/M)	29/22
Geographical region (Asia/Africa)	1/50
Mean PP dose received ± S.D. (mg/kg)	9.2 $\pm$ 1.7
Median PP dose (range) (mg/kg)	9.0 (6.7 – 13.8)
Median age (range) (years)	5 (0.5 – 14)
Median weight (range) (kg)	18.0 (8.0 – 44.0)
Median height (range) (cm)	104 (64 – 158)
Median BMI (range) (kg/m^2)	16.0 (12.1– 23.8)
Median LBW (range) (kg)	15.6 (6.8 – 38.5)
Baseline parasite count (range) (per μL)	11,560 (78 – 297,529)
Median baseline Alanine Aminotransferase (range) (U/L)	25 (7 – 36)
Median baseline Aspartate Aminotransferase (range) (U/L)	38 (21 –79)
Median baseline hematocrit (range) (%)	31 (23.7 – 36.9)
Median baseline hemoglobin (range) (g/L)	104 (80 – 133)
Median baseline erythrocyte count (range) ($x10^{12}$ /L)	4.1 (3.1 – 5.7)

Table 4.5 Comparison of pharmacokinetic parameters (mean ± SD) for pediatric patients in the treatment failure versus success groups.

Parameter	Pediatric Population		p-value†
	Treatment failure group (n=23)	Success group (n=296)	
Ka (d^{-1})	27.1 ± 2.8	28.6 ± 8.2	0.511
CL/F (L/d)	456 ± 323	473 ± 210	0.137
V2/F (L)	5,070 ± 3,898	3,757 ± 3,366	0.099
$T_{½\alpha}$ (d)	1.5 ± 0.6	1.3 ± 0.5	0.12
$T_{½\beta}$ (d)	15.6 ± 9.9	10.7 ± 5.0	0.046Ŧ
Weight-normalized parameters			
CL/F (L/d/kg)	21.4 ± 7.3	19.9 ± 4.3	0.578
V2/F (L/kg)	287 ± 249	165 ± 143	0.033Ŧ

† P-value based on two-sided Wilcoxon rank-sum test.

Ŧ Statistically significant at α=0.05.

Figure 4.1 Natural log-transformed blood pyronaridine concentrations versus time. The solid line is loess smoothing lines.

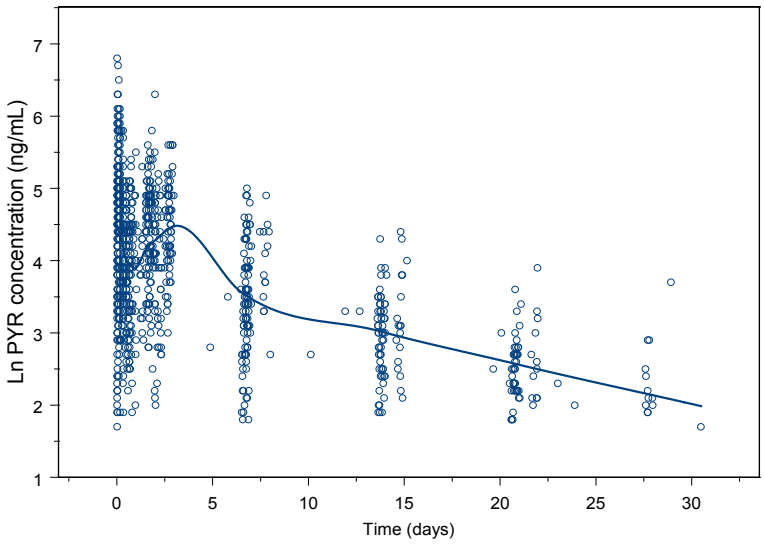

Figure 4.2 Natural log-transformed blood pyronaridine concentrations versus time after dose. The solid line is loess smoothing lines.

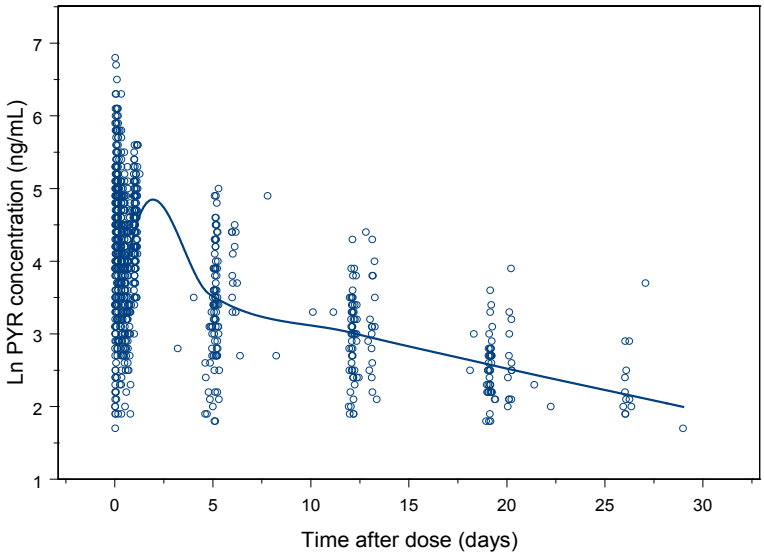

Figure 4.3 Box plots showing median age (left panel) and weight (right panel) for patients received PA tablets (FORM=0) and granule formulation (FORM=1); bars represent 25th and 75th percentiles; whiskers represent 10th and 90th percentiles.

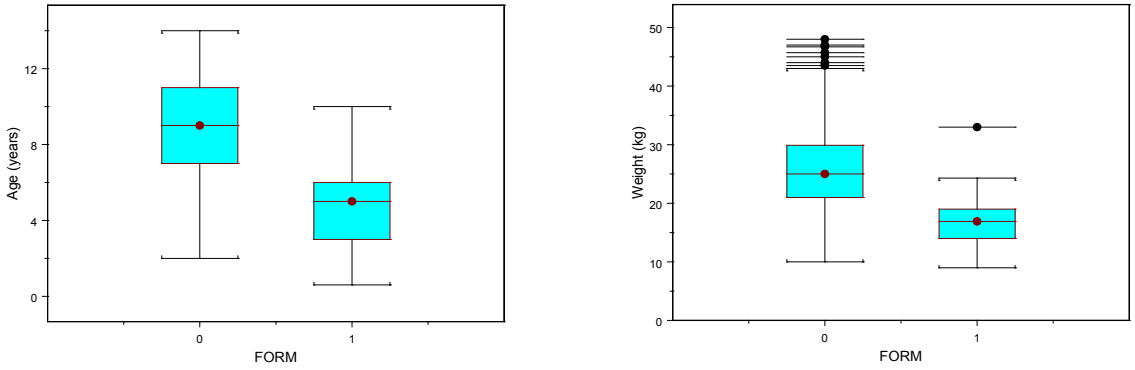

Figure 4.4 Box-plots depicting age (left panel) and weight (right panel) distribution in pediatric Asian population (GEO=0) and African population (GEO=1); bars represent 25th and 75th percentiles; whiskers represent 10th and 90th percentiles.

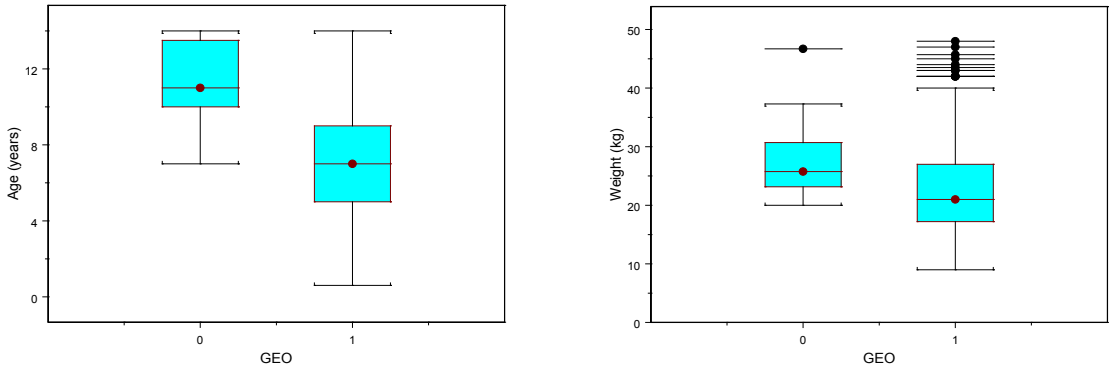

Figure 4.5 Observed concentrations versus Population and individual predicted concentrations plots for the final model. The solid lines are lines of identity.

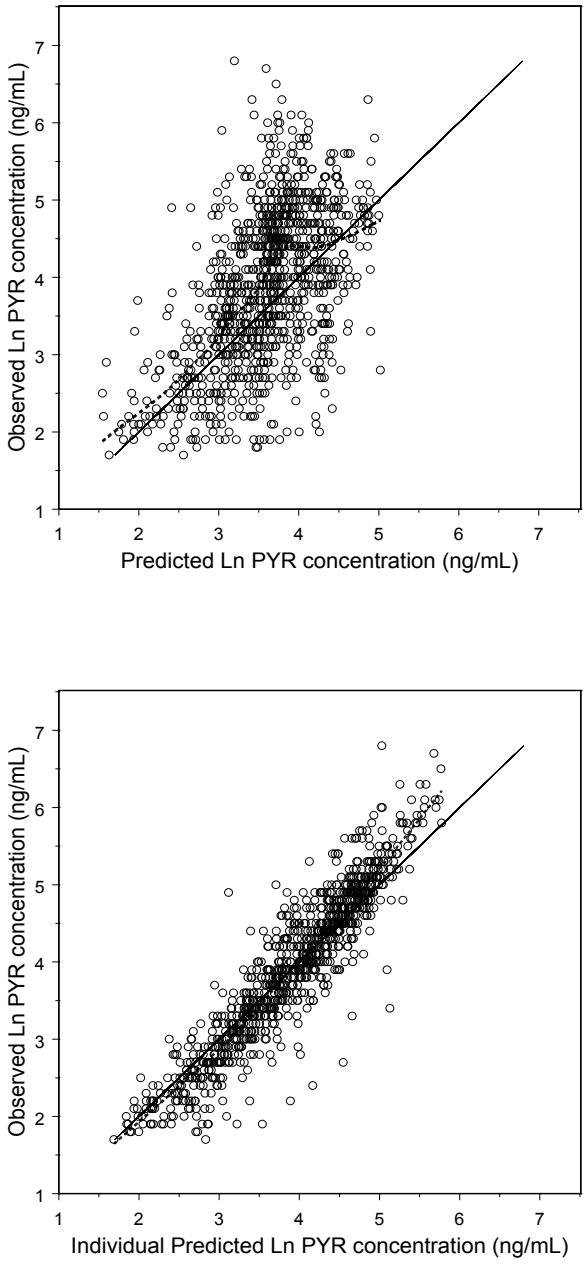

Figure 4.6 Conditional weighted residual plots for the final model. The dotted lines are smoothing lines.

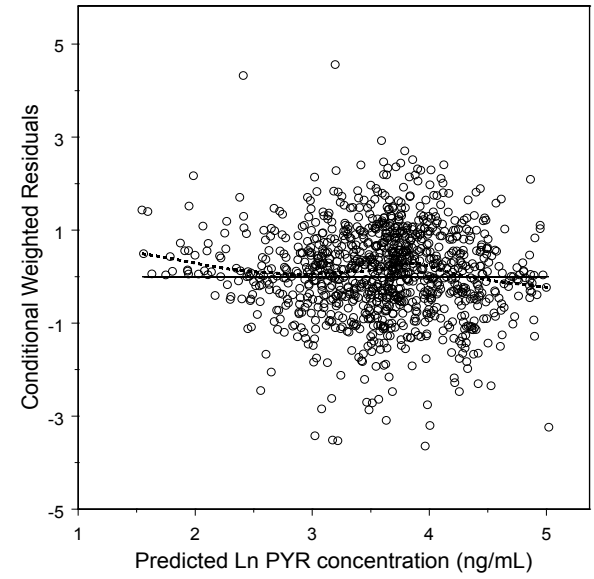

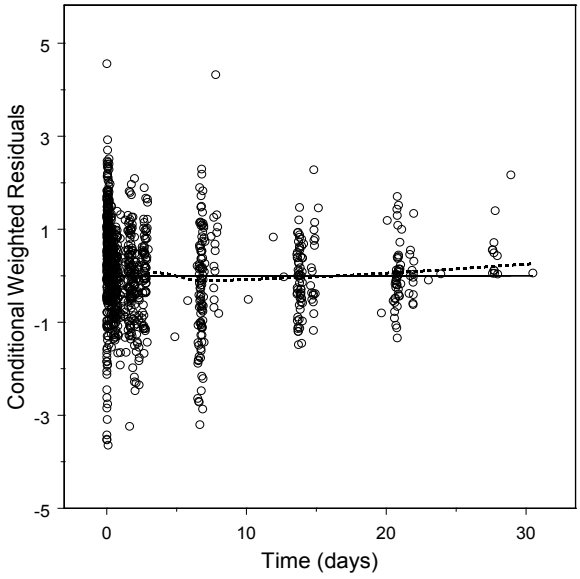

Figure 4.7 Plots of pyronaridine observations (open) and predictions (solid) from the final model for individual subjects with intensive pharmacokinetic sampling.

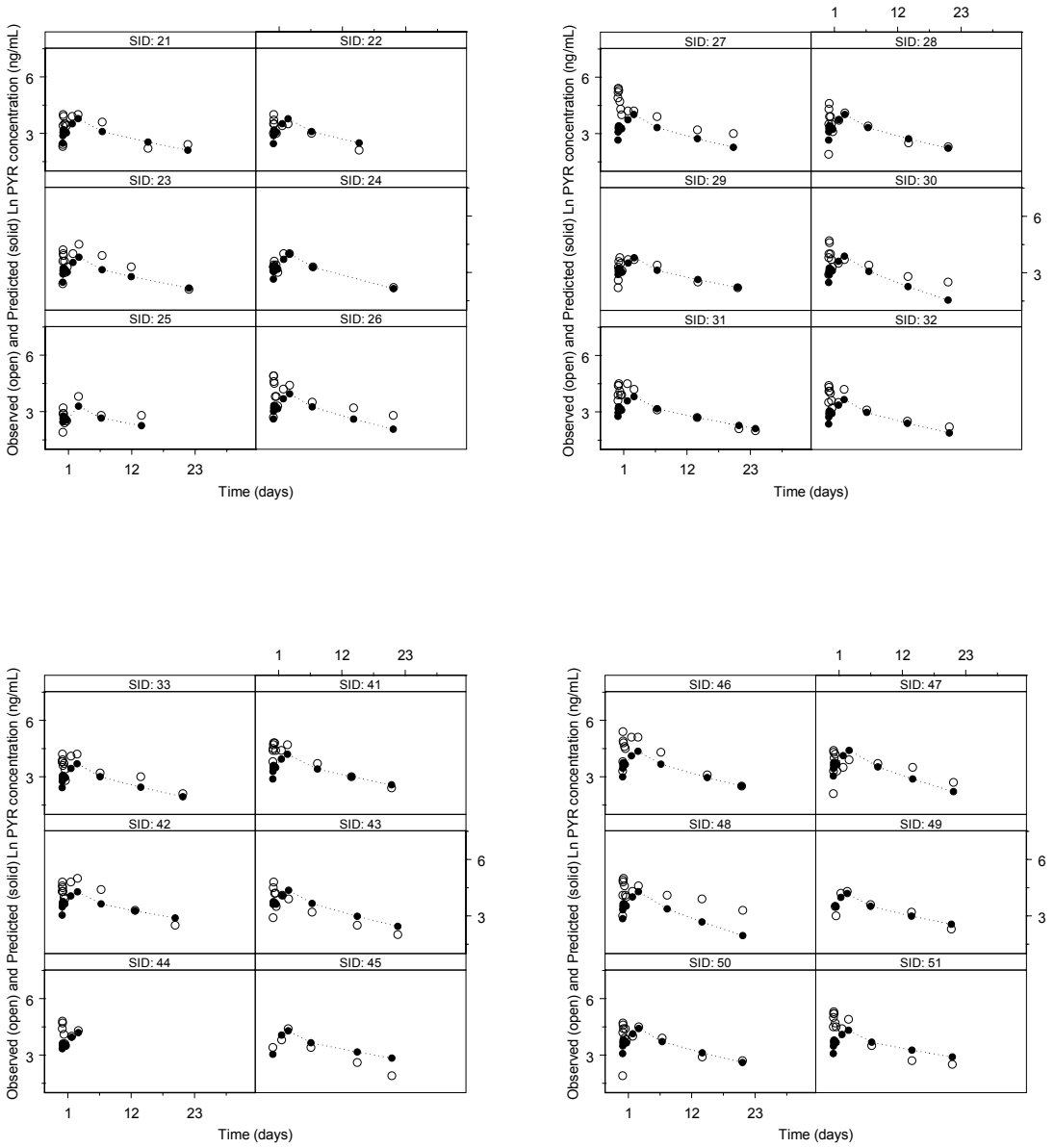

Figure 4.7 continued

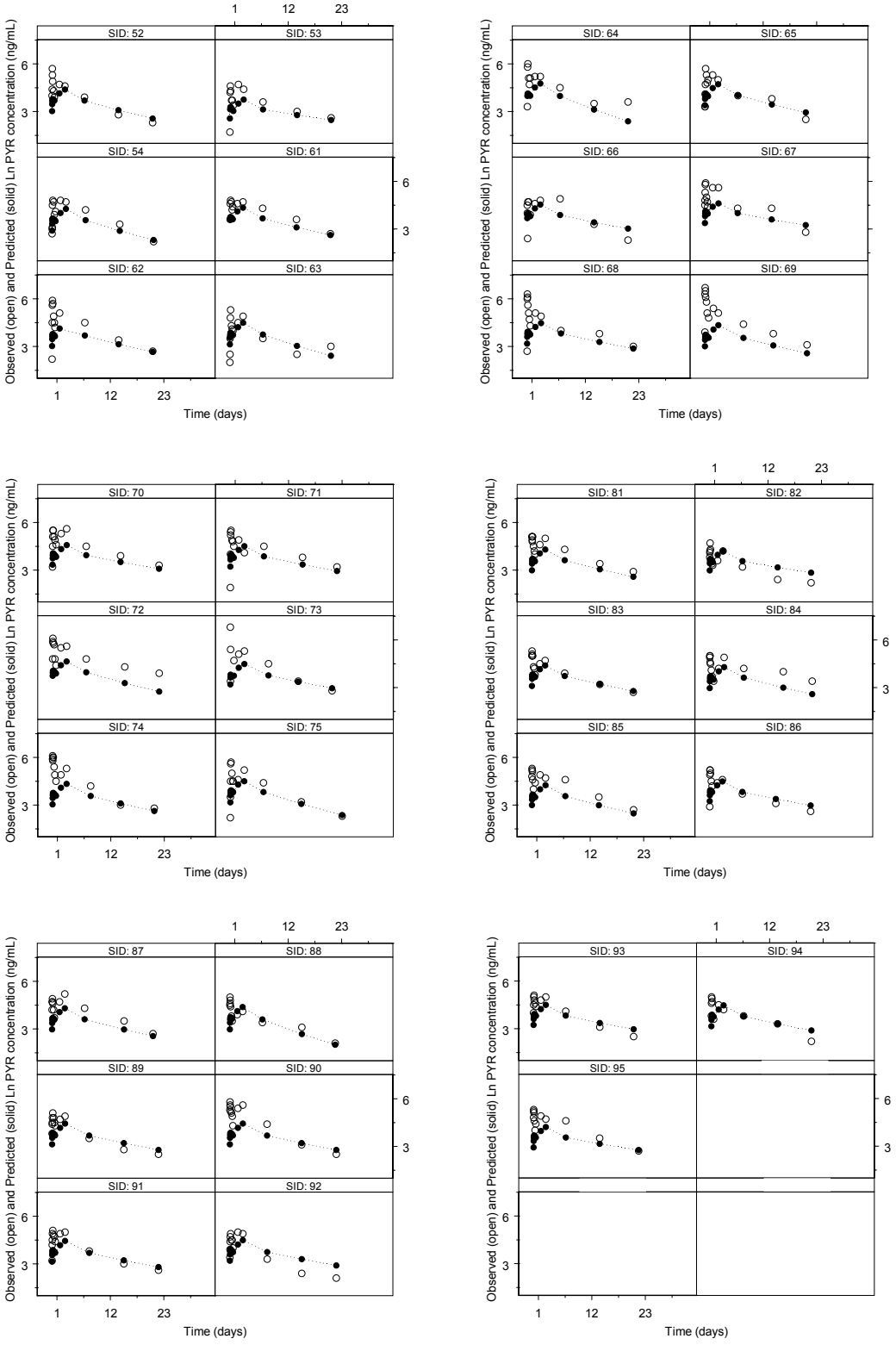

Note: The last three plots were intentionally left blank.

Figure 4.8 Visual Predictive Check of the final model in the adult population. The open circles represent the observed concentrations, solid lines represent the 5th and 95th quantiles, the dashed line represents the 10th and 90th quantiles, and the dotted line represents the 50th percentile obtained from the simulations. The lower graph shows an expanded time scale

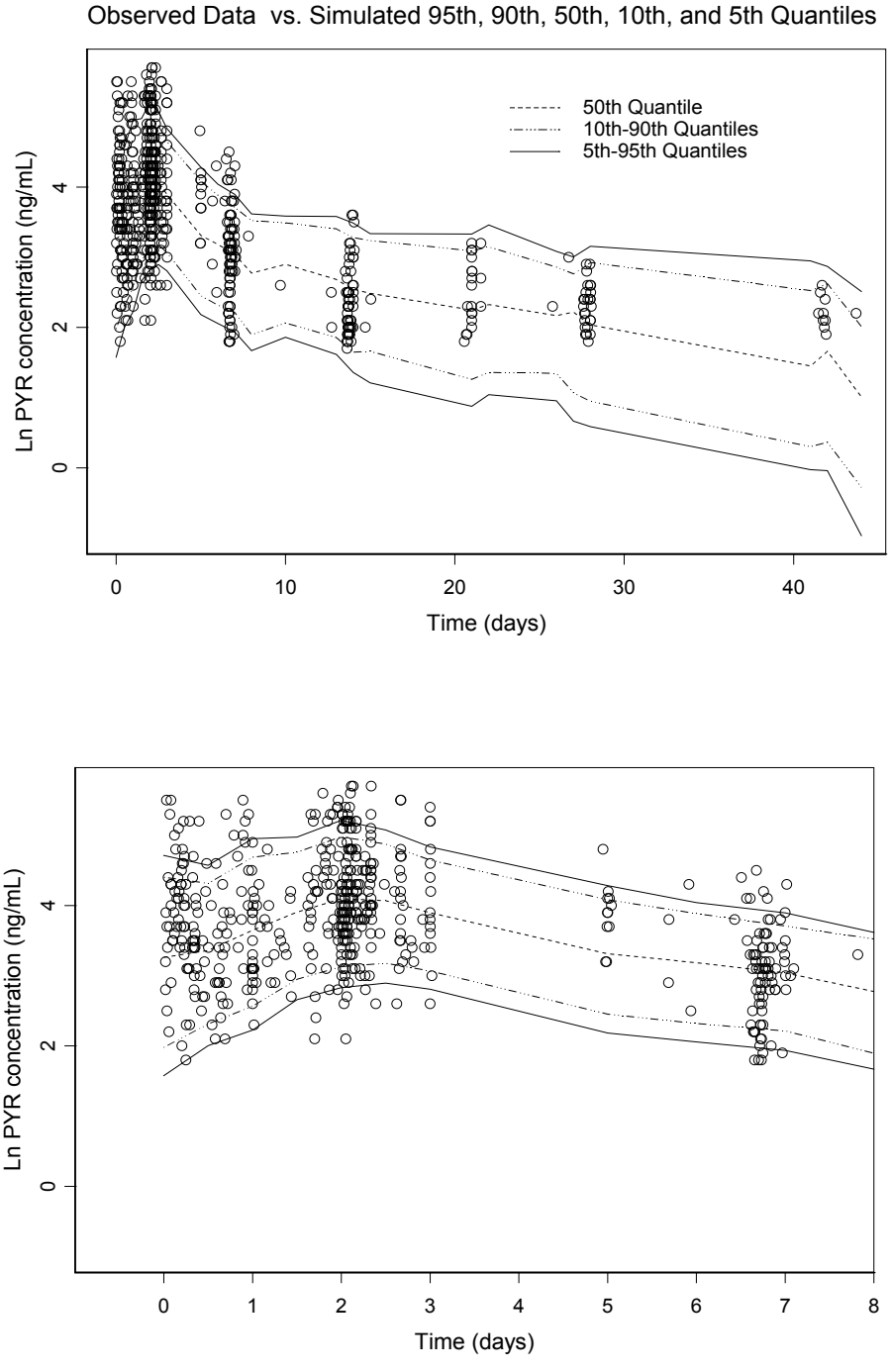

CHAPTER V

COMPARISONS OF STUDY POPULATIONS

Pyronaridine, a promising partner drug in Artemisinin-based combination therapies, has been used extensively as monotherapy to treat malaria in some provinces in China since 1970s[84]. It has been found to be safe and effective in the treatment of uncomplicated malaria[27, 28, 41, 43], but the usage is limited outside China due to the failure to meet international regulatory standards. As a result, there is very limited published data on pharmacokinetics of pyronaridine in humans.

In this thesis, the population pharmacokinetics (PPKs) of pyronaridine has been studied in different populations. In Chapter II, we first explored the structural model of pyronaridine based on extensive data of 91 healthy Korean subjects. The pharmacokinetics of pyronaridine was best characterized with a two-compartment model with first-order absorption and elimination from the central compartment. The pharmacokinetic parameters were estimated with high degree of precision and they were consistent with noncompartmental analysis. Pyronaridine has a large total apparent volume of distribution. Marked variability in drug absorption was evident.

In Chapters III and IV, we examined the PPKs of pyronaridine in 321 adult and 319 pediatric malaria patients, respectively. Pyronaridine pharmacokinetic data from Clinical Phase II and III trials were pooled and we used the cut-off of 14 years of age to perform PPK analysis in adults and children separately. The same structural pharmacokinetic model used in the healthy population also best described the pharmacokinetics of pyronaridine in patient populations. Considerable variability in the absorption rate constant (Ka) and the central compartment volume (V2/F) was observed in patient populations.

We found that the pharmacokinetic properties of pyronaridine are different among the three studied populations, as discussed earlier. Since the same structural

pharmacokinetic model was used in each population, in this chapter we directly compare the results from each analysis to summarize our findings. All statistical analyses were conducted using SPSS 17 (SPSS Inc., Chicago, IL). Since the Shapiro-Wilk test for normality for the data revealed that not all variables follow normal distribution, a two-sided Wilcoxon–Mann–Whitney test was used to test statistical significance at the $\alpha = 0.05$ level.

Comparison of Population Pharmacokinetics of Pyronaridine between Adult malaria patients and Healthy volunteers

Table 5.1 shows a comparison of demographic and pharmacokinetic data between adult patients and healthy subjects. Subject characteristics were significantly different between the two groups. The characteristics of the healthy population were much more homogenous and the healthy Korean subjects' body sizes were generally larger than adult malaria patients. Overall, the healthy population received a higher median dose of Pyronaridine Tetraphosphate (PP) than the adult patient population (11.6 mg/kg versus 10.0 mg/kg, respectively) and the range of studied doses was wider in the Phase I study. This is due to the fact that there were 4 studied dose levels: 6, 9, 12 and 15 mg/kg in the Phase I study and the majority of healthy subjects received 12 mg/kg of PP. In the Clinical Phase II trial, the studied doses were 6, 9 and 12 mg/kg and all patients in the Clinical Phase III trials received a PP dose of 9 mg/kg.

All pharmacokinetic parameters significantly differed between the two populations. In patients, the typical absorption rate constant (Ka) and its inter-subject variability (ISV) were about twice that found in healthy subjects (median Ka = 29.3 and 15.3 d^{-1}, and an ISV of 109 and 54%, in patients and healthy subjects, respectively). This suggests that pyronaridine was absorbed faster and more variably in patients. Patients have higher oral clearance (CL/F), but the drug is eliminated more slowly than healthy

subjects due to a considerable increase in volume of distribution of the drug. Median elimination half-lives were 16.7 days in patients and 8.5 days in healthy subjects. The blood levels of pyronaridine were followed for a longer time period in Phase II and III studies (21 – 42 days) than in Phase I studies (10 days) which likely contributed to the longer half-life in patients.

Five-hundred pyronaridine concentration-time profiles were simulated to illustrate its pharmacokinetics in each population. The median weight of the patient population (52 kg) was used and the PP dose was calculated based on the typical dose used in adult and children for the treatment of malaria (9 mg/kg body weight). The simulated profiles of healthy subjects and adult patients are shown in Figure 5.1 and 5.2, respectively. The concentration-time curve for patients significantly differed from that for healthy subjects. In patients, the maximum concentration (Cmax) was significantly lower than those of healthy subjects and the decline of blood concentrations in the terminal phase was slower. Figure 5.3 shows a comparison of the median simulated profiles of the two populations.

Comparison of Population Pharmacokinetics of Pyronaridine between Adult and Pediatric Malaria patients

A comparison of demographic and pharmacokinetic data between adult and pediatric patients is shown in Table 5.2. Interestingly, although the studied dose levels were similar across adult and pediatric Phase II studies (PP dose of 6, 9 and 12 mg/kg) and across Phase III studies (PP dose of 9 mg/kg), the PP doses in these two populations were significantly different. Overall, PP dose in the pediatric population is lower with a wider range. These differences are due to dose stratification according to the study protocol and the difficulty of adjusting the dose for the children taking tablets. For example, Table 5.3 shows the dosing regimen used in three adult and pediatric Phase III studies (SP-C-004-06, SP-C-005-06, and SP-C-006-06), which tends to provide an

average PP dose of 10 mg/kg for a subject weighing above 25 kg and an average PP dose of 8 mg/kg for a subject weighing 25 kg and less.

There were significant differences between the pyronaridine pharmacokinetics of adult patients and those of pediatric patients. Since the sample sizes were large, even small differences, such as in Ka and CL/F, between the two populations were found to be statistically significant. However, these differences seem clinically unimportant. As a result of a substantially larger volume of distribution in adults, the elimination half-life in the adult population was longer. Figure 5.4 illustrates 500 simulated concentration-time profiles in children using the final model based on the median value of weight (22 kg) of the pediatric population and the standard PP dose of 9 mg/kg. Figure 5.5 shows the comparison of median simulated profiles between adult and pediatric populations. As a result of a smaller central volume of distribution in children, the simulated Cmax of pediatric patients was higher than those of adult patients. It is worth mentioning again that the median PP dose in adults was higher than in children included in the analysis. The simulated profile also illustrates that the terminal decline in concentrations in children was faster.

In the adult population, lean body weight (LBW) was a significant covariate of central compartment volume (V2/F). There was an increase in V2/F as LBW increased. The relationship was best described by an exponential model (Figure 5.6). LBW was also identified as an important covariate of V2/F during the stepwise forward addition in the Phase 1 study but it was not significant enough to remain in the final model. This result is most likely because the healthy population is relatively homogenous in body size. Unlike the adult patient population, actual body weight (WT) was a significant predictor of V2/F and CL/F in pediatric patient population. Power models were used to characterize the relationships with estimated power terms of 0.83 and 1.17 for V2/F and CL/F, respectively (Figure 5.7 and 5.8). V2/F increases with increasing WT, but not weight-normalized V2/F. Young children tends to have high weight-normalized V2/F and this

would result in low blood concentrations of pyronaridine in the central compartment which represents the concentrations at target sites of pyronaridine. This could be therapeutically important because young children are vulnerable to the disease, as their immune systems are not fully developed.

In summary, the pharmacokinetic properties of pyronaridine were characterized by a two-compartment disposition model with first-order absorption and elimination from the central compartment. Residual variability was evaluated using an additive error model after natural logarithmic transformation of the observed blood concentrations. The final models were stable and showed good robustness. The parameters were plausible and estimated with acceptable precision.

Pyronaridine exhibits a very large apparent volume of distribution and a slow elimination phase. The absorption and distribution of pyronaridine showed considerable variability in patient populations. Pharmacokinetic modeling suggests that LBW is an important predictor of V2/F in adult patients while WT is a significant covariate of V2/F and CL/F in children. Further study will be necessary to examine other covariates that could influence the drug absorption and disposition.

Table 5.1 Comparison of demographic and pharmacokinetic data between adult patients and healthy volunteers.

Parameter	Median (range) for:		P-value[¥]
	Adult Patients (n=321)	Healthy Subjects (n=91)	
Age (years)	26 (15 – 60)	23 (19 – 40)	0.005[§]
Weight (kg)	52.0 (24.8 – 80.0)	61.5 (50.1 – 70.0)	0.000[§]
Height (cm)	161 (127 – 178)	171 (154 – 183)	0.000[§]
BMI (kg/m^2)	20.1 (14.0 – 35.6)	21.1 (18.1– 23.8)	0.000[§]
LBW (kg)	42.9 (22.4 – 57.1)	50.2 (37.9 – 57.4)	0.000[§]
PP dose (mg/kg)	10.0 (6.2 – 13.3)	11.6 (5.7 – 15.2)	0.000[§]
Ka (d^{-1})	29.3 (8.8 – 70.4)	15.3 (5.2 – 39.0)	0.000[§]
CL/F (L/d/kg)	22.6 (8.1 – 69.0)	9.4 (4.5 – 39.9)	0.000[§]
V2/F (L/kg)	160.6 (24.7 – 1274.9)	12.0 (8.2 – 18.7)	0.000[§]
V3/F (L/kg)	254[€]	71.4 (62.7 – 87.6)	NA[†]
$t_{½,\alpha}$ (d)	1.5 (0.4 – 4.5)	0.3 (0.1 – 0.4)	0.000[§]
$t_{½,\beta}$ (d)	16.7 (8.5 – 54.1)	8.5 (2.7 – 16.5)	0.000[§]

[¥] P-value based on two-side Wilcoxon rank-sum test.

[§] Statistically significant at $\alpha = 0.05$.

[€] The value was calculated for a subject with median weight as no ISV on this parameter.

[†] The statistic comparison has been omitted since ISV in the patient population cannot be estimated.

Table 5.2 Comparison of demographic and pharmacokinetic data between adult and pediatric patients.

Parameter	Median (range) for: Adult Patients (n=321)	Pediatric Patients (n=319)	P-value[¥]
Age (years)	26 (15 – 60)	7 (0.6 – 14)	0.000[§]
Weight (kg)	52.0 (24.8 – 80.0)	22 (9.0 – 48.0)	0.000[§]
Height (cm)	161 (127 – 178)	120 (65 – 160)	0.000[§]
BMI (kg/m^2)	20.1 (14.0 – 35.6)	15.5 (6.0– 26.5)	0.000[§]
LBW (kg)	42.9 (22.4 – 57.1)	19.3 (7.3 – 40.7)	0.000[§]
PP dose (mg/kg)	10.0 (6.2 – 13.3)	9.3 (4.2 – 16.3)	0.013[§]
Ka (d^{-1})	29.3 (8.8 – 70.4)	28.0 (8.1 – 96.9)	0.000[§]
CL/F (L/d/kg)	22.6 (8.1 – 69.0)	19.7 (8.7 – 45.0)	0.000[§]
V2/F (L/kg)	160.6 (24.7 – 1274.9)	125.5 (13.6 – 920.9)	0.000[§]
V3/F (L/kg)	254[€]	90[€]	NA[†]
$t_{½, \alpha}$ (d)	1.5 (0.4 – 4.5)	1.3 (0.2 – 2.4)	0.000[§]
$t_{½, \beta}$ (d)	16.7 (8.5 – 54.1)	10.4 (4.0 – 36.4)	0.000[§]

[¥] P-value based on two-side Wilcoxon rank-sum test.

[§] Statistically significant at $\alpha = 0.05$.

[€] The values were calculated for a subject with median weight as no ISV on this parameter.

[†] The statistic comparison has been omitted since ISV cannot be estimated.

Table 5.3 Dosing regimen of Pyronaridine Artesunate (PA) 180:60 mg tablet used in three phase III studies in children and adult patients studies (SP-C-004-06, SP-C-005-06, and SP-C-006-06).

Weight (kg)	Number of PA tablet to be administered once daily on day 0, 1, 2	The amount of PP[†] (mg)	Estimated average and range[§] of PP [†] dose (mg/kg)
20 – 25	1	180	8.1 (7.2 – 9.0)
26 – 44	2	360	11.0 (8.2 – 13.8)
45 – 64	3	540	10.2 (8.4 – 12.0)
65 – 90	4	720	9.5 (8.0 – 11.1)

[†] Pyronaridine tetraphosphate

[§] Calculated using minimum and maximum weight in each level

Figure 5.1 Plots of 500 simulated pyronaridine concentration-time profiles using the final model from Phase I studies. A median weight of the adult patient population of 52 kg and a standard dose of pyronaridine tetraphosphate of 9 mg/kg were used. The open circles represent the simulated concentrations, solid lines represent the 90% confidence interval obtained from the simulations, and the dashed line represents the 50th percentile of the simulations.

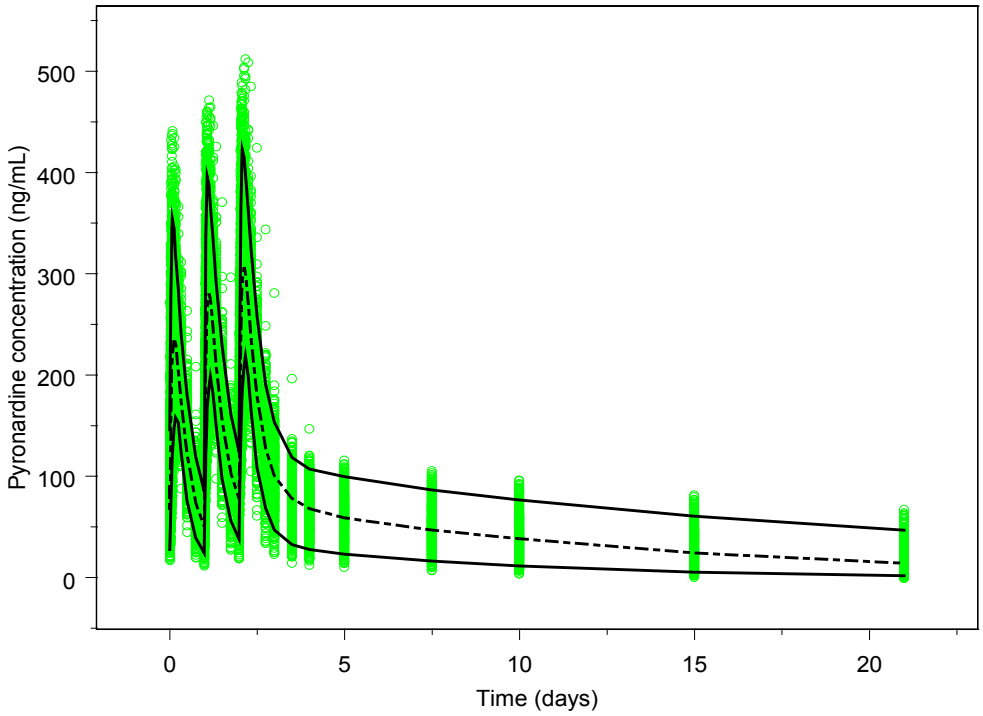

Figure 5.2 Plots of 500 simulated pyronaridine concentration-time profiles using the final model from adult patients data. A median weight of 52 kg and a standard dose of pyronaridine tetraphosphate of 9 mg/kg were used. The open circles represent the simulated concentrations, solid lines represent the 90% confidence interval obtained from the simulations, and the dashed line represents the 50^{th} percentile of the simulations.

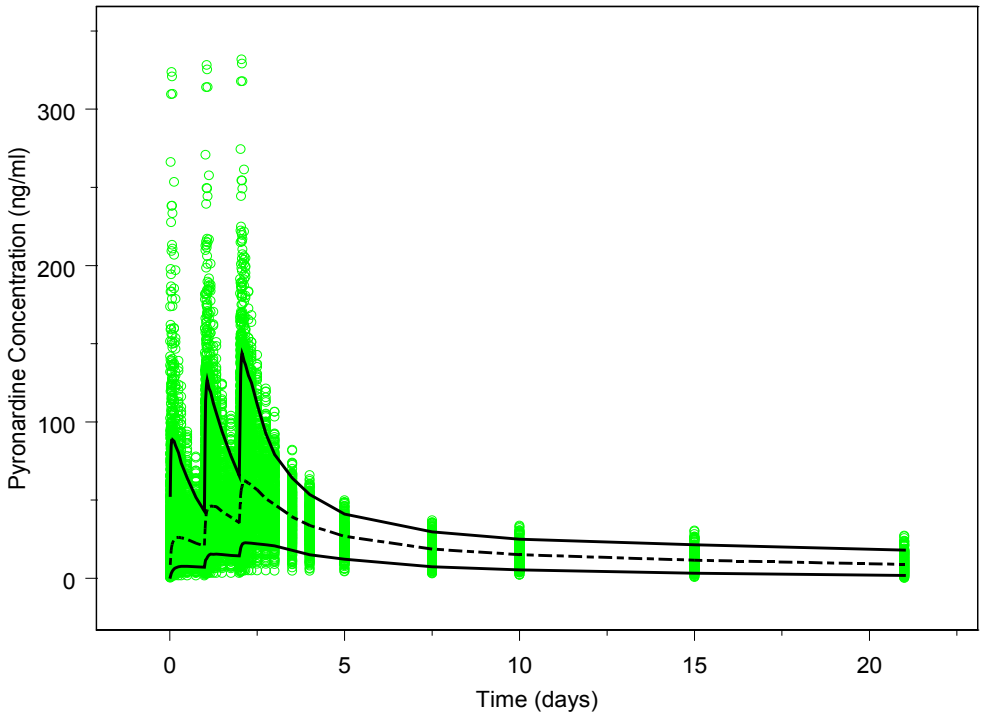

Figure 5.3 Comparison of the median simulated profiles of adult patients versus healthy subjects. The median weight of 52 kg of the adult patient population and the standard PP dose of 9 mg/kg were used.

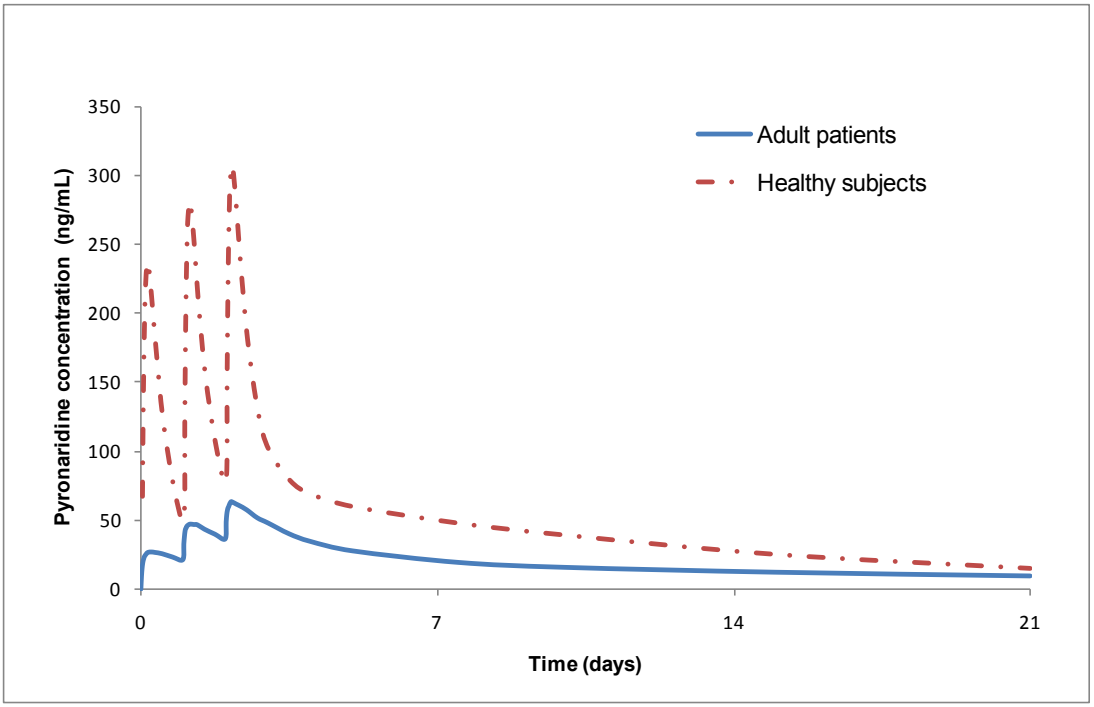

Figure 5.4 Plots of 500 simulated pyronaridine concentration-time profiles using the final model from pediatric patients data. A median weight of 22 kg and a standard dose of pyronaridine tetraphosphate of 9 mg/kg were used. The open circles represent the simulated concentrations, solid lines represent the 90% confidence interval obtained from the simulations, and the dashed line represents the 50th percentile of the simulations.

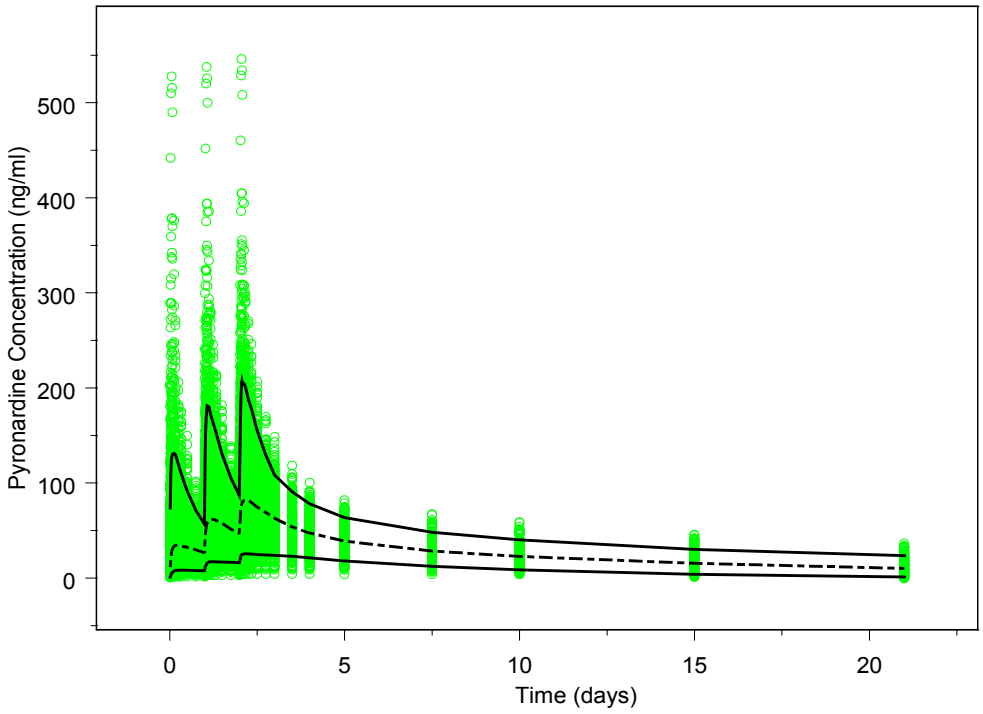

Figure 5.5 Comparison of the median simulated profiles of 52-kg adult versus 22-kg pediatric patients. The standard PP dose of 9 mg/kg were used.

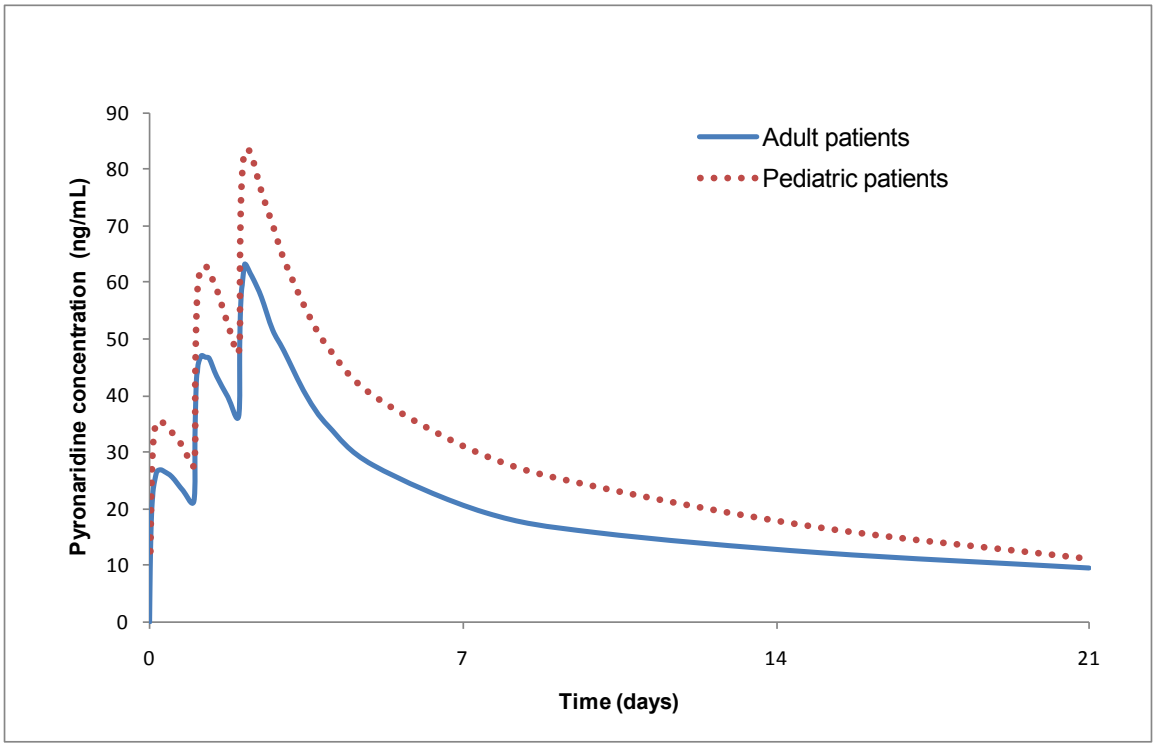

Figure 5.6 Relationship of pyronaridine central compartment volume (V2/F) and lean body weight (LBW) in the adult patient population. The lower panel shows the same relationship with a different unit of V2/F (L/kg of LBW).

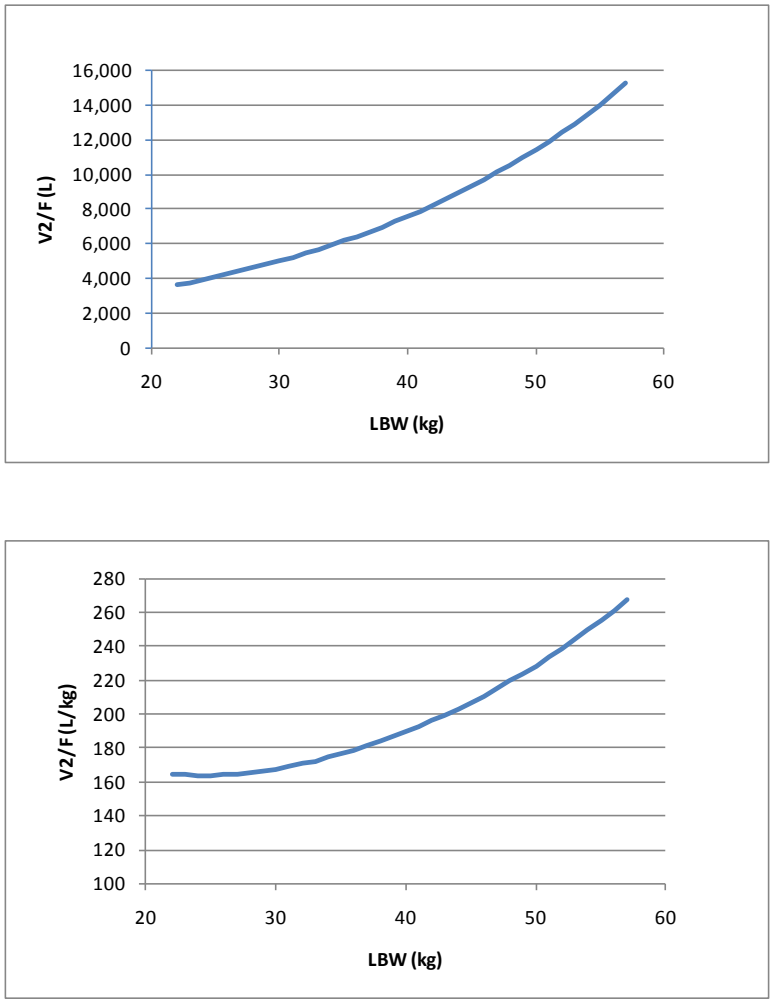

Figure 5.7 Relationship of pyronaridine central compartment volume (V2/F) and actual body weight (WT) in the pediatric patient population. The lower panel shows the same relationship with a different unit of V2/F (L/kg of WT).

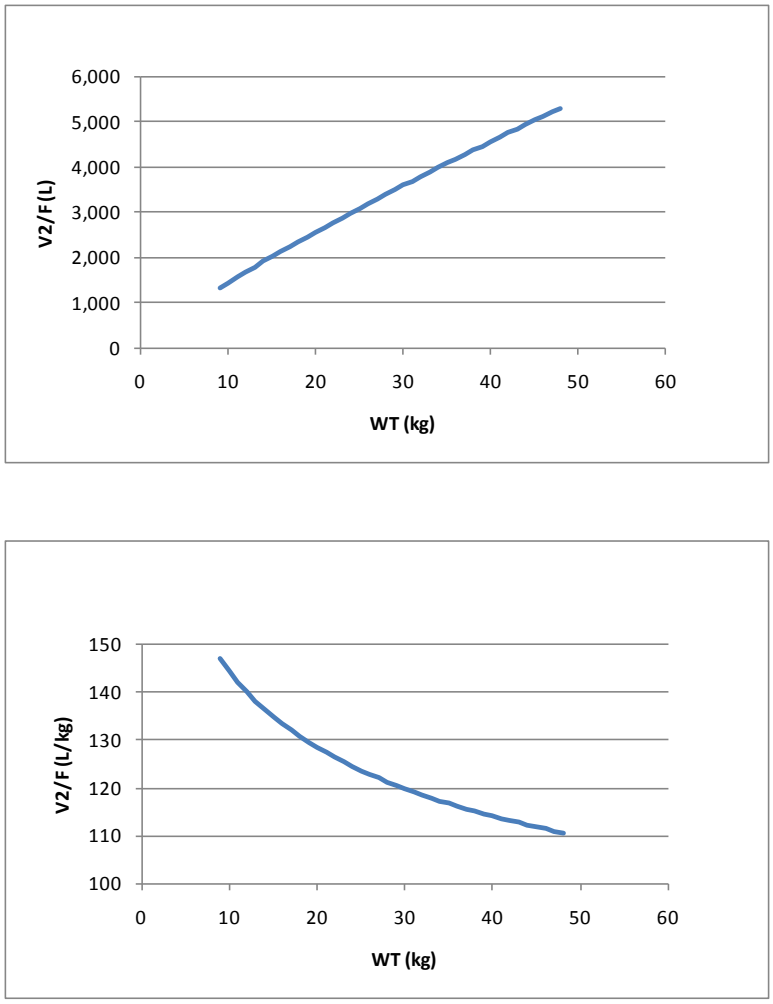

Figure 5.8 Relationship of pyronaridine oral clearance (CL/F) and actual body weight (WT) in the pediatric population. The lower panel shows the same relationship with a different unit of CL/F (L/d/kg of WT).

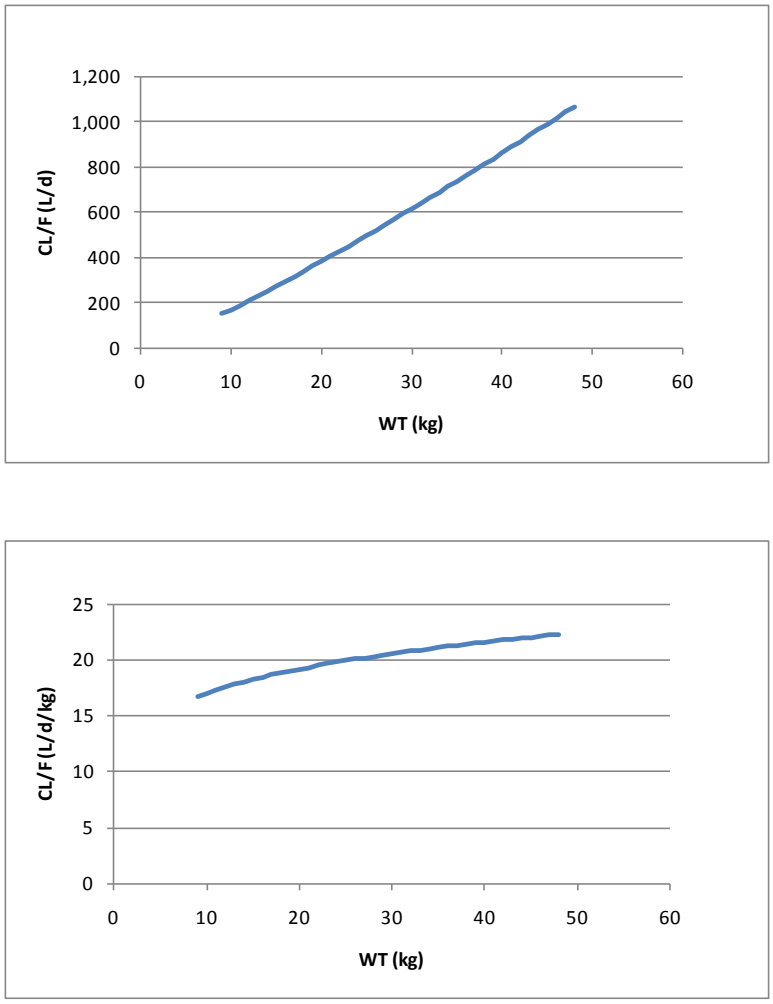

CHAPTER VI

CONCLUSIONS

Pyronaridine pharmacokinetics was best described by a two-compartment model with first order absorption and elimination from the central compartment. The modeling suggests that pharmacokinetic properties of pyronaridine were different among healthy, adult patient and pediatric patient populations. Pyronaridine absorption was faster and more variable in patient populations. Pyronaridine has a large total apparent volume of distribution (V/F). The weighted-normalized V/F in adult and pediatric patient populations were approximately 5 and 3 times, respectively, larger than in healthy subjects. Adult and pediatric patients had a mean weight-normalized oral clearance (CL/F) approximately twice that found in healthy subjects but the drug is eliminated more slowly in patient populations due to a much larger V/F. The average estimated elimination half-lives were 8, 11 and 18 days in healthy, pediatric patient and adult patient populations, respectively.

Pharmacokinetic modeling suggests that lean body weight is an important covariate of apparent central volume of distribution (V2/F) in the adult patient population while actual body weight is a significant predictor of V2/F and CL/F in the pediatric patient population. Further study in a broader patient population, including time-varying covariates will be necessary to examine factors that could influence the absorption and disposition of pyronaridine.

APPENDIX A

NONMEM CONTROL FILE FOR THE FINAL MODEL IN CHAPTER II

```
$PROB RUN# 090107
$INPUT C ID TIME TSLD AMT DV XDV MDV AGE SEX WT HT BMI LBW ART REM=DROP CAT=DROP TOD=DROP
IOV=DROP STD=DROP
$DATA 020709PYRPHASE1WOFOOD.CSV IGNORE=C
$ABB COMRES=6
$SUBROUTINES ADVAN4 TRANS4
$PK
   TVKA=THETA(1)
   KA=TVKA*EXP(ETA(1))
   TVCL=THETA(2)
   CL=TVCL*EXP(ETA(2))
   TVV2=THETA(3)
   V2=TVV2*EXP(ETA(3))
   TVQ=THETA(4)
   Q=TVQ*EXP(ETA(4))
   TVV3=THETA(5)
   V3=TVV3*EXP(ETA(5))
   S2=V2/1000
   TAD=TSLD
   K20=CL/V2
   K23=Q/V2
   K32=Q/V3
   BETA=((K23+K32+K20)-SQRT(((K23+K32+K20)**2) - 4*K32*K20))*0.5
   ALPHA=K32*K20/BETA
   TBETA=LOG(2)/BETA
   TALPHA=LOG(2)/ALPHA
$INFN
IF (ICALL.EQ.3) THEN
 OPEN(50,FILE='CWTAB090100.est')
 WRITE (50,*) 'ETAS'
DO WHILE(DATA)
IF (NEWIND.LE.1) WRITE(50,*) ETA
ENDDO
 WRITE (50,*) 'THETAS'
 WRITE (50,*) THETA
 WRITE (50,*) 'OMEGAS'
 WRITE (50,*) OMEGA(BLOCK)
 WRITE (50,*) 'SIGMAS'
 WRITE (50,*) SIGMA(BLOCK)
ENDIF
$ERROR
   IPRED=0
   IF (F.GT.0) IPRED=LOG(F)
   W = 1; additive error model
   IRES = DV-IPRED
   IWRES = IRES/W
   Y = IPRED + W*ERR(1)
"LAST
"  COM(1)=G(1,1)
"  COM(2)=G(2,1)
"  COM(3)=G(3,1)
"  COM(4)=G(4,1)
"  COM(5)=G(5,1)
"  COM(6)=HH(1,1)
$EST METHOD=1 INTERACTION PRINT=5 MAX=9999 SIG=3     MSFO=090107.msf
$THETA
  (0, 20) ;[KA]
  (0, 800) ;[CL]
  (0, 1000) ;[V2]
  (0, 2000) ;[Q]
  (0, 8000) ;[V3]
$OMEGA
  0.1 ;[P] omega(1,1)
  0.1 ;[P] omega(2,2)
  0.1 ;[P] omega(3,3)
  0.1 ;[P] omega(4,4)
  0, FIXED ;[P] omega(5,5)
$SIGMA
  0.1 ;[A] sigma(1,1)
```

```
$COV PRINT=E
$TABLE ID TIME TAD IPRED IWRES KA CL V2 V3 Q TBETA TALPHA TSS CLW V2W V3W VSS AUC SEX AGE
WT HT BMI LBW ONEHEADER NOPRINT FILE=090107.tab
$TABLE ID KA CL V2 V3 Q FIRSTONLY NOAPPEND NOPRINT FILE=090107FOCEI.par
$TABLE ID ETA1 ETA2 ETA3 ETA4 ETA5  FIRSTONLY NOAPPEND NOPRINT FILE=090107FOCEI.eta
$TABLE ID COM(1)=G11 COM(2)=G21 COM(3)=G31 COM(4)=G41 COM(5)=G51 COM(6)=H11 IPRED IWRES
MDV ONEHEADER NOPRINT FILE=090107FOCEI.deriv
```

APPENDIX B

THE OUTPUT SUMMARY FOR THE FINAL MODEL IN CHAPTER II

```
MINIMIZATION STATUS
  MINIMIZATION SUCCESSFUL
  NO. OF FUNCTION EVALUATIONS USED:      226
  NO. OF SIG. DIGITS IN FINAL EST.:  3.4

  ETABAR IS THE ARITHMETIC MEAN OF THE ETA-ESTIMATES,
  AND THE P-VALUE IS GIVEN FOR THE NULL HYPOTHESIS THAT THE TRUE MEAN IS 0.

  ETABAR:  -0.18E-01  0.13E-01 -0.13E-01 -0.14E-01  0.00E+00
  SE:       0.46E-01  0.44E-01  0.17E-01  0.23E-01  0.00E+00

  P VAL.:   0.69E+00  0.77E+00  0.47E+00  0.55E+00  0.10E+01
  MINIMUM VALUE OF OBJECTIVE FUNCTION :    -1145.091

ETABAR P VAL. FOR NO ETA < 0.05

MODEL DEFINITION
   TVKA=THETA(1)
   KA=TVKA*EXP(ETA(1))
   TVCL=THETA(2)
   CL=TVCL*EXP(ETA(2))
   TVV2=THETA(3)
   V2=TVV2*EXP(ETA(3))
   TVQ=THETA(4)
   Q=TVQ*EXP(ETA(4))
   TVV3=THETA(5)
   V3=TVV3*EXP(ETA(5))
   S2=V2/1000
```

	FINAL ESTIMATE	%RSE	95% CONFIDENCE INTERVAL LBOUND	UBOUND	DESCRIPTOR/ VARIABILITY	
THETA						
1	15.4	10.1%	12.4	18.4		KA
2	614	4.30%	562	666		CL
3	738	5.89%	653	823		V2
4	1.27e+003	5.24%	1.14e+003	1.40e+003		Q
5	4.39e+003	7.97%	3.70e+003	5.08e+003		V3
OMEGA					INTERINDIVIDUAL VARIABILITY	
1,1	0.291	20.2%	0.176	0.406	CV =	53.9%
2,2	0.203	22.4%	0.114	0.292	CV =	45.1%
3,3	0.0590	41.5%	0.0110	0.107	CV =	24.3%
4,4	0.0956	37.2%	0.0258	0.165	CV =	30.9%
SIGMA					RESIDUAL VARIABILITY	
1,1	0.150	10.7%	0.118	0.182	SD =	0.387

```
*Indicates 95% confidence interval that includes zero
%RSE is percent relative standard error (100% x SE/EST)

        Akaike Information Criterion: -1125.09
        Schwarz Bayesian Criterion:   -1069.99
CONDITION NUMBER = 42.9 (DOES NOT EXCEED 1000)
```

APPENDIX C

NONMEM CONTROL FILE FOR THE FINAL MODEL IN CHAPTER III

```
$PROB RUN# 278
$INPUT C ID AMT TIME TAD XDV=DROP DV MDV EVID SEX AGE WT HT BMI LBW PARA ALT AST HCT HGB
RBC IFXN=DROP GEO=DROP COUN=DROP OCC=DROP FORM=DROP TOUT=DROP
$DATA ADT.CSV IGNORE=C
$ABB COMRES=6
$SUBROUTINES ADVAN4 TRANS4
$PK
   TVKA=THETA(1)
   KA=TVKA*EXP(ETA(1))
   TVCL=THETA(2)
   CL=TVCL*EXP(ETA(2))
   TVV2=(THETA(3)*EXP((LBW-42.9)*THETA(6)))
   V2=TVV2*EXP(ETA(3))
   TVV3=THETA(4)
   V3=TVV3*EXP(ETA(4))
   TVQ=THETA(5)
   Q=TVQ*EXP(ETA(5))
   S2=V2/1000
   K20=CL/V2
   K23=Q/V2
   K32=Q/V3
   BETA=((K23+K32+K20)-SQRT(((K23+K32+K20)**2) - 4*K32*K20))*0.5
   ALPHA=K32*K20/BETA
   TBETA=LOG(2)/BETA
   TALPHA=LOG(2)/ALPHA
$INFN
IF (ICALL.EQ.3) THEN
 OPEN(50,FILE='CWTAB278.est')
 WRITE (50,*) 'ETAS'
DO WHILE(DATA)
IF (NEWIND.LE.1) WRITE(50,*) ETA
ENDDO
 WRITE (50,*) 'THETAS'
 WRITE (50,*) THETA
 WRITE (50,*) 'OMEGAS'
 WRITE (50,*) OMEGA(BLOCK)
 WRITE (50,*) 'SIGMAS'
 WRITE (50,*) SIGMA(BLOCK)
ENDIF
$ERROR
   IPRED=0
   IF (F.GT.0) IPRED=LOG(F)
   W = 1; additive error model
   IRES = DV-IPRED
   IWRES = IRES/W
   Y = IPRED + W*ERR(1)
"LAST
"  COM(1)=G(1,1)
"  COM(2)=G(2,1)
"  COM(3)=G(3,1)
"  COM(4)=G(4,1)
"  COM(5)=G(5,1)
"  COM(6)=HH(1,1)
$EST METHOD=1  INTERACTION PRINT=5 MAX=9999 SIG=3     MSFO=278.msf
$THETA
  (3, 20);[KA]
  (0, 1000);[CL]
  (500, 6000);[V2]
  (500, 10000);[V3]
  (0, 3000);[Q]
  (-INF, 0.5, INF);[THETA6 LBW ON V2]
$OMEGA
  0.3 ;[P] omega(1,1)
  0.3 ;[P] omega(2,2)
  0.3 ;[P] omega(3,3)
  0, FIXED ;[P] omega(4,4)
  0, FIXED ;[P] omega(5,5)
$SIGMA
  0.3 ;[A] sigma(1,1)
```

```
$COV PRINT=E
$TABLE ID TIME TAD DV PRED IPRED IWRES CL V2 Q V3 KA TBETA TALPHA SEX AGE WT HT BMI LBW
PARA ALT AST HCT HGB RBC ONEHEADER NOPRINT FILE=278.tab
$TABLE ID CL V2 Q V3 KA FIRSTONLY NOAPPEND NOPRINT FILE=278.par
$TABLE ID ETA1 ETA2 ETA3 ETA4 ETA5  FIRSTONLY NOAPPEND NOPRINT FILE=278.eta
$TABLE ID COM(1)=G11 COM(2)=G21 COM(3)=G31 COM(4)=G41 COM(5)=G51 COM(6)=H11 IPRED MDV
ONEHEADER NOPRINT FILE=CWTAB278.deriv
```

APPENDIX D

THE OUTPUT SUMMARY FOR THE FINAL MODEL IN CHAPTER III

```
MINIMIZATION STATUS
  MINIMIZATION SUCCESSFUL
  NO. OF FUNCTION EVALUATIONS USED:      312
  NO. OF SIG. DIGITS IN FINAL EST.:  3.1

  ETABAR IS THE ARITHMETIC MEAN OF THE ETA-ESTIMATES,
  AND THE P-VALUE IS GIVEN FOR THE NULL HYPOTHESIS THAT THE TRUE MEAN IS 0.

  ETABAR:  -0.19E-01  0.84E-02  0.14E-01  0.00E+00  0.00E+00
  SE:       0.12E-01  0.16E-01  0.38E-01  0.00E+00  0.00E+00

  P VAL.:   0.11E+00  0.60E+00  0.72E+00  0.10E+01  0.10E+01
  MINIMUM VALUE OF OBJECTIVE FUNCTION :    8.470

ETABAR P VAL. FOR NO ETA < 0.05

MODEL DEFINITION
   TVKA=THETA(1)
   KA=TVKA*EXP(ETA(1))
   TVCL=THETA(2)
   CL=TVCL*EXP(ETA(2))
   TVV2=(THETA(3)*EXP((LBW-42.9)*THETA(6)))
   V2=TVV2*EXP(ETA(3))
   TVV3=THETA(4)
   V3=TVV3*EXP(ETA(4))
   TVQ=THETA(5)
   Q=TVQ*EXP(ETA(5))
   S2=V2/1000
```

	FINAL ESTIMATE	%RSE	95% CONFIDENCE INTERVAL LBOUND	UBOUND	DESCRIPTOR/ VARIABILITY
THETA					
1	29.2	19.9%	17.8	40.6	KA
2	1.18e+003	10.1%	947	1.41e+003	CL
3	8.54e+003	7.30%	7.32e+003	9.76e+003	V2
4	1.32e+004	24.3%	6.91e+003	1.95e+004	V3
5	1.72e+003	22.6%	958	2.48e+003	Q
6	0.0412	23.7%	0.0221	0.0603	THETA6 LBW ON V2
OMEGA					INTERINDIVIDUAL VARIABILITY
1,1	1.19	41.8%	0.214	2.17	CV = 109%
2,2	0.252	15.9%	0.174	0.330	CV = 50.2%
3,3	0.679	12.6%	0.511	0.847	CV = 82.4%
SIGMA					RESIDUAL VARIABILITY
1,1	0.143	15.4%	0.0999	0.186	SD = 0.378

```
*Indicates 95% confidence interval that includes zero
%RSE is percent relative standard error (100% x SE/EST)

        Akaike Information Criterion: 28.47
        Schwarz Bayesian Criterion:   73.5278
CONDITION NUMBER = 30.8 (DOES NOT EXCEED 1000)
```

APPENDIX E

NONMEM CONTROL FILE FOR THE FINAL MODEL IN CHAPTER IV

```
$PROB RUN# 280
$INPUT C ID AMT TIME TAD XDV=DROP DV MDV EVID SEX AGE WT HT=DROP BMI LBW PARA ALT AST HCT
  HGB
RBC=DROP IFXN=DROP GEO=DROP COUN=DROP OCC=DROP FORM TOUT=DROP
$DATA PED.CSV IGNORE=C
$ABB COMRES=6
$SUBROUTINES ADVAN4 TRANS4
$PK
   TVKA=THETA(1)
   KA=TVKA*EXP(ETA(1))
   TVCL=(THETA(2)*((WT/22)**THETA(6)))
   CL=TVCL*EXP(ETA(2))
   TVV2=(THETA(3)*((WT/22)**THETA(7)))
   V2=TVV2*EXP(ETA(3))
   TVV3=THETA(4)
   V3=TVV3*EXP(ETA(4))
   TVQ=THETA(5)
   Q=TVQ*EXP(ETA(5))
   S2=V2/1000
   K20=CL/V2
   K23=Q/V2
   K32=Q/V3
   BETA=((K23+K32+K20)-SQRT(((K23+K32+K20)**2) - 4*K32*K20))*0.5
   ALPHA=K32*K20/BETA
   TBETA=LOG(2)/BETA
   TALPHA=LOG(2)/ALPHA
   PP=AMT/WT/0.57
$INFN
IF (ICALL.EQ.3) THEN
 OPEN(50,FILE='CWTAB280.est')
 WRITE (50,*) 'ETAS'
DO WHILE(DATA)
IF (NEWIND.LE.1) WRITE(50,*) ETA
ENDDO
 WRITE (50,*) 'THETAS'
 WRITE (50,*) THETA
 WRITE (50,*) 'OMEGAS'
 WRITE (50,*) OMEGA(BLOCK)
 WRITE (50,*) 'SIGMAS'
 WRITE (50,*) SIGMA(BLOCK)
ENDIF
$ERROR
   IPRED=0
   IF (F.GT.0) IPRED=LOG(F)
   W = 1; additive error model
   IRES = DV-IPRED
   IWRES = IRES/W
   Y = IPRED + W*ERR(1)
"LAST
"  COM(1)=G(1,1)
"  COM(2)=G(2,1)
"  COM(3)=G(3,1)
"  COM(4)=G(4,1)
"  COM(5)=G(5,1)
"  COM(6)=HH(1,1)
$EST METHOD=1PRINT=5 MAX=9999 SIG=3     MSFO=280.msf
$THETA
  (0, 29);[KA]
  (0, 500);[CL]
  (0, 900);[V2]
  (0, 3000);[V3]
  (0, 1100);[Q]
  (-INF, 0.5, INF);[THETA WT ON CL]
  (-INF, 0.5, INF);[THETA WT ON V2]
$OMEGA
  0.3 ;[P] omega(1,1)
  0.3 ;[P] omega(2,2)
  0.3 ;[P] omega(3,3)
  0, FIXED ;[P] omega(4,4)
  0, FIXED ;[P] omega(5,5)
```

```
$SIGMA
  0.3 ;[A] sigma(1,1)
$COV PRINT=E
$TABLE ID TIME TAD DV PRED IPRED IWRES PP CL V2 Q V3 KA TALPHA TBETA SEX AGE WT PARA HGB
  IFXN GEO COUN FORM TOUT OCC ONEHEADER NOPRINT FILE=280.tab
$TABLE ID COM(1)=G11 COM(2)=G21 COM(3)=G31 COM(4)=G41 COM(5)=G51 COM(6)=H11 IPRED MDV
  ONEHEADER NOPRINT FILE=CWTAB280.deriv
```

APPENDIX F

THE OUTPUT SUMMARY FOR THE FINAL MODEL IN CHAPTER IV

```
MINIMIZATION STATUS
  MINIMIZATION SUCCESSFUL
  NO. OF FUNCTION EVALUATIONS USED:      298
  NO. OF SIG. DIGITS IN FINAL EST.:  3.0

  ETABAR IS THE ARITHMETIC MEAN OF THE ETA-ESTIMATES,
  AND THE P-VALUE IS GIVEN FOR THE NULL HYPOTHESIS THAT THE TRUE MEAN IS 0.

  ETABAR:  -0.15E-01  0.31E-02  0.10E-01  0.00E+00  0.00E+00
  SE:       0.14E-01  0.12E-01  0.44E-01  0.00E+00  0.00E+00

  P VAL.:   0.30E+00  0.80E+00  0.82E+00  0.10E+01  0.10E+01
  MINIMUM VALUE OF OBJECTIVE FUNCTION :    193.167

ETABAR P VAL. FOR NO ETA < 0.05

MODEL DEFINITION
   TVKA=THETA(1)
   KA=TVKA*EXP(ETA(1))
   TVCL=THETA(2)*((WT/22)**THETA(6))
   CL=TVCL*EXP(ETA(2))
   TVV2=THETA(3)*((WT/22)**THETA(7))
   V2=TVV2*EXP(ETA(3))
   TVV3=THETA(4)
   V3=TVV3*EXP(ETA(4))
   TVQ=THETA(5)
   Q=TVQ*EXP(ETA(5))
   S2=V2/1000
```

	FINAL ESTIMATE	%RSE	95% CONFIDENCE INTERVAL LBOUND	UBOUND	DESCRIPTOR/ VARIABILITY
THETA					
1	28.0	14.8%	19.9	36.1	KA
2	429	6.46%	375	483	CL
3	2.78e+003	6.22%	2.44e+003	3.12e+003	V2
4	1.98e+003	11.2%	1.54e+003	2.42e+003	V3
5	524	10.0%	421	627	Q
6	1.17	11.6%	0.903	1.44	THETA WT ON CL
7	0.825	20.7%	0.490	1.16	THETA WT ON V2
OMEGA					INTERINDIVIDUAL VARIABILITY
1,1	0.671	26.7%	0.320	1.02	CV = 81.9%
2,2	0.157	40.6%	0.0320	0.282	CV = 39.6%
3,3	0.852	8.97%	0.702	1.00	CV = 92.3%
SIGMA					RESIDUAL VARIABILITY
1,1	0.226	13.1%	0.168	0.284	SD = 0.475

```
*Indicates 95% confidence interval that includes zero
%RSE is percent relative standard error (100% x SE/EST)

        Akaike Information Criterion: 215.167
        Schwarz Bayesian Criterion:   269.477
CONDITION NUMBER = 17.5 (DOES NOT EXCEED 1000)
```

REFERENCES

1. World Malaria Report 2008. WHO press, 2008. (Accessed Sept, 2009, at http://www.who.int/malaria/wmr2008/malaria2008.pdf)

2. World Malaria Report 2009. WHO press 2009. (Accessed Dec, 2009, at http://www.who.int/malaria/world_malaria_report_2009/en/index.html.)

3. Mouala C, Houze S, Guiguet M, et al. Imported malaria in HIV-infected patients enrolled in the ANRS CO4 FHDH study. J Acquir Immune Defic Syndr 2008;49:55-60.

4. Mali S, Steele S, Slutsker L, Arguin PM. Malaria surveillance--United States, 2006. MMWR Surveill Summ 2008;57:24-39.

5. Mali S, Steele S, Slutsker L, Arguin PM. Malaria surveillance--United States, 2007. MMWR Surveill Summ 2009;58:1-16.

6. Kantele A, Marti H, Felger I, Muller D, Jokiranta TS. Monkey malaria in a European traveler returning from Malaysia. Emerg Infect Dis 2008;14:1434-6.

7. Breman JG. Eradicating malaria. Sci Prog 2009;92:1-38.

8. Mueller I, Galinski MR, Baird JK, et al. Key gaps in the knowledge of Plasmodium vivax, a neglected human malaria parasite. Lancet Infect Dis 2009;9:555-66.

9. Tolle MA. Mosquito-borne diseases. Curr Probl Pediatr Adolesc Health Care 2009;39:97-140.

10. Ashley E, McGready R, Proux S, Nosten F. Malaria. Travel Med Infect Dis 2006;4:159-73.

11. Guidelines for the treatment of malaria. World Health Organization, 2006. (Accessed at http://apps.who.int/malaria/docs/TreatmentGuidelines2006.pdf.)

12. Mendis K, Rietveld A, Warsame M, Bosman A, Greenwood B, Wernsdorfer WH. From malaria control to eradication: The WHO perspective. Trop Med Int Health 2009;14:802-9.

13. Kilama W, Ntoumi F. Malaria: a research agenda for the eradication era. Lancet 2009;374:1480-2.

14. World Health Organization. Guidelines for the treatment of malaria. In. Geneva: WHO Press; 2006. [http://apps.who.int/malaria/docs/TreatmentGuidelines2006.pdf].

15. Sinclair D, Zani B, Donegan S, Olliaro P, Garner P. Artemisinin-based combination therapy for treating uncomplicated malaria. Cochrane Database Syst Rev 2009:CD007483.

16. White N. Antimalarial drug resistance and combination chemotherapy. Philos Trans R Soc Lond B Biol Sci 1999;354:739-49.

17. Zheng XY, Xia Y, Gao FH, Chen C. [Synthesis of 7351, a new antimalarial drug (author's transl)]. Yao Xue Xue Bao (abstract) 1979;14:736-7.

18. Chang C, Lin-Hua T, Jantanavivat C. Studies on a new antimalarial compound: pyronaridine. Trans R Soc Trop Med Hyg 1992;86:7-10.

19. New Drug Group of the Former Department of Malaria. [Experimental studies on chemotherapeutic effects and toxicities of a new antimalarial drug 7351 (author's transl)]. Yao Xue Xue Bao (abstract) 1980;15:630-2.

20. Zheng XY, Chen C, Gao FH, Zhu PE, Guo HZ. [Synthesis of new antimalarial drug pyronaridine and its analogues (author's transl)]. Yao Xue Xue Bao (abstract) 1982;17:118-25.

21. Fu S, Bjorkman A, Wahlin B, Ofori-Adjei D, Ericsson O, Sjoqvist F. In vitro activity of chloroquine, the two enantiomers of chloroquine, desethylchloroquine and pyronaridine against Plasmodium falciparum. Br J Clin Pharmacol 1986;22:93-6.

22. Shao BR. A review of antimalarial drug pyronaridine. Chin Med J (Engl) 1990;103:428-34.

23. World Health Organization. Practical chemotherapy of malaria. Report of a WHO Scientific Group. World Health Organ Tech Rep Ser 1990;805:122-4.

24. Fu S, Xiao SH. Pyronaridine: A new antimalarial drug. Parasitol Today 1991;7:310-3.

25. Chen C, Zheng X. Development of the new antimalarial drug pyronaridine: a review. Biomed Environ Sci 1992;5:149-60.

26. Basco LK, Le Bras J. In vitro activity of pyronaridine against African strains of Plasmodium falciparum. Ann Trop Med Parasitol 1992;86:447-54.

27. Looareesuwan S, Kyle DE, Viravan C, Vanijanonta S, Wilairatana P, Wernsdorfer WH. Clinical study of pyronaridine for the treatment of acute uncomplicated falciparum malaria in Thailand. Am J Trop Med Hyg 1996;54:205-9.

28. Ringwald P, Bickii J, Basco L. Randomised trial of pyronaridine versus chloroquine for acute uncomplicated falciparum malaria in Africa. Lancet 1996;347:24-8.

29. Kurth F, Pongratz P, Belard S, Mordmuller B, Kremsner PG, Ramharter M. In vitro activity of pyronaridine against Plasmodium falciparum and comparative evaluation of anti-malarial drug susceptibility assays. Malar J 2009;8:79.

30. Olliaro PL, Trigg PI. Status of antimalarial drugs under development. Bull World Health Organ 1995;73:565-71.

31. Wiesner J, Ortmann R, Jomaa H, Schlitzer M. New antimalarial drugs. Angew Chem Int Ed Engl 2003;42:5274-93.

32. Adegoke OA, Babalola CP, Oshitade OS, Famuyiwa AA. Determination of the physicochemical properties of pyronaridine - a new antimalarial drug. Pak J Pharm Sci 2006;19:1-6.

33. Wu LJ, Rabbege JR, Nagasawa H, Jacobs G, Aikawa M. Morphological effects of pyronaridine on malarial parasites. Am J Trop Med Hyg 1988;38:30-6.

34. Kawai S, Kano S, Chang C, Suzuki M. The effects of pyronaridine on the morphology of Plasmodium falciparum in Aotus trivirgatus. Am J Trop Med Hyg 1996;55:223-9.

35. Auparakkitanon S, Chapoomram S, Kuaha K, Chirachariyavej T, Wilairat P. Targeting of hematin by the antimalarial pyronaridine. Antimicrob Agents Chemother 2006;50:2197-200.

36. Childs GE, Hausler B, Milhous W, et al. In vitro activity of pyronaridine against field isolates and reference clones of Plasmodium falciparum. Am J Trop Med Hyg 1988;38:24-9.

37. Schildbach S, Wernsdorfer WH, Suebsaeng L, Rooney W. In vitro sensitivity of multiresistant Plasmodium falciparum to new candidate antimalarial drugs in western Thailand. Southeast Asian J Trop Med Public Health 1990;21:29-38.

38. Warsame M, Wernsdorfer WH, Payne D, Bjorkman A. Positive relationship between the response of Plasmodium falciparum to chloroquine and pyronaridine. Trans R Soc Trop Med Hyg 1991;85:570-1.

39. Elueze EI, Croft SL, Warhurst DC. Activity of pyronaridine and mepacrine against twelve strains of Plasmodium falciparum in vitro. J Antimicrob Chemother 1996;37:511-8.

40. Looareesuwan S, Olliaro P, Kyle D, Wernsdorfer W. Pyronaridine. Lancet 1996;347:1189-90.

41. Ringwald P, Bickii J, Basco LK. Efficacy of oral pyronaridine for the treatment of acute uncomplicated falciparum malaria in African children. Clin Infect Dis 1998;26:946-53.

42. Ringwald P, Bickii J, Same-Ekobo A, Basco LK. Pyronaridine for treatment of Plasmodium ovale and Plasmodium malariae infections. Antimicrob Agents Chemother 1997;41:2317-9.

43. Ramharter M, Kurth F, Schreier AC, et al. Fixed-dose pyronaridine-artesunate combination for treatment of uncomplicated falciparum malaria in pediatric patients in Gabon. J Infect Dis 2008;198:911-9.

44. Development Projects: PYRAMAX®(pyronaridine-artesunate)-Phase III. MMV, 2010. (Accessed Jan, 2010, at http://www.mmv.org/article.php3?id_article=48&recherche=pyramax.)

45. Feng Z, Wu ZF, Wang CY, Jiang NX. [Pharmacokinetics of pyronaridine in malaria patients]. Zhongguo Yao Li Xue Bao 1987;8:543-6.

46. Feng Z, Jiang NX, Wang CY, Zhang W. [Pharmacokinetics of pyronaridine, an antimalarial in rabbits]. Yao Xue Xue Bao (abstract) 1986;21:801-5.

47. Chen YC, Fleckenstein L. Improved assay method for the determination of pyronaridine in plasma and whole blood by high-performance liquid chromatography for application to clinical pharmacokinetic studies. J Chromatogr B Biomed Sci Appl 2001;752:39-46.

48. Lee J, Son J, Chung SJ, Lee ES, Kim DH. In vitro and in vivo metabolism of pyronaridine characterized by low-energy collision-induced dissociation mass spectrometry with electrospray ionization. J Mass Spectrom 2004;39:1036-43.

49. Ette EI, Williams PJ. Pharmacometrics: impacting drug development and pharmacotherapy. In: Ette EI, Williams PJ, eds. Pharmacometrics: The science of quantitative pharmacology. Hoboken, NJ: John Wiley & Sons; 2007:1-21.

50. Powell JR, Gobburu JV. Pharmacometrics at FDA: evolution and impact on decisions. Clin Pharmacol Ther 2007;82:97-102.

51. Pharmacometrics at FDA. United States Food and Drug Administration, 2009. (Accessed Dec, 2009, at http://www.fda.gov/AboutFDA/CentersOffices/CDER/ucm167032.htm.)

52. Gobburu JV, Lesko LJ. Quantitative disease, drug, and trial models. Annu Rev Pharmacol Toxicol 2009;49:291-301.

53. Barrett JS, Fossler MJ, Cadieu KD, Gastonguay MR. Pharmacometrics: a multidisciplinary field to facilitate critical thinking in drug development and translational research settings. J Clin Pharmacol 2008;48:632-49.

54. Bhattaram VA, Booth BP, Ramchandani RP, et al. Impact of pharmacometrics on drug approval and labeling decisions: a survey of 42 new drug applications. AAPS J 2005;7:E503-12.

55. Bhattaram VA, Bonapace C, Chilukuri DM, et al. Impact of pharmacometric reviews on new drug approval and labeling decisions--a survey of 31 new drug applications submitted between 2005 and 2006. Clin Pharmacol Ther 2007;81:213-21.

56. Guidance for Industry: Population Pharmacokinetics. United States Food and Drug Administration, 1999. (Accessed Dec, 2009, at www.fda.gov/downloads/Drugs/.../Guidances/UCM072137.pdf)

57. Guideline on reporting the results of population pharmacokinetic analyses. European Medicines Agency 2008. (Accessed Dec, 2009, at

58. Hochhaus G, Barrett JS, Derendorf H. Evolution of pharmacokinetics and pharmacokinetic/dynamic correlations during the 20th century. J Clin Pharmacol 2000;40:908-17.

59. Aarons L. Population pharmacokinetics: theory and practice. Br J Clin Pharmacol 1991;32:669-70.

60. Sheiner LB, Beal SL. Evaluation of methods for estimating population pharmacokinetics parameters. I. Michaelis-Menten model: routine clinical pharmacokinetic data. J Pharmacokinet Biopharm 1980;8:553-71.

61. Sheiner BL, Beal SL. Evaluation of methods for estimating population pharmacokinetic parameters. II. Biexponential model and experimental pharmacokinetic data. J Pharmacokinet Biopharm 1981;9:635-51.

62. Sheiner LB, Beal SL. Evaluation of methods for estimating population pharmacokinetic parameters. III. Monoexponential model: routine clinical pharmacokinetic data. J Pharmacokinet Biopharm 1983;11:303-19.

63. Bonate P. Pharmacokinetic-pharmacodynamic modeling and simulation. New York: Springer; 2006.

64. Boeckmann AJ, Sheiner LB, Beal SL. NONMEM Users Guides - Part V. San Francisco: NONMEM Project Group, University of California at San Francisco; 1994.

65. Ette EI, Williams PJ, eds. Pharmacometrics: The science of quantitative pharmacology. Hoboken, NJ: John Wiley & Sons; 2007.

66. Whiting B, Kelman AW, Grevel J. Population pharmacokinetics. Theory and clinical application. Clin Pharmacokinet 1986;11:387-401.

67. Mandema JW, Verotta D, Sheiner LB. Building population pharmacokinetic--pharmacodynamic models. I. Models for covariate effects. J Pharmacokinet Biopharm 1992;20:511-28.

68. Ette EI, Williams PJ, Lane JR. Population pharmacokinetics III: design, analysis, and application of population pharmacokinetic Studies. Ann Pharmacother 2004;38:2136-44.

69. Brendel K, Dartois C, Comets E, et al. Are population pharmacokinetic and/or pharmacodynamic models adequately evaluated? A survey of the literature from 2002 to 2004. Clin Pharmacokinet 2007;46:221-34.

70. Tshefu AK, Gaye O, Kayentao K, et al. Efficacy and safety of a fixed-dose oral combination of pyronaridine-artesunate compared with artemether-lumefantrine in children and adults with uncomplicated Plasmodium falciparum malaria: a randomised non-inferiority trial. Lancet 2010;375:1457-67.

71. Malaria Pictures. Hardin MD/University of Iowa and CDC, 2009. (Accessed Sept, 2009, at http://www.lib.uiowa.edu/hardin/md/cdc/malaria5.html.)

72. Schema of the Life Cycle of Malaria. Centers for Disease Control and Prevention (CDC), 2009. (Accessed Sept, 2009, at http://www.cdc.gov/malaria/biology/life_cycle.htm.)

73. Vivas L, Rattray L, Stewart L, et al. Anti-malarial efficacy of pyronaridine and artesunate in combination in vitro and in vivo. Acta Trop 2008;105:222-8.

74. Olliaro P, Wells TN. The global portfolio of new antimalarial medicines under development. Clin Pharmacol Ther 2009;85:584-95.

75. Ringwald P, Eboumbou EC, Bickii J, Basco LK. In vitro activities of pyronaridine, alone and in combination with other antimalarial drugs, against Plasmodium falciparum. Antimicrob Agents Chemother 1999;43:1525-7.

76. Beal SL, Sheiner LB, Boeckmann AJ, eds. NONMEM Users Guides. San Francisco: NONMEM Project Group, University of California at San Francisco; 1989-2006.

77. Jonsson EN, Karlsson MO. Xpose--an S-PLUS based population pharmacokinetic/pharmacodynamic model building aid for NONMEM. Comput Methods Programs Biomed 1999;58:51-64.

78. Pradines B, Mabika Mamfoumbi M, Parzy D, et al. In vitro susceptibility of African isolates of Plasmodium falciparum from Gabon to pyronaridine. Am J Trop Med Hyg 1999;60:105-8.

79. Pradines B, Tall A, Parzy D, et al. In-vitro activity of pyronaridine and amodiaquine against African isolates (Senegal) of Plasmodium falciparum in comparison with standard antimalarial agents. J Antimicrob Chemother 1998;42:333-9.

80. Alin MH, Bjorkman A, Ashton M. In vitro activity of artemisinin, its derivatives, and pyronaridine against different strains of Plasmodium falciparum. Trans R Soc Trop Med Hyg 1990;84:635-7.

81. Assessment and monitoring of antimalarial drug efficacy for the treatment of uncomplicated falciparum malaria. WHO press 2003. (Accessed Dec, 2009, at http://www.who.int/malaria/publications/atoz/whohtmrbm200350/en/index.html.)

82. Naik H, Imming P, Schmidt MS, Murry DJ, Fleckenstein L. Development and validation of a liquid chromatography-mass spectrometry assay for the determination of pyronaridine in human blood for application to clinical pharmacokinetic studies. J Pharm Biomed Anal 2007;45:112-9.

83. Sachs J, Malaney P. The economic and social burden of malaria. Nature 2002;415:680-5.

84. Nwaka S, Riopel L, Ubben D, Craft JC. Medicines for Malaria Venture new developments in antimalarials. Travel Med Infect Dis 2004;2:161-70.

85. Eastman RT, Fidock DA. Artemisinin-based combination therapies: a vital tool in efforts to eliminate malaria. Nat Rev Microbiol 2009;7:864-74.